AD-A054 174 TRANSPORTATION SYSTEMS CENTER CAMBRIDGE MASS F/G 4/2

WIND SHEAR REQUIREMENTS AND THEIR APPLICATION TO LASER SYSTEMS.(U)

FEB 78 R M KALAFUS

UNCLASSIFIED DOT-TSC-FAA-77-5 FAA/RD-77-120 NL

1 OF 2

ADA 054174

1 OF 2
ADA
054174

1·0 2·8 2·5 3·15 2·2 3·5 2·0 4·0 1·1 4·5 1·8 1·25 1·4 1·6

NATIONAL BUREAU OF STANDARDS
MICROCOPY RESOLUTION TEST CHART

Report No. FAA-RD-77-~~123~~120

WIND SHEAR REQUIREMENTS AND THEIR APPLICATION TO LASER SYSTEMS

Rudolph M. Kalafus

U.S. Department of Transportation
Transportation Systems Center
Kendall Square
Cambridge MA 02142

FEBRUARY 1978

FINAL REPORT

DOCUMENT IS AVAILABLE TO THE U.S. PUBLIC THROUGH THE NATIONAL TECHNICAL INFORMATION SERVICE, SPRINGFIELD, VIRGINIA 22161

Prepared for

U.S. DEPARTMENT OF TRANSPORTATION
FEDERAL AVIATION ADMINISTRATION
Systems Research and Development Service
Washington DC 20591

NOTICE

This document is disseminated under the sponsorship of the Department of Transportation in the interest of information exchange. The United States Government assumes no liability for its contents or use thereof.

NOTICE

The United States Government does not endorse products or manufacturers. Trade or manufacturers' names appear herein solely because they are considered essential to the object of this report.

ERRATA

Report No. FAA-RD-77-123

WIND SHEAR REQUIREMENTS AND THEIR APPLICATION TO LASER SYSTEMS

Rudolph M. Kalafus

U.S. Department of Transportation
Transportation Systems Center
Kendall Square
Cambridge MA 02142

FEBRUARY 1978

FINAL REPORT

Front Cover and Form DOT F 1700.7: Change number of the above title report from FAA-RD-77-123 to FAA-RD-77-120.

Released April 24, 1978

Technical Report Documentation Page

1. Report No. FAA/RD 77-123	2. Government Accession No.	3. Recipient's Catalog No.
4. Title and Subtitle WIND SHEAR REQUIREMENTS AND THEIR APPLICATION TO LASER SYSTEMS.		5. Report Date Feb[redacted]78
		6. Performing Organization Code
7. Author(s) Rudolph M. Kalafus		8. Performing Organization Report No. DOT-TSC-FAA-77-5
9. Performing Organization Name and Address U.S. Department of Transportation Transportation Systems Center Kendall Square Cambridge MA 02142		10. Work Unit No. (TRAIS) FA742 R8105
		11. Contract or Grant No.
12. Sponsoring Agency Name and Address U.S. Department of Transportation Federal Aviation Administration Systems Research and Development Service Washington DC 20591		13. Type of Report and Period Covered Final Report. Mar[redacted]-Dec[redacted]76
		14. Sponsoring Agency Code

15. Supplementary Notes

16. Abstract

The requirements for a ground-based wind shear sensing system are developed. System coverage, accuracy, resolution, and data update rate are treated in detail. The differing requirements for synoptic shear conditions and thunderstorm-associated shears are discussed. Several candidate sensing systems are considered. The hybrid CW/pulsed laser is discussed in detail because of its potential for providing advance warning for all shear conditions. Propagational characteristics of laser beams are treated and equipment design implications are developed. A system concept is outlined which provides the framework for a future operational system.

17. Key Words	18. Distribution Statement
Boundary Layer, Carbon Dioxide Lasers, Fronts, Heterodyne Laser Sensors, Thunderstorms, Wind Profiles, Wind Shears	DOCUMENT IS AVAILABLE TO THE U.S. PUBLIC THROUGH THE NATIONAL TECHNICAL INFORMATION SERVICE, SPRINGFIELD, VIRGINIA 22161

19. Security Classif. (of this report)	20. Security Classif. (of this page)	21. No. of Pages	22. Price
Unclassified	Unclassified	140	

Form DOT F 1700.7 (8-72) Reproduction of completed page authorized

407 082

PREFACE

I would especially like to acknowledge the help of Jim Hallock, who provided a sounding board for many of the topics discussed here, and who wrote Appendix C and the other material on boundary layer shears. My special thanks also go to my colleagues Bill Wood, Ed Spitzer, and Ian McWilliams for numerous helpful discussions and criticisms, and to Chuck Sonnenschein for his help on laser propagation. Finally, I would like to thank Leo Gumina, Frank Coons and Guice Tinsley of the FAA Wind Shear Program Office for their encouragement and support.

METRIC CONVERSION FACTORS

Approximate Conversions to Metric Measures

Symbol	When You Know	Multiply by	To Find	Symbol
		LENGTH		
in	inches	2.5	centimeters	cm
ft	feet	30	centimeters	cm
yd	yards	0.9	meters	m
mi	miles	1.6	kilometers	km
		AREA		
in^2	square inches	6.5	square centimeters	cm^2
ft^2	square feet	0.09	square meters	m^2
yd^2	square yards	0.8	square meters	m^2
mi^2	square miles	2.6	square kilometers	km^2
	acres	0.4	hectares	ha
		MASS (weight)		
oz	ounces	28	grams	g
lb	pounds	0.45	kilograms	kg
	short tons (2000 lb)	0.9	tonnes	t
		VOLUME		
tsp	teaspoons	5	milliliters	ml
Tbsp	tablespoons	15	milliliters	ml
fl oz	fluid ounces	30	milliliters	ml
c	cups	0.24	liters	l
pt	pints	0.47	liters	l
qt	quarts	0.95	liters	l
gal	gallons	3.8	liters	l
ft^3	cubic feet	0.03	cubic meters	m^3
yd^3	cubic yards	0.76	cubic meters	m^3
		TEMPERATURE (exact)		
°F	Fahrenheit temperature	5/9 (after subtracting 32)	Celsius temperature	°C

Approximate Conversions from Metric Measures

Symbol	When You Know	Multiply by	To Find	Symbol
		LENGTH		
mm	millimeters	0.04	inches	in
cm	centimeters	0.4	inches	in
m	meters	3.3	feet	ft
m	meters	1.1	yards	yd
km	kilometers	0.6	miles	mi
		AREA		
cm^2	square centimeters	0.16	square inches	in^2
m^2	square meters	1.2	square yards	yd^2
km^2	square kilometers	0.4	square miles	mi^2
ha	hectares (10,000 m^2)	2.5	acres	
		MASS (weight)		
g	grams	0.035	ounces	oz
kg	kilograms	2.2	pounds	lb
t	tonnes (1000 kg)	1.1	short tons	
		VOLUME		
ml	milliliters	0.03	fluid ounces	fl oz
l	liters	2.1	pints	pt
l	liters	1.06	quarts	qt
l	liters	0.26	gallons	gal
m^3	cubic meters	35	cubic feet	ft^3
m^3	cubic meters	1.3	cubic yards	yd^3
		TEMPERATURE (exact)		
°C	Celsius temperature	9/5 (then add 32)	Fahrenheit temperature	°F

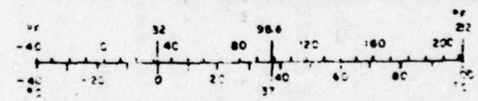

TABLE OF CONTENTS

TABLE OF CONTENTS (CONTINUED)

LIST OF ILLUSTRATIONS

LIST OF ILLUSTRATIONS (CONTINUED)

LIST OF ILLUSTRATIONS (CONTINUED)

LIST OF ILLUSTRATIONS (CONTINUED)

LIST OF TABLES

LIST OF ABBREVIATIONS

cm	centimeters
dB	decibels, equal to 20 $\log_{10}$ (ratio of two numbers)
fpm	feet per minute
ft	feet (or foot); 1 foot equals 0.3048 meters
hr	hour
Hz	Hertz, or cycles per second
in	inches
kHz	kilohertz
km	kilometers
knots	nautical miles per hour; 1 knot equals 0.5149 m/sec
kphf	knots per hundred feet; 1 kphf equals 0.0169 m/sec/m
KW	kilowatts
lb	pounds; 1 lb equals 454 grams
m	meters
mg	milligrams
MHz	megahertz
microns	1 micron equals 10^{-6}m
MW	megawatts
nm	nautical miles; 1 nm equals 6076 feet, or 1.852 km
pps	pulses per second
sec	seconds
sr	steradian
W	watts
σ	standard deviation of error; 1σ is one standard deviation, 3σ is three standard deviations, etc.

1. INTRODUCTION

Sharp gradients in the wind encountered by an aircraft on takeoff or on final approach have caused several serious, in some cases fatal, accidents to occur. Of the three components of wind as seen from the aircraft, namely headwinds, crosswinds, and downdrafts, gradients in headwinds appear to be the single most dangerous condition. Sudden crosswinds have contributed to accidents by distracting the pilot from vertical position instruments (e.g., NTSB, 1973c), but have not been identified as the cause of a serious accident. Sudden changes of headwind are critical because of the relation between airspeed and lift, and are doubly insidious because of the lack of distinctive accelerative cues felt by pilot and crew. In several accidents pilots were seeking to acquire visual contact with runway indicators at the time that instruments were indicating descent below the glideslope and excessive sink rates; even after visual contact was obtained, neither visual nor accelerative cues were distinctive enough to depict the gravity of the situation in time (NTSB, 1974b,c, 1967a,c).

There are three meteorological conditions which are frequently accompanied by regions of severe wind shear (Langweil, 1976).

a. Boundary layer shears--inversions and jets; characterized by horizontal strata existing for several miles, but having a vertical profile with significant shears (vertical shear); while these can be quite abrupt and reach significant values (e.g., 20 kphf (see glossary) or 0.3 m/sec/m), they have yet to be positively identified with a serious accident.

b. Frontal shears--cold and warm; fronts causing hazardous shears are characterized by abrupt wind shift zones having considerably different wind directions on either side. Warm fronts have shallow slopes compared with approach and departure paths, and thus present a vertical shear region to an ascending or descending aircraft; cold fronts have steep slopes in the atmospheric boundary layer, so that even aircraft flying at constant altitude may encounter shear zones (horizontal shear). The Iberia Airlines accident (NTSB, 1974c) appears to have been caused by a warm front shear.

c. Thunderstorms--gust fronts and downburst cells; characterized by localized zones of rapidly varying wind currents, which an aircraft experiences as downdrafts and sudden changes in headwind and crosswind. These have been identified as a prime contributing factor in several accidents (NTSB, 1974, 1976).

The need exists for a sensor which can remotely detect, identify, and track such wind shears around the airport and provide safety assurance to both departing and approaching aircraft up to 1500 feet (450m) or more in altitude. Point sensors, such as anemometers and pressure jump sensors, and vertical looking probes, such as acoustic sodars, FM/CW radars, and CW laser radars, must be placed off the airport surface if they are to detect gust fronts or downburst cells. There are two technologies which can be placed on the airport surface and provide the potential of remotely sensing shear events beyond the airport boundaries: pulsed Doppler radar operating off returns either from precipitation or index of refraction variations, and pulsed Doppler laser radar, operating off returns from precipitation or particulate aerosols. Both are promising techniques. Lasers have now reached a state of maturity that makes the feasibility of a combined vertical probe and remote sensor possible; it is given primary emphasis in the later sections.

Section 2 discusses the meteorology of wind shear events. Section 3 develops the major requirements that any sensing system should meet, and some candidate sensors. Section 4 deals with the particular propagational and implementation features associated with laser systems, and Section 5 presents the system concept.

Some of the results derived here were given in a presentation in November 1976 (Kalafus and Hallock, 1976).

2. WIND SHEAR DESCRIPTION

2.1 BOUNDARY LAYER SHEARS

Low-level wind shears result from the interaction of synoptic scale flow with the surface of the earth. The boundary layer can be segmented into a constant wind direction layer and a wind turning layer. The constant wind direction layer extends from the surface up to about 150 meters (500 feet) and wind shear results from the boundary condition that the steady-state wind speed must be zero at the ground. The turning layer occurs above the constant wind direction layer and exhibits a marked turning of the steady-state wind vector with an increase in altitude.

Neutral and unstable conditions rarely produce wind shears that are hazardous to aviation. Stable conditions, on the other hand, can lead to appreciable wind shears. Negative buoyant forces suppress the turbulence and decouple the layers, allowing them to slip relative to each other. With very stable conditions the flow is laminar, very little mixing occurs, and the overriding air remains separated from the underlying air. Large changes in wind direction (in excess of 40°) and/or wind magnitude (15m/sec, or 30 knots) are possible in altitude changes of less than 30 meters (100 feet). This is discussed further in Appendix C.

During the night an inversion can build up and relax the constraint imposed on the wind by daytime mixing. As a result the wind at the top of the inversion accelerates, becomes supergeostropic, and oscillates inertially--a low-level nocturnal jet. The low-level jet is a thin, well-defined region of high-speed air at typical altitude of about 300 meters, with no indication of such a wind near the ground. The jet begins to build up in the late afternoon as the earth cools, reaches its maximum in the middle of the night, and decays in the early morning. The nocturnal jets can produce significantly large values of low-level wind shear. At the peak of the jet the winds in its core, between 250 and 700 meters (800 and 2200 feet) in altitude, can attain between 15 and 35 m/sec (30 to 70 knots), decreasing to 5 or 10 m/sec (10 or 20 knots) between 1000 and 1400 meters (3000 and 4500 feet), and to 0 at the ground (see Fig. 2-1). It is a local phenomenon which can be 1500 kilometers long (800 nm) and 70 to 700 kilometers wide (40-400 nm). In the United States the occurrence of the nocturnal jet is most pronounced in the Great Plains. Tower measurements have recorded low-level jet shears in excess of 0.4 m/sec/m (24 kphf). This corresponds to a headwind change of 12 meters/second (23 knots) within a change of altitude of 30 meters (100 feet) (a corresponding change of 2-3 meters/second (4-6 knots) can be hazardous for some aircraft).

A vertical looking probe will adequately measure such a shear. These conditions occur over large areas and last for long periods of time. Thus the probe measurements are highly correlated in space and time with aircraft flight profiles so that the measured information should provide the pilot with an accurate picture of what conditions to expect.

This type of condition is less dangerous to aircraft than fronts or storms for several reasons: (1) airport anemometers give good indications of wind speeds at the surface, so that pilots have some indication of the presence of a shear by comparison of reported surface winds and winds aloft; (2) reports of previous pilots tend to be consistent and reliable; (3) the shear at the upper part of the jet is at a high enough altitude to be manageable; (4) there are fewer operations during this period of time; and (5) visibility is good, and visual cues are clear.

2.2 FRONTAL SYSTEMS

Fronts are the zones of discontinuity between cold and warm air, typically polar and tropical air masses. These zones are characterized by differences in temperature, wind, and humidity between the adjacent air masses, and are frequently accompanied by stormy weather. The effect of the earth's surface is to slow the advance of a front, so that warm air always lies above the cold air of the front. This frictional effect also causes a cold front to have a "nose" so that the slope of a rapidly advancing

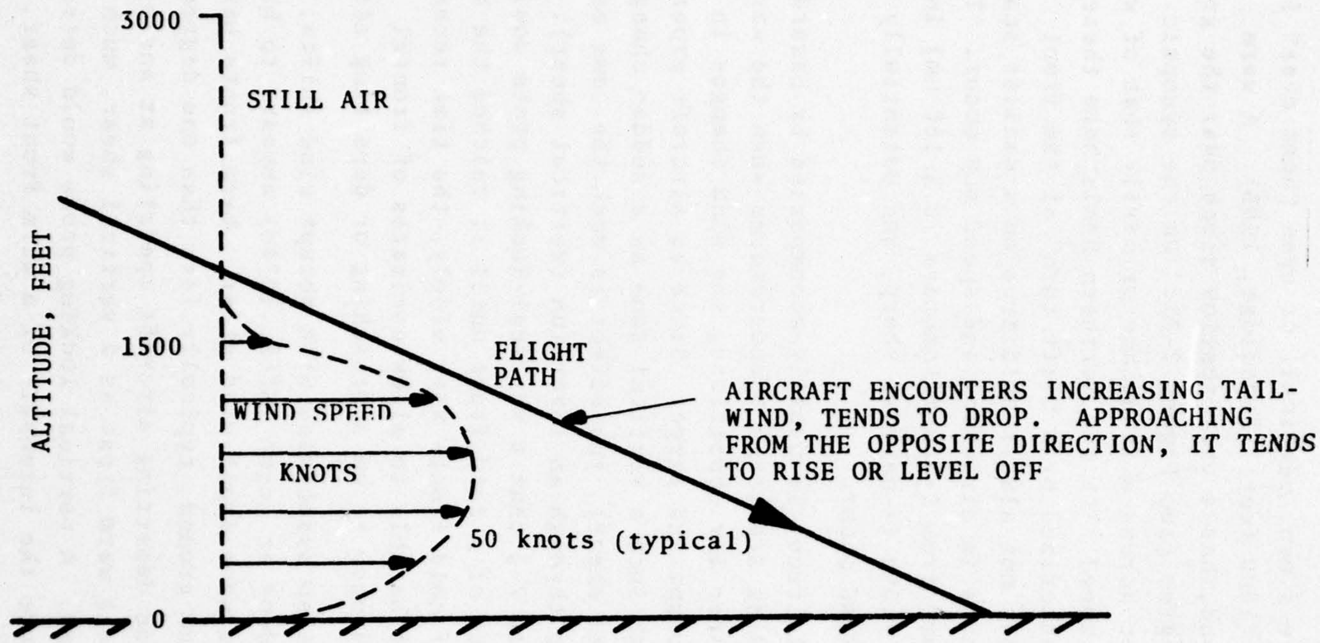

FIGURE 2-1. VERTICAL WIND PROFILE ASSOCIATED WITH A NOCTURNAL JET

cold front can be quite steep, vertical, or even "bent over" in the lowest 300 meters (1000 feet) (Brundidge, 1965). A warm front, on the other hand, has a very shallow slope near the ground, usually less than a degree (see Figure 2-2). On the synoptic scale, the wind changes across a front are primarily that of wind direction rather than speed. In the Northern Hemisphere these wind changes are characterized by a "left turn" at the front (Figure 2-2). This does not always hold true on a smaller scale, because localized changes in direction and speed may occur. The zones of transition vary from 1-300 kilometers (0.5-160 nm) in width. When the zone width is narrow, sharp, and potentially hazardous changes in wind occur.

A fast-moving cold front is usually accompanied by hazardous flying weather, including scattered thunderstorms when the warm air is moist. Even under dry conditions, the wind changes in the frontal zone can be abrupt and large. Since an aircraft experiences a passage through such a vertical zone as a sudden change in headwind (horizontal shear), the effect is much the same as for an aircraft descending through an inversion (vertical shear). It can be seen from Figure 2-2 that a vertical-looking probe would not detect the presence of a cold front until it reached the airport. Since slopes of cold fronts vary widely, the time record of such a probe would not be able to allow estimates of frontal speed or severity of danger to an approaching or departing aircraft.

Warm fronts are also associated with abrupt wind shifts; the Iberia Air Lines accident at Logan (NTSB, 1974c) appears to have been associated with a warm front wind shear. Warm fronts have shallow slopes near the ground, typically less than one degree, so that approaching and departing aircraft operating at angles of 3-6 degrees experience a warm front as a vertical shear, much like an inversion shear. A vertical-looking probe would detect the presence and measure the intensity of a warm front shear, but would not give speed or slope (see Fig. 2-3).

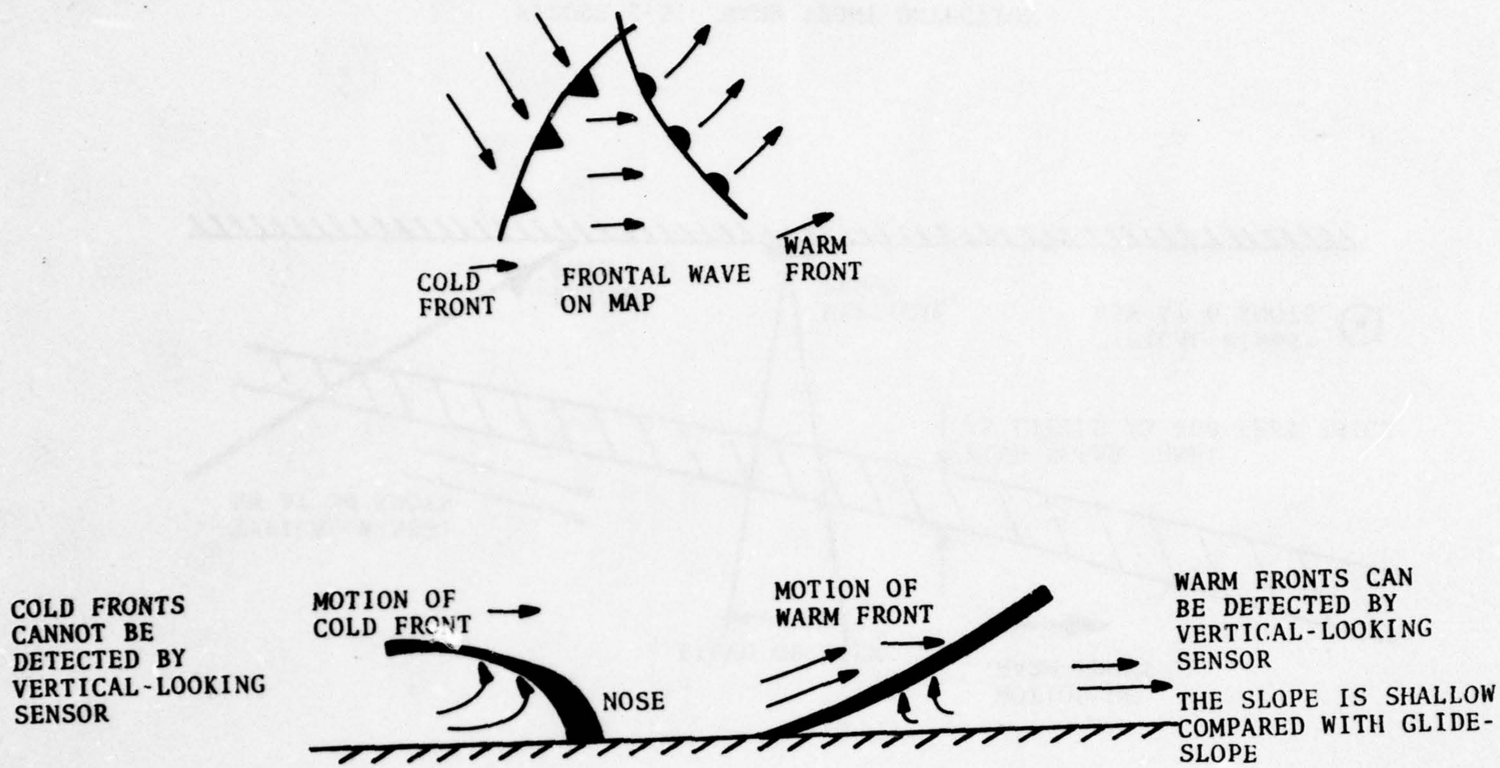

FIGURE 2-2. TYPICAL FRONTAL PROFILES

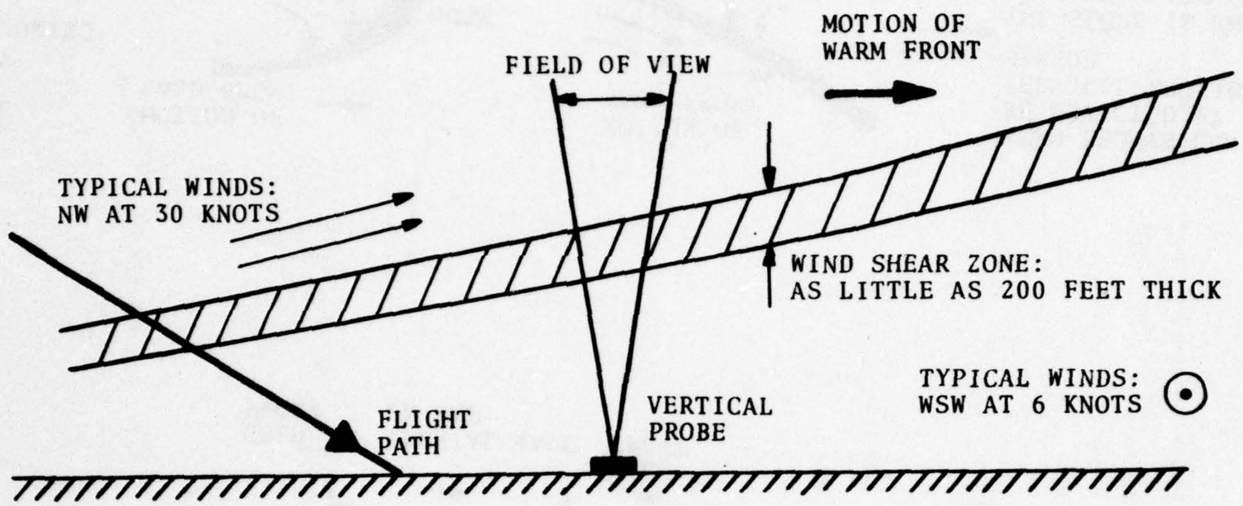

FIGURE 2-3. WARM FRONT DETECTION
WITH A VERTICAL PROBE

2.3 THUNDERSTORMS

In mature thunderstorms both updrafts and downdrafts occur which make it difficult for an approaching aircraft to hold the glidepath. In the lowest 300 meters (1000 feet) of altitude, the effect of the earth's surface is to cause an outflow from a downdraft. Usually a downdraft is accompanied by heavy rain, but there have been cases where the precipitation evaporated before reaching the ground (NTSB, 1976b). The outflow results in a gust front ahead of the downdraft of a thunderstorm (Figure 2-4). The gust front may precede the precipitation by up to 18 nm (30 km). The gust front varies from 1-3 kilometers (0.7-2 nm) in thickness (Goff, 1975). An aircraft penetrating the gust front usually experiences updrafts, an increasing headwind, and a change in crosswind. The slope of the front is much steeper than the path of aircraft, so that it is characterized by a horizontal shear. Headwind gradients reported by Goff (1975) reached values of 0.1 m/sec/m (6 knots per thousand feet), which corresponds to a headwind speed change of 3.5 m/sec (7 knots) in 5 seconds for an aircraft traveling at 70 m/sec (140 knots).

Within a large thunderstorm system there can be several intense downburst cells (Caracena, 1976 and Fujita, 1975). These cells can produce downdrafts of 10 m/sec (33 fps) and extreme wind speed changes. In the Stapleton accident (NTSB, 1976b) a loss of headwind of 12 m/sec (23 knots) in 5 seconds was recorded. The cells are as little as 3 kilometers (2 nm) across, and can be traversed by an aircraft in less than a minute. Similarly, behind the gust front, large scale turbulence can take the form of updrafts and downdrafts or secondary surges; these secondary surges exhibit similar characteristics to the downburst cells, but are not accompanied by rain, and are not visible to the pilot. Downdraft cells such as these are believed to be the most dangerous hazard to landing and departing aircraft. Within 40 seconds the pilot may have to successively handle an increasing headwind (gust front), decreasing headwind, blinding rain, downdraft and crosswind, increasing tailwind, and increasing headwind (gust front),

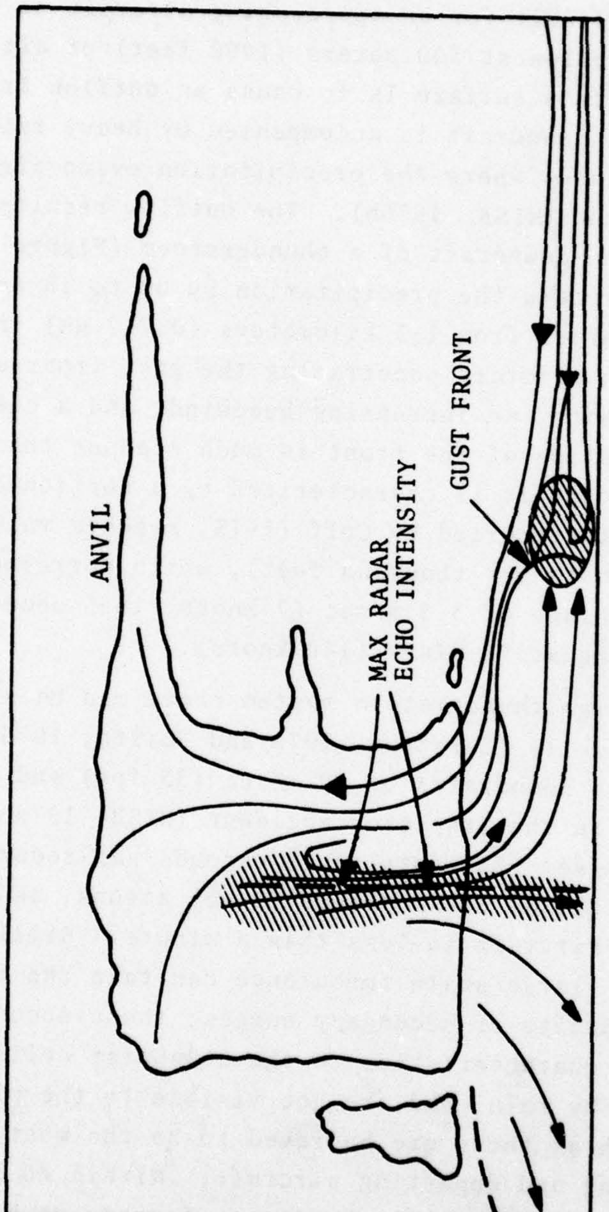

FIGURE 2-4. GUST FRONT OF A THUNDERSTORM

while simultaneously acquiring visual contact with the runway. This situation is portrayed in Figure 3-4 and Table 3-2.

3. MAJOR REQUIREMENTS FOR A GROUND-BASED SYSTEM

Within the constraints of cost, system requirements are dictated primarily by the intended use of the information acquired. In the case of wind shear, the data will be used to detect the existence of a hazardous shear event, and provide the pilot and controller with sufficient information on the intensity and altitude of the expected encounter, so that decisions can be safely made relative to (1) execution of a missed approach (or choosing not to depart) or (2) continuation of the operation with a knowledge of what preventive and corrective actions will ensure the safety of the flight. In the present context, this means detecting shear zones, tracking them, measuring their intensity and estimating their time of arrival at the corridor.

3.1 SYSTEM RANGE

System range should be large enough to protect the approach and departure corridors out to a point where an aircraft has a high probability of recovering after encountering a severe wind shear event. The National Transportation Safety Board has made the following recommendations (NTSB, 1976b):

"Expedite the program to develop and install equipment which would facilitate the detection and classification, by severity, of thunderstorms within 4 nm of the departure or threshold ends of active runways at airports having precision instrument approaches. (A-76-32.)"

"Install equipment capable of detecting variations in the speed of the longitudinal, lateral, and vertical components of the winds as they exist along the projected takeoff and approach flightpaths within 1 nm of the ends of active runways which serve air carrier aircraft. (A-76-33.)"

On the basis of these and other recommendations, the FAA Wind Shear Program Office has adopted the requirement of coverage to the outer marker, until results from simulations, hazard and accident studies indicate otherwise. This implies a system range of about 7 nm (13 km) for a sensor placed in a centerfield location.

Rather than deriving a specific number for system range, the remainder of this discussion is aimed at outlining the steps by which this number can be determined, using results from the various study efforts. The major considerations are:

a. Where along the flight path have shear situations been encountered which historically have caused (or contributed to) accidents (or near accidents)?

b. Based on simulations and reasonable operating assumptions, what is the minimum coverage such that, if no shear events exist in the coverage area, the probability of an accident is small?

c. How do these factors relate to the type of shear encountered?

The accident analysis should be used to back up the coverage requirement resulting from (b) and (c).

The first question to be addressed is whether system range should be based on approach requirements or departure requirements. On takeoff, the aircraft is typically climbing at rates of 1200 fpm (6 m/sec) or more, and reaches a safe airspeed and altitude within 0.5-1 nm (1-2 km) of the runway end. On approach, the aircraft is operating near stall speeds farther out from touchdown. Thus system range must be premised on approach requirements. System range is determined by: first, establishing the minimum range for which an aircraft can readily recover after encountering an event farther out (critical zone); second, establishing th amount of advance warning time needed to assure that no shear event can move into the critical zone before pilots can be alerted.

Clearly, a shear which causes a plane to stall is dangerous at any altitude. There are no accidents of this type known to the author. However, shears can be dangerous without causing stalls; the extent of the danger then depends on the altitude of the aircraft at the time of encounter--the lower the altitude the more dangerous the situation. The zone to be protected is the approach corridor from threshold out to a distance sufficiently far so that, if an aircraft encounters a shear event outside the zone, recovery is virtually certain (see Figure 3-1).

The ability of an aircraft to recover depends on:

a. The mass, available thrust, and responsiveness of the aircraft.

b. The type of shear event, its intensity, and its duration.

c. The information available to the pilot.

d. The pilot's skill.

A ground-based system should be conservative: the aircraft studied should be primarily high-mass, slow-response aircraft; the shear events assumed should be based on the worst observed conditions: minimal information should be assumed (no heads-up display or inertial system, for examples), and pilot response should be assumed to be slow.

There are several reasons for believing that the danger decreases for events encountered farther up the glide path:

a. The aircraft has more altitude and time for recovery;

b. The pilot has fewer duties: decision height is not yet reached, the aircraft may still be on autopilot and margins are greater.

c. In the important case of a downburst event, the danger is greatest below 500 feet; this is discussed at some length below.

Collectively, these factors imply a marked decrease in the danger from a shear event encountered above about 500-feet altitude (150 m).

The downdrafts associated with a thunderstorm constitute the single most dangerous wind shear event known. Convincing evidence has only recently been obtained on the severity of these events, but this evidence is dramatic.

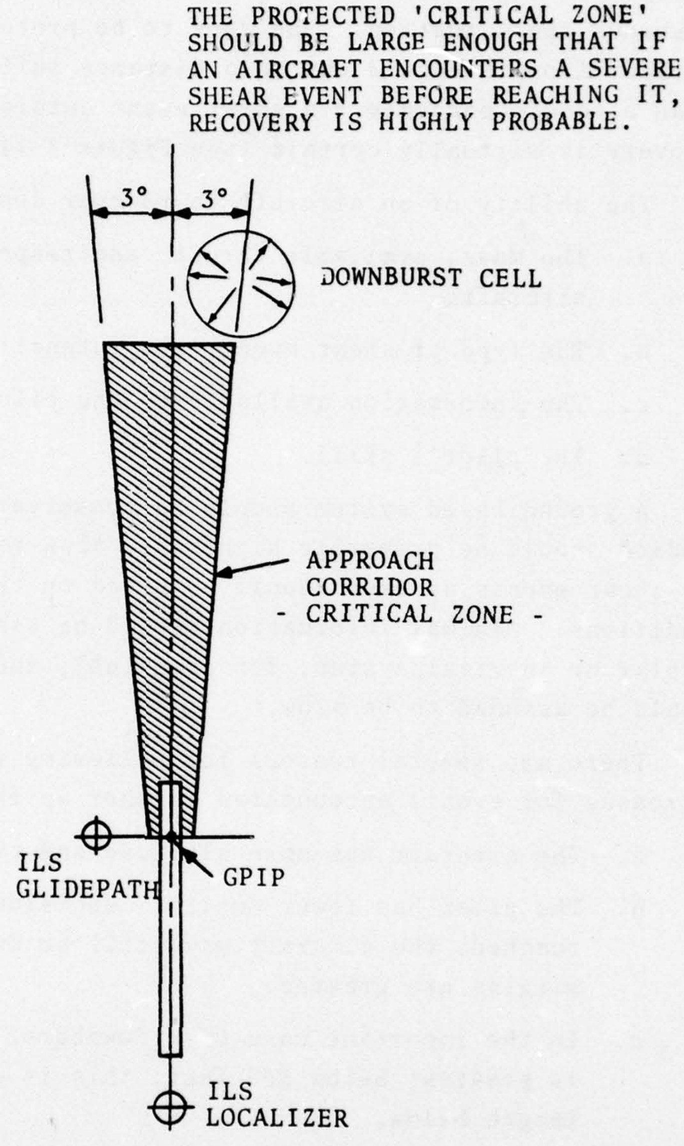

FIGURE 3-1. APPROACH CORRIDOR REQUIRING PROTECTION

While downdrafts from a thunderstorm outflow can occur over a larger area, such wide-scale drafts are believed to be small, on the order of 2-5 feet per second (0.6-1.5 m/sec) at altitudes below 500 feet (150 m). In downburst cells the intense drafts are tightly confined, being on the order of 1000-2000 feet (300-600 m) wide. This statement is premised on limited data, but the effect is observed in data from Goff (1976), Caracena (1976) and Fujita (1975). Below 300-500 feet (90-150m) the effect of the ground is to convert the downwash into an outflow (see Figure 3-2). The outflow is approximately radially outward from the center of the downwash cell; the magnitude varies substantially, as the wind apparently tends to concentrate in sectors. Figure 3-3, taken from Caracena (1975), shows the horizontal streamlines associated with a thunderstorm outflow. The isotachs in that study indicate wind speeds that vary from 6 knots to 40 knots in the radial streamlines around the downwash cell associated with the Denver Stapleton accident (NTSB, 1976b). An aircraft traversing the cell below 300-500 feet (90-150 m) would encounter a decreasing head-wind shear, coupled with a downdraft and possible crosswinds. The archetypal model is shown in Figure 3-4 and Table 3-2.

To ascertain the relative effects of the downdraft and a horizontal shear associated with a downburst cell, the analog computer study by Snyder (1968) was used. There he simulated a swept-wing transport aircraft on final approach, and subjected it to several events: (1) a sudden 5 knot (500 fpm, or 2.5 m/sec) downdraft, sustained; (2) a sudden 15 knot (8 m/sec) drop in air-speed, sustained; and (3) a sudden shear of 5 (and 10) kphf (0.084 and 0.17 m/sec/m), also sustained. Controls are fixed, providing a good picture of what happens in the absence of pilot intervention. The response to a downdraft is a temporary pitchup, which increases lift, thus countering the downward thrust of the draft to some extent; eventually the aircraft stabilizes in the new air mass at a sink rate equal to the original sink rate plus the downdraft speed. The response to a headwind loss is an initial pitchdown; this and the loss of airspeed both act to increase the sink rate. Snyder's computations were premised on a rather fast approach speed of 160 knots (95 m/sec airspeed) and initial trim at an 800 fpm (4 m/sec) sink rate. Table 3-1 shows the sink rates associated with the three shear types.

TABLE 3-1. SINK RATES ASSOCIATED WITH SHEAR EVENTS (FROM SNYDER, 1968)

SHEAR EVENT	AFTER 5 SECONDS	AFTER 10 SECONDS
5 knot downdraft	1000 fpm (5 m/sec)	1300 fpm (6.5 m/sec)
15 knot headwind loss	1900 fpm (9.5m/sec)	2500 fpm (12.5m/sec)
5 kphf shear	950 fpm (4.8m/sec)	1400 fpm (7 m/sec)
10 kphf shear	1100 fpm (5.5m/sec)	2100 fpm (10.5m/sec)

Using Snyder's formulation, TSC performed computations which duplicated his results and were run for other shear severities and approach speeds of 145 and 120 knots. The results were consistent with Snyder's.

It can be seen from the table that a 5 knot downdraft is comparable to a 5 kphf (0.08 m/sec/m) shear for about 10 seconds; thereafter the shear is worse, since the sink rate continues to increase. Whether a 10 knot downdraft is comparable to a 10 kphf (0.17 m/sec/m) shear is not known, but it appears to be a reasonable assumption. There is no firm relationship between the downdraft speed and the equivalent vertical shear in a downburst cell, for the obvious reason that the air mass flow is not uniformly distributed in angle. Thus the shear encountered by an aircraft depends on the direction from which the cell is approached, as well as the region within the cell that is traversed. However, based on a simple flow model, it appears that a 5 kphf (0.08 m/sec/m) shear is a typical average shear that would be associated with a 5 knot (2.5 m/sec) downdraft.

The conclusion to be drawn from this is that in general an aircraft encountering a downdraft at higher altitudes will deviate from the glidepath less than if it encounters the same downburst

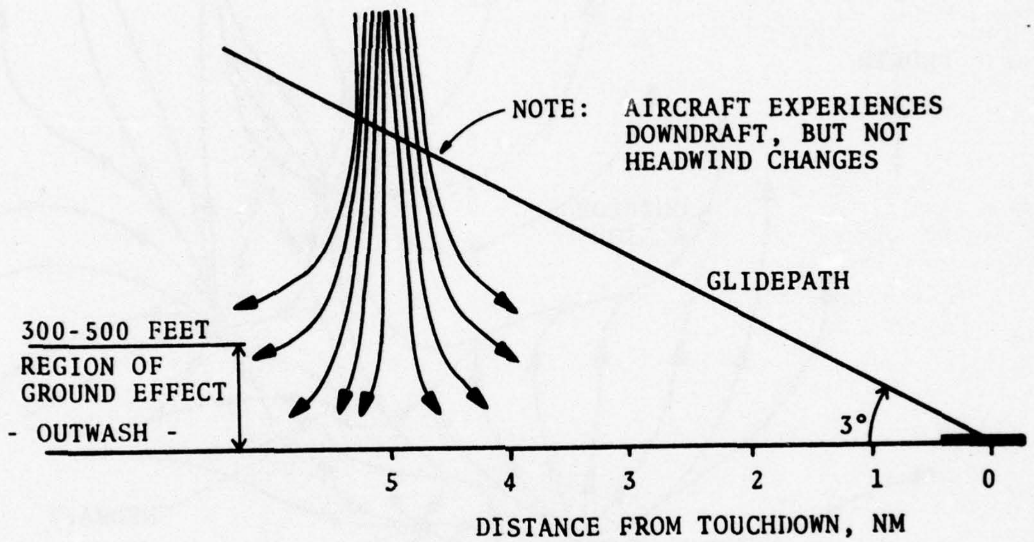

FIGURE 3-2. DOWNBURST CELL SHOWING OUTWASH DUE TO THE PRESENCE OF THE GROUND

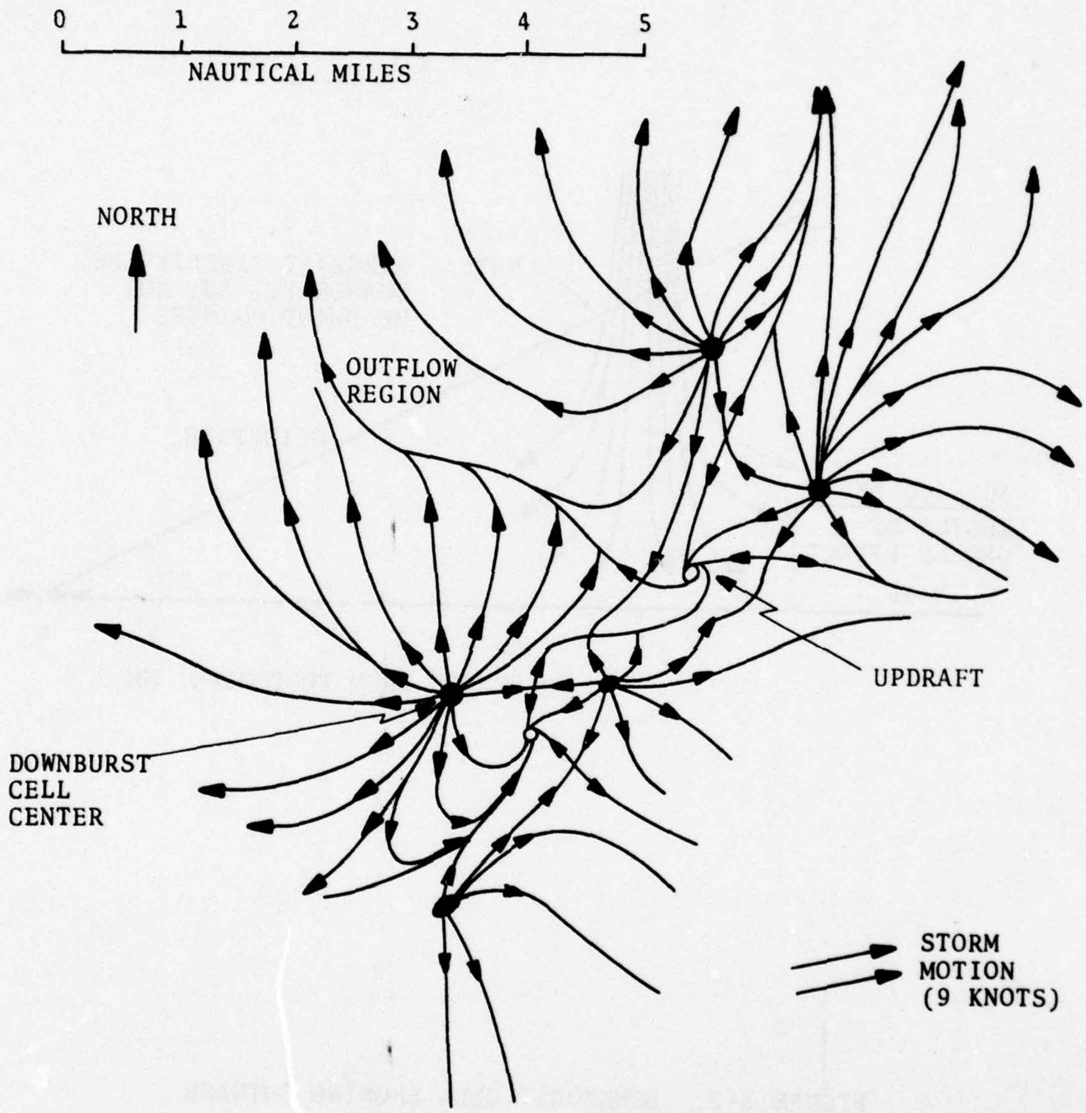

FIGURE 3-3. STREAMLINES ASSOCIATED WITH STAPLETON ACCIDENT, AUGUST 1975 (FROM CARACENA, 1976)

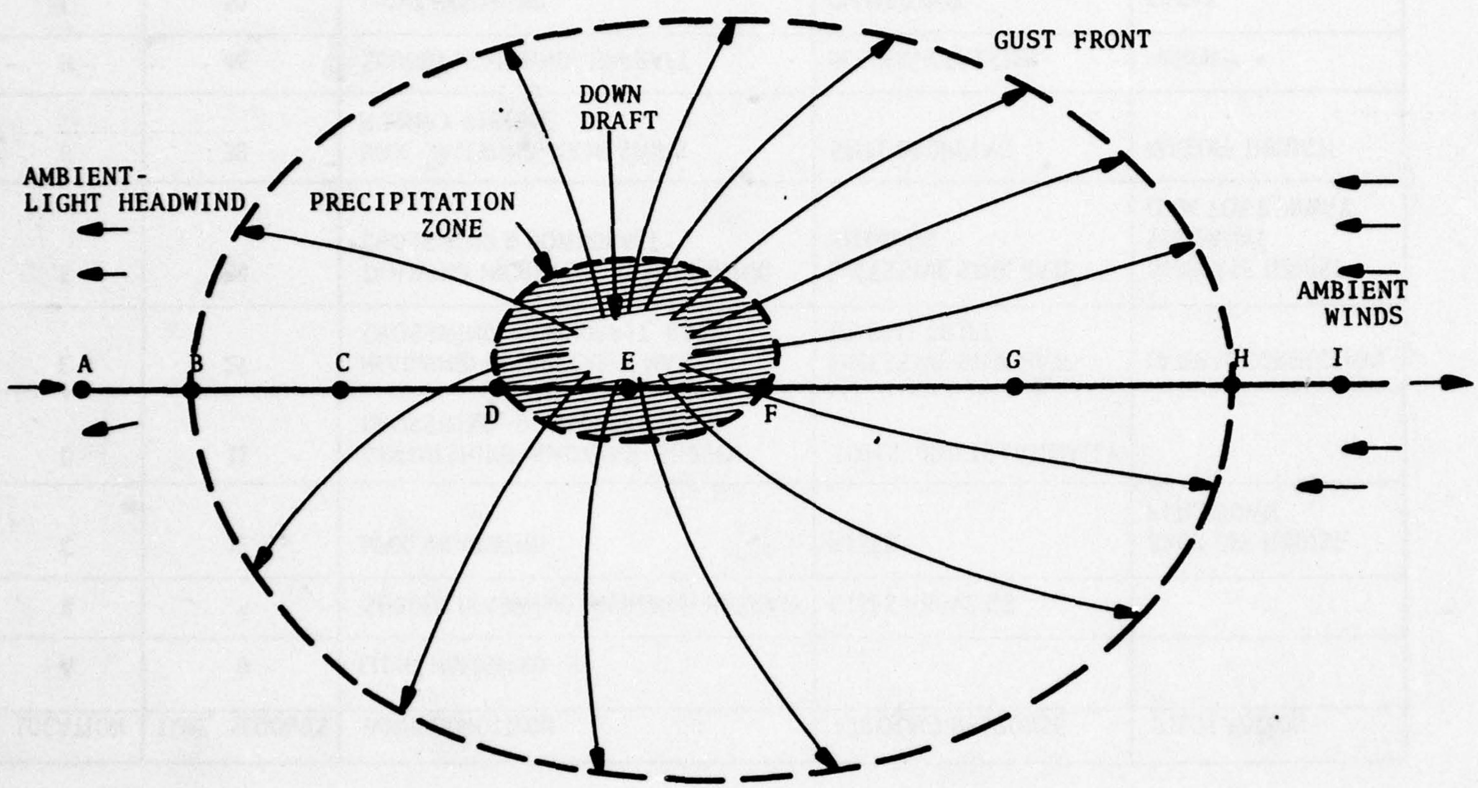

FIGURE 3-4. CLASSIC DOWNBURST ENCOUNTER--STREAMLINES

TABLE 3-2. CLASSIC DOWNBURST ENCOUNTER-EVENTS

LOCATION	TIME, SECONDS	WIND CONDITION	AIRCRAFT RESPONSE	PILOT ACTION
A	0	LIGHT HEADWIND	-	-
B	5	SUDDEN HEADWIND INCREASE; UPDRAFT	RISES ABOVE GS	-
C	12	MAX. HEADWIND	RISES	BACK OFF THRUST; PITCHDOWN
D	18	DIMINISHING HEADWIND; SUDDEN CROSSWIND, DOWNDRAFT, RAIN	SINKS; DRIFTS LATERALLY	-
E	25	HEADWIND DISAPPEARS: MAX. CROSSWIND, DOWNDRAFT, RAIN	EXCESSIVE SINK RATE; LATERAL DRIFT	LATERAL CORRECTION
F	30	TAILWIND INCREASES; DIMINISHING CROSSWIND & DOWNDRAFT	EXCESSIVE SINK RATE - BELOW GS	INCREASE THRUST SOMEWHAT LOOK FOR RUNWAY
G	38	MAX. TAILWIND; RAIN STOPS RUNWAY VISIBLE	STILL DROPPING	TAKEOFF THRUST!
H	46	SUDDEN HEADWIND, UPDRAFT	DESCENT ARRESTED	"WHEW!"
I	50	LIGHT HEADWIND	CLIMBS OUT	SWEAT

at lower altitudes where the downdraft is coupled with a diminishing headwind shear.

The extent of the critical zone does not, by itself, establish the system range. It was asserted earlier that once the extent of the critical zone is established, the system should provide advance warning. Thus the system coverage must be large enough to guarantee that an event does not move into the critical zone before it can be detected, identified, and a warning issued and acknowledged. This is discussed in the next section.

3.2 DATA UPDATE RATE AND COVERAGE

The maximum rate at which the airport wind shear situation is surveyed is limited by the sensor. Regardless of the sensor used, the minimum update rate depends on the coverage, the duration and speed of the phenomenon, the time required to divert an aircraft from landing or departing, and the basic concept of the use of the information. Since there is frequently a cost/performance tradeoff between update rate and other system parameters, the minimum update rate is the important system parameter to be determined.

Minimum coverage and update rate are determined by landing, rather than departure requirements, because the approaching aircraft is slower, and is in a more critical configuration near the ground for a longer period of time. If the meteorological situation did not change during the approach, it would be sufficient to protect the zone shown in Figure 3-1. That is, by assuming that there was no shear event in the critical zone, approaching aircraft would be protected.

This kind of protection would be sufficient for wide-scale synoptic events such as those encountered in inversions and shallow sloped warm fronts. There the basic wind patterns change very slowly with time. Where thunderstorms or cold fronts with steep slopes are involved, however, wind patterns can change significantly in less than a minute. In these situations the information must be updated frequently, and the coverage must be expanded to detect shear events moving toward the corridor.

An examination of gust front speeds (Goff, 1975 and 1976) and storm system motions (Caracena, 1976 and Fujita, 1975) suggests that velocities of 10-15 knots are typical, while velocities of 30 knots have been observed. There were two cases in Goff (1975) of faster gust front motion, but the associated shears were mild. For the purposes of this analysis, 30 knots (15 m/sec) will be used as a working figure for rapidly moving shear events. In the 2-2.5 minutes that an approaching aircraft takes to fly from the outer marker to touchdown, such a wind shear event can move over a nautical mile.

Any real sensor has a time delay associated with it: the effect must be observed for some period of time before it registers; a sampling system has a delay between zero and the update period, when it first appears to the sensor. Thus any point sensor or vertical-looking sensor will not register an alarm until the wind shear event has been present above the sensor for some period of time. If this period of time is excessive, e.g., more than a minute, such a sensor located in the critical zone of Figure 3-5 would not provide adequate protection. Even half a minute would be marginal, since the shear event could move about 1500 feet (450 m); shear events can occur on a scale of 1000-1500 feet (300-450 m) (see section 3.3) and thus could be outside the corridor at one time and inside the corridor half a minute later.

Where sensor coverage encompasses a wider area, the shear event can be detected before it reaches the critical zone. If this area is sampled sufficiently often, the event can be observed several times before it reaches the operating corridor. It is anticipated that a downburst cell will maintain its shape and intensity to a sufficient degree to be tracked; i.e., be unique and consistent enough from sample to sample so that its intensity, speed, and direction can be determined. This would enable an algorithm to be employed which would give advance warning of the time of arrival of the event in the operating corridor.

A hit is defined as one observation of a shear event. Two hits are necessary to establish a velocity, and probably 3 to 4 hits will prove necessary for validation and elimination of false alarms, before an alarm is issued. The additional coverage this implies is shown in Figure 3-5 for 3- and 4-hit criteria, assuming a fast 30 knot front velocity. Also included is the time T required between the time an alarm is issued and the time the pilot is alerted, or a decision made to close the runway.

The establishment of the time duration T is an important parameter which needs to be addressed. Once it is established, the additional coverage required for each approach corridor would be that shown in Figure 3-6. The composite coverage for a typical airport would then resemble Figure 3-7.

3.3 SPATIAL RESOLUTION

Spatial resolution depends on the size of the phenomenon: the thickness of the shear zone, its shape, and its extent. It also depends on the aircraft response scale. Even if shears existed on a 10 foot (3 m) scale, if an aircraft responded on a 100 foot (30 m) scale it would not be affected by them; stated another way, shear effects which are seen by an aircraft at high frequencies compared with the frequency response of the aircraft are not significant.

A typical aircraft will deviate from the flight path in response to frequencies below about one radian per second. Translated to an aircraft traveling 120 knots (62 m/sec), this corresponds to a horizontal scale of about 1300 feet (400 m), and a vertical scale of 70 feet (20 m). This suggests that a horizontal resolution of 1500 feet (450 m) or less would be desirable from the point of view of aircraft response. Similarly, a vertical resolution of 75 feet (23 m) or less would be desirable.

This discussion is included to show that the relative scales are reasonable: disturbances on a smaller scale than 1000 feet (300 m) may cause aircraft control surface motion and buffeting, but do not move the aircraft significantly. Of equal importance

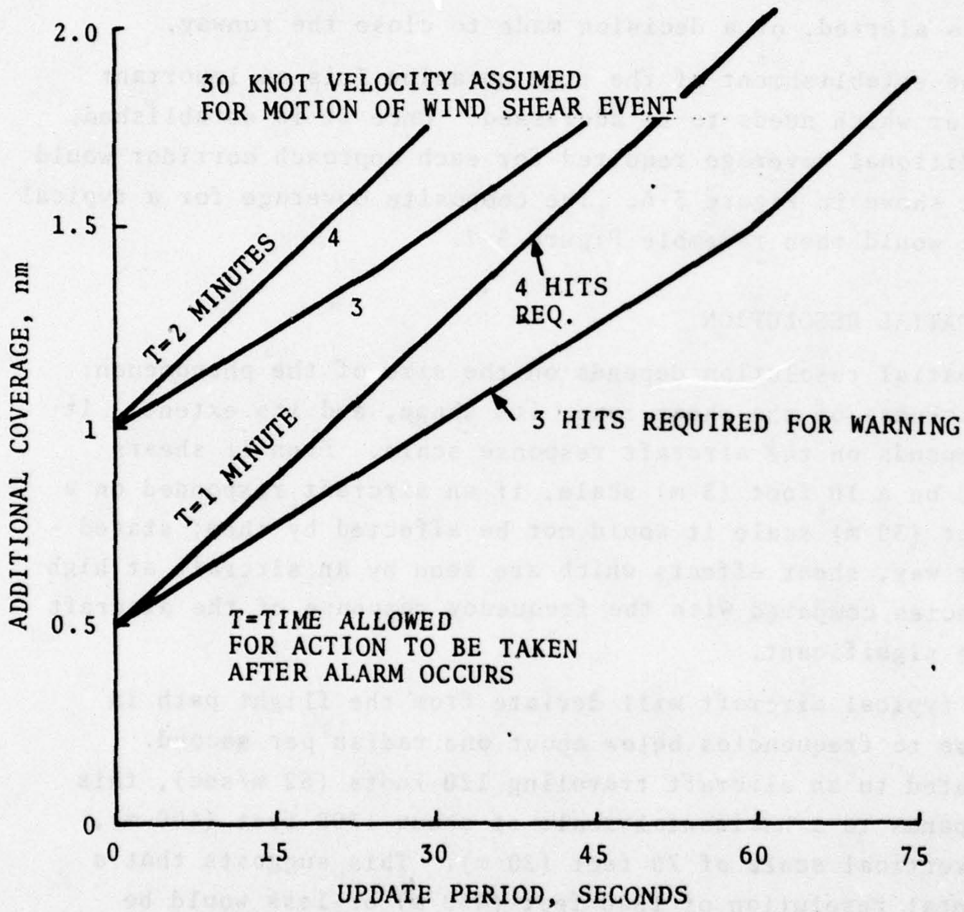

FIGURE 3-5. ADDITIONAL COVERAGE
REQUIRED FOR ADVANCED WARNING
FOR VARIOUS UPDATE RATES

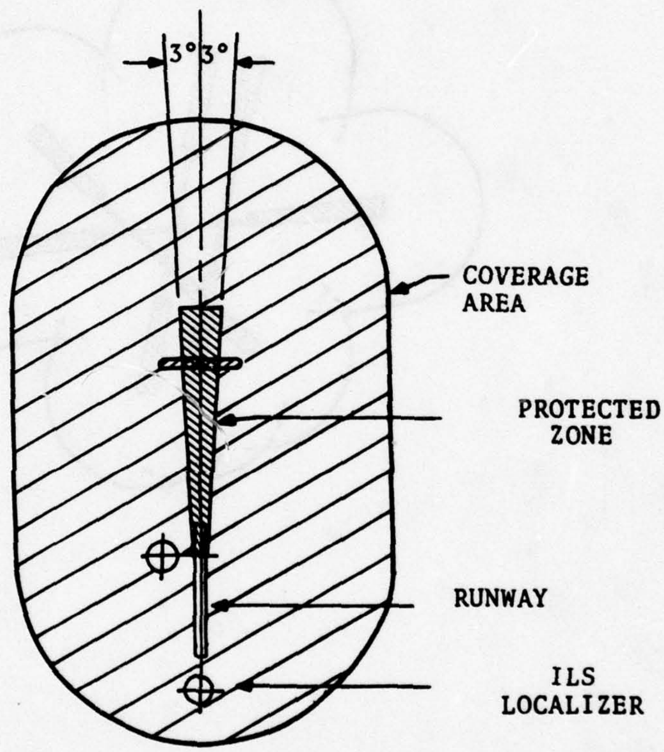

FIGURE 3-6. COVERAGE ZONE FOR AN APPROACH CORRIDOR

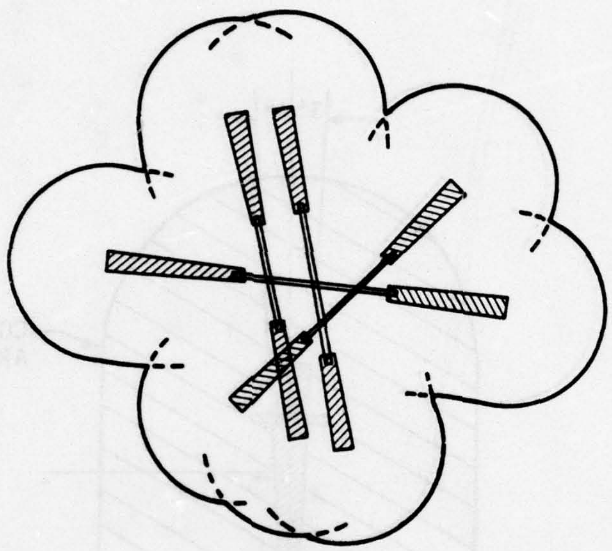

FIGURE 3-7. COVERAGE ZONE FOR A TYPICAL AIRPORT

is the scale on which wind changes take place in shear events. If these changes occur only on scales much larger than 1000 feet, resolution would not need to be so fine-grained.

For large-scale synoptic phenomena, wind gradients are gradual in the horizontal dimension, and are significant only in the vertical dimension. Thus, the shear events are adequately represented by a vertical shear measurement such as would be obtained by a vertical-looking probe.

In the case of the boundary layer shears, a logarithmic profile near the ground yields a good approximation to the observed values. Here the winds change in a regular fashion between, say, 500 feet (150 m) height AGL and the surface. A height resolution of 100 feet (30 m) would be adequate to describe the shear conditions.

However, the profiles found in fronts (NTSB, 1974c and Coons, 1976) often exhibit less regular profiles, ones whose winds change significantly over a 100 foot (30 m) altitude movement, but change less sharply elsewhere. In these cases a 100 foot resolution would not be fine enough to characterize the shear; this is shown in Figure 3-8. On the other hand, a 50 foot (15 m) resolution is quite adequate. Thus for vertical-looking probes, a 50 foot altitude resolution is recommended.

Cold fronts and thunderstorm downwash surges are not as well characterized by vertical shear derived from a vertical profile measurement as by horizontal shear. An aircraft on final approach experiences both vertical and horizontal shears as changes in headwind (actually, in crosswind as well), so there are similarities between the two types. However, with different descent rates aircraft flying through a horizontal shear will experience similar headwind changes.

Cold fronts have "noses" caused by frictional retardation at the ground. The slope near the ground can be quite shallow (slow-moving), quite steep, or even "bent over." The scale is such that the shear could be horizontal or vertical, or something

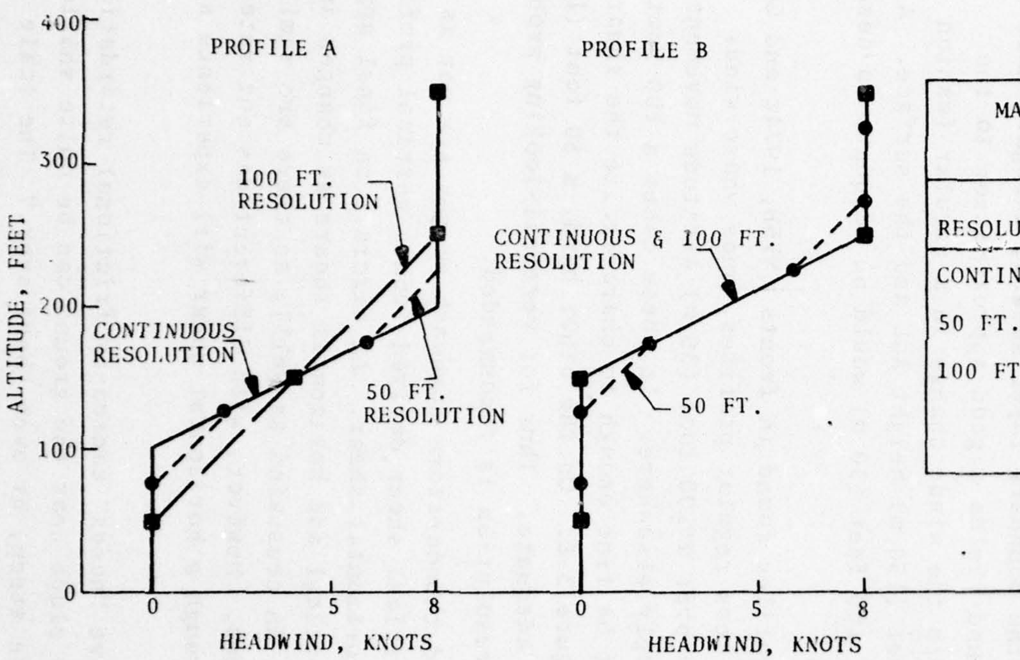

MAXIMUM ESTIMATED SHEAR kphf		
RESOLUTION	PROFILE A	PROFILE B
CONTINUOUS	8	8
50 FT.	8	8
100 FT.	4	8

FIGURE 3-8. EFFECT OF RESOLUTION ON ESTIMATED WIND PROFILE AND SHEAR

in between. Brundidge (1965) reports examples where the wind shift zones vary from 1000 to 5000 feet in extent (300 m to 1500 m).

Gust fronts associated with thunderstorm outflows typically exhibit updrafts and severe shears which an aircraft would experience as an increasing headwind as it travels through them. An example is shown in Figure 3-9, taken from storm data at NSSL (Goff, 1975). The contours in the bottom record represent constant values of the wind component normal to the front. There is a shear zone about a mile long wherein the headwind gradient experienced by an aircraft having a ground speed of 120 knots (62 m/sec) would be about 16 knots (8 m/sec) per 10 seconds of travel, and a total headwind increase of 32 knots (16 m/sec) in about 45 seconds. An interesting aspect of this is that an aircraft will experience an increasing headwind regardless of which way it flies through the gust front. For wind speed contours like this one, even range resolution as large as 4000 feet would satisfactorily characterize the total wind change, since on either side of the gust front fairly uniform winds are encountered. This large a resolution would not adequately estimate the shear for reasons described in Figure 3-8, but 1000-2000 foot (300-600 m) resolution is quite satisfactory.

Intense, concentrated downwash cells are believed to be associated with the Eastern 66 and Continental 426 accidents (Fujita, Caracena). These cells appear to be as little as 2nm (4 km) in diameter, and are accompanied by severe downdrafts. The headwinds encountered by aircraft traversing the cell would resemble those depicted in Figure 3-10. Along paths AA and A'A' cross-track gusts would also be experienced, complicating pilot workload and causing lateral deviations from the extended runway centerline. Downdrafts would be experienced in all paths, being worst in path BB. Headwind changes observed in such cells have ranged from 20 knots (10 m/sec) in 12 seconds (Coons and Mandel, 1976) to 40 knots (20 m/sec) in 5 seconds (NTSB, 1976b); in the first case, the headwinds changed from zero to 25 knots (13 m/sec)

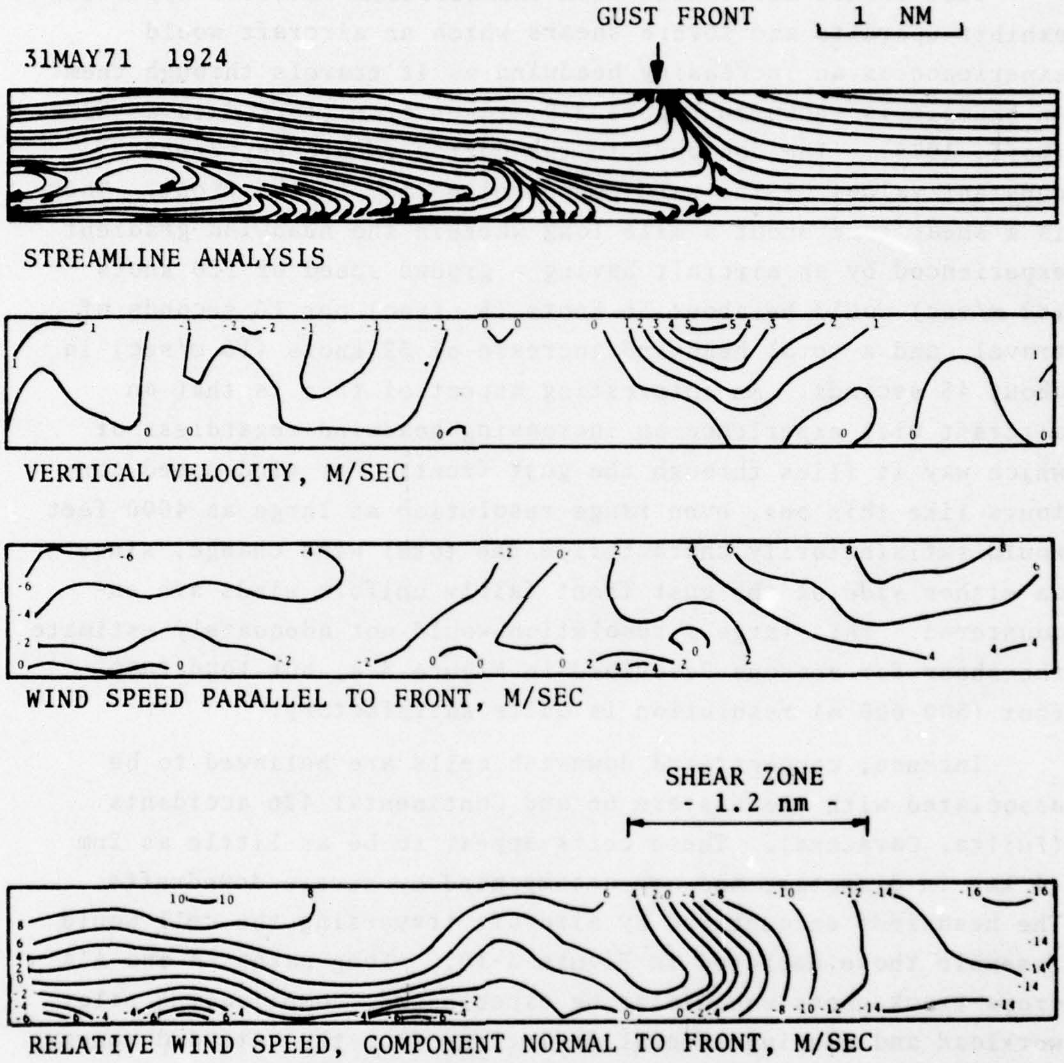

FIGURE 3-9. GUST FRONT WIND PATTERNS
(From Goff, 1975)

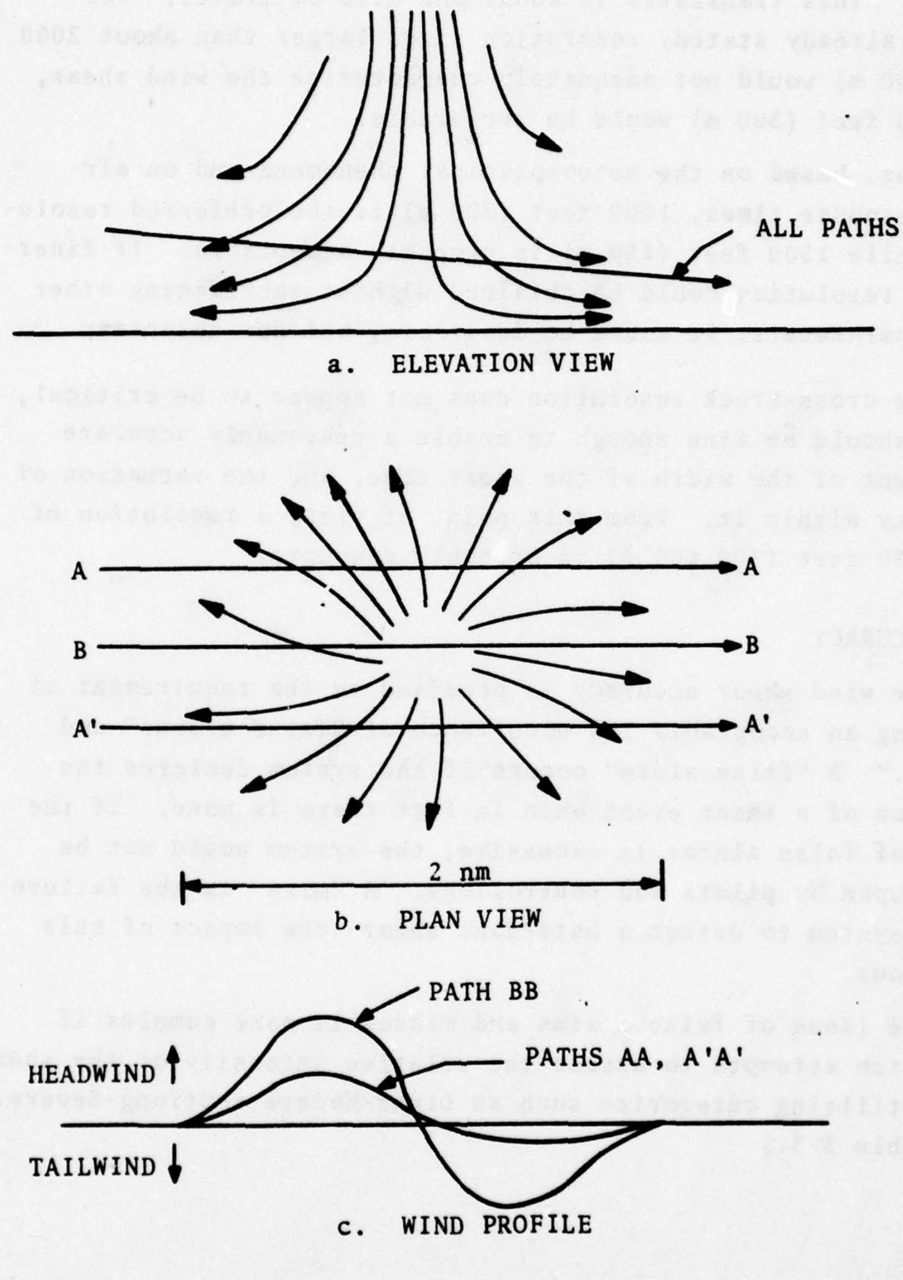

FIGURE 3-10. WINDS ASSOCIATED WITH A THUNDERSTORM DOWNBURST CELL

to zero in 300 feet (90 m) of altitude change, i.e., in about 25 seconds. This translates to about one mile of travel. For reasons already stated, resolution sizes larger than about 2000 feet (600 m) would not adequately characterize the wind shear, and 1000 feet (300 m) would be preferable.

Thus, based on the meteorological phenomena and on aircraft response times, 1000 feet (300 m) is the preferred resolution, while 1500 feet (450 m) is probably acceptable. If finer-grained resolution could be obtained without sacrificing other system parameters, it would be desirable, but not necessary.

The cross-track resolution does not appear to be critical, but it should be fine enough to enable a reasonably accurate assessment of the width of the shear zone, and the variation of intensity within it. From this point of view, a resolution of 1000-2000 feet (300-600 m) is probably adequate.

3.4 ACCURACY

The wind shear accuracy is premised on the requirement of achieving an acceptably low occurrence of "false alarms" and "misses." A "false alarm" occurs if the system declares the existence of a shear event when in fact there is none. If the number of false alarms is excessive, the system would not be relied upon by pilots and controllers. A "miss" is the failure of the system to detect a hazardous shear--the impact of this is obvious.

The issue of false alarms and misses is more complex if the system attempts to assess the relative intensity of the shear, e.g., utilizing categories such as Light-Moderate-Strong-Severe. (See Table 3-3.)

TABLE 3-3. WIND SHEAR DESCRIPTORS, SIMILAR TO ICAO RECOMMENDATIONS (ICAO, 1976)

DESCRIPTION	SHEAR MAGNITUDE
Light	0-4 kphf (0-0.07 m/sec/m)
Moderate	5-8 kphf (0.08 - 0.14 m/sec/m)
Strong	9-12 kphf (0.15 - 0.20 m/sec/m)
Severe	13 or more kphf (>0.22 m/sec/m)

An example of a false alarm here would be the declaration of a strong shear, when in fact the shear is moderate. A miss would be an under-assessment of the intensity, e.g., the declaration of a moderate shear when the shear is actually strong.

For the purpose of establishing the accuracy requirement, a shear/no shear model will be employed. Appendix D develops the probabilities of misses and false alarms as a function of wind shear error, taking into account the fact that severe shears are less probable than light shears. Two system thresholds are chosen for consideration: 4.5 kphf (0.076 m/sec/m) and 7.5 kphf (0.13m/sec/m) (for 4.5 kphf, 0-4 kphf is considered "no shear," and 5 or more is considered a "shear"). The results are plotted in Figure 3-11. It can be seen that if the threshold is set too high, the miss probability increases, while the false alarm probability drops.

The chart should be read in the following way: for example, given a measurement error of σ kphf, the probability that a shear of 5 kphf or more will be mistakenly interpreted as a no-shear condition is given by the miss curve for $\sigma = 4.5$. A different question is the following: Given that a shear is a particular value, e.g., 9 kphf, what is the probability of this being mistakenly interpreted as a no-shear condition? This is given in Figure 3-13. From this it can be seen that most of the misses of Figure 3-12 occur for shears just above threshold.

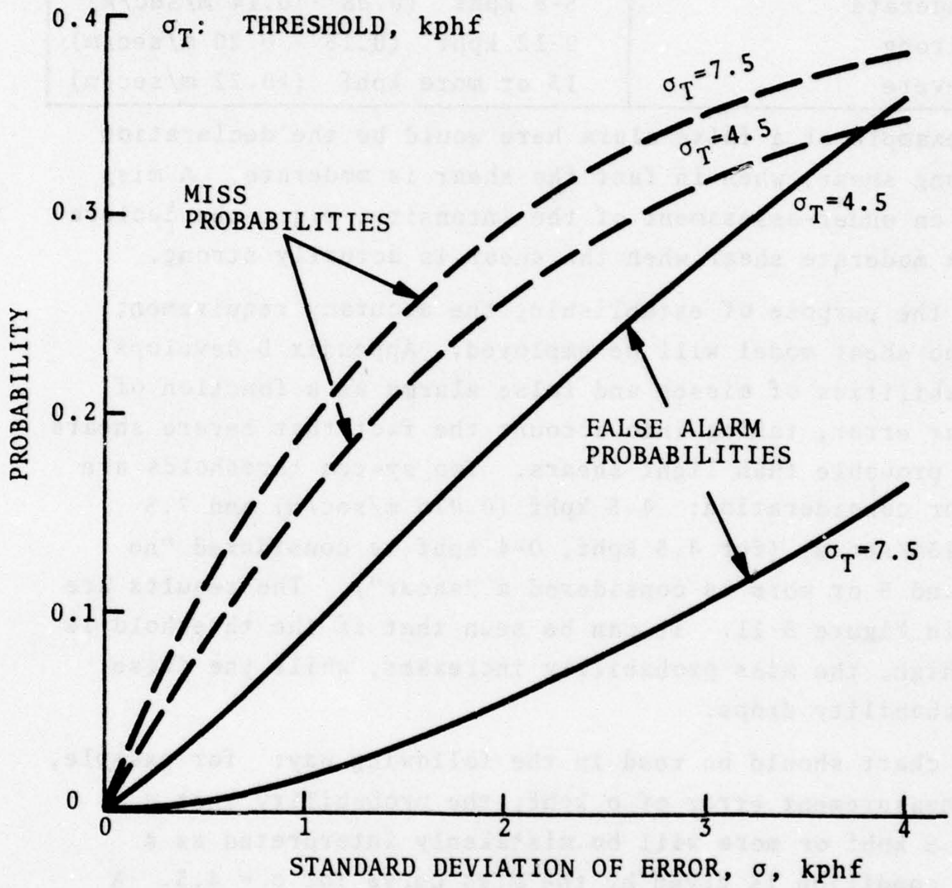

FIGURE 3-11. VARIATION OF MISS AND FALSE ALARM PROBABILITIES WITH SYSTEM THRESHOLD

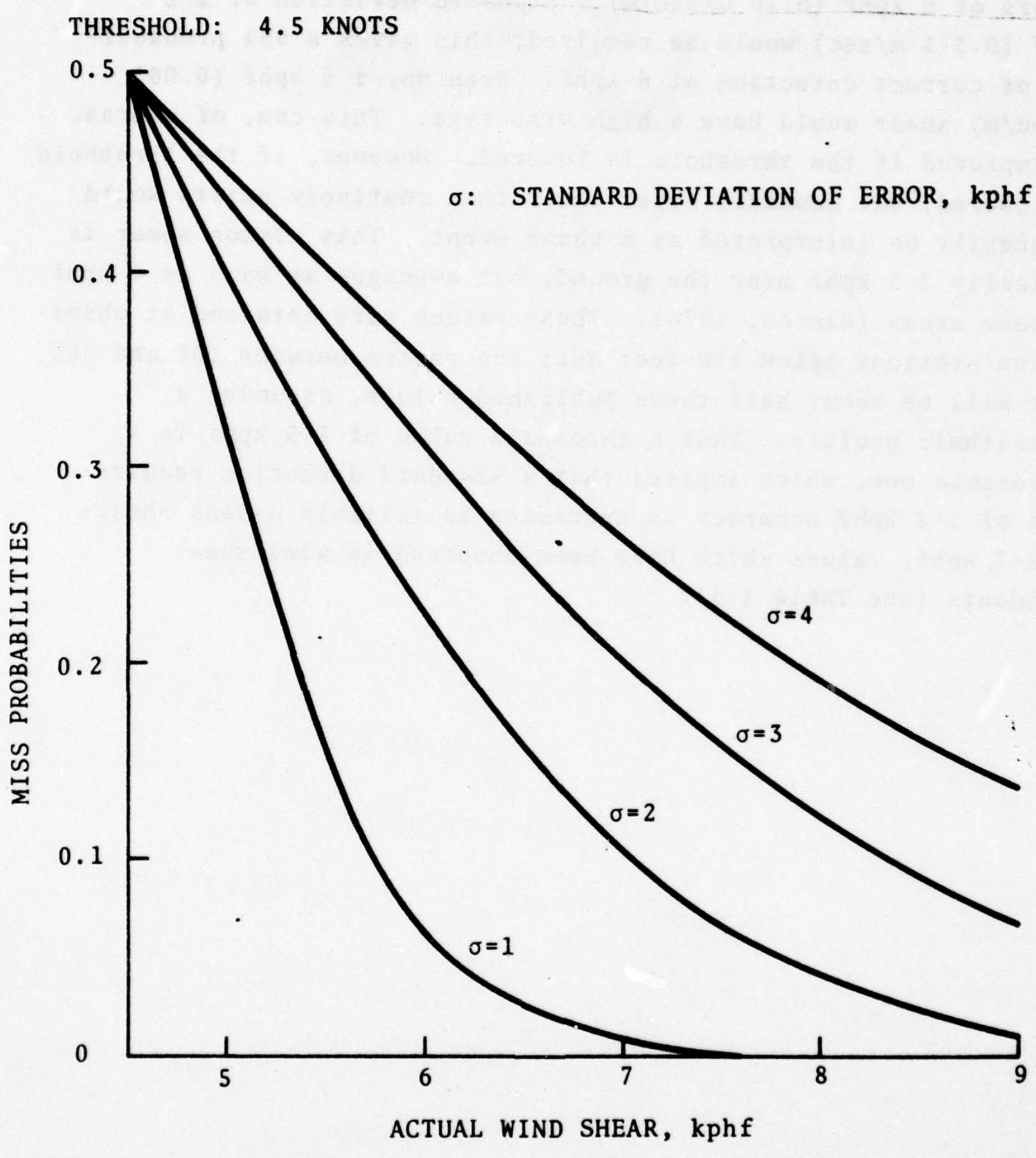

FIGURE 3-12. PROBABILITY OF MISTAKING A SHEAR EVENT FOR A NO-SHEAR EVENT FOR VARIOUS SYSTEM ERRORS

From these figures it is evident that to reliably identify shears of 6 kphf (0.10 m/sec/m) a standard deviation of 1-2 kphf (0.5-1 m/sec) would be required; this gives a 95% probability of correct detection at 6 kphf. Even so, a 5 kphf (0.083 m/sec/m) shear would have a high miss rate. This can, of course, be improved if the threshold is lowered. However, if the threshold is lowered, the boundary layer shear that routinely exists would frequently be interpreted as a shear event. This common shear is typically 2-3 kphf near the ground, but averages as much as 4 kphf in some areas (Nancoo, 1974). These values were obtained at observation stations below 150 feet AGL; the shears between 100 and 300 feet will be about half these published values, assuming a logarithmic profile. Thus a threshold value of 3-5 kphf is a reasonable one, which implies that a standard deviation requirement of 1-2 kphf accuracy is necessary to reliably assess shears of 5-7 kphf, values which have been observed in wind shear accidents (see Table 3-4).

TABLE 3-4. ESTIMATED SHEARS FOR SEVERAL ACCIDENTS OR NEAR-ACCIDENTS

FLIGHT	LOCATION	APPROACH SPEED, KNOTS	MAXIMUM VERTICAL SHEAR, KPHF	MAXIMUM HEADWIND GRADIENTS, KNOTS/SEC	TOTAL HEADWIND CHANGE, KNOTS/SEC
EA66	JFK NY	140	-14*	-2.8	-18/8
EA902	JFK NY	140	-12*	-2.0	-14/8
CO426	DEN CO	160**	N.A.	-8.8	-40/5
IA933	BOS MA	150	+7	+1.4*	+21/20
DL516	CHA TN	130	5*	-1.0	-15/15

* Equivalent - see text

** Maximum takeoff speed

The preceding discussion has used kphf, a measure of vertical shear, for convenience; however, the reasoning applies as well to horizontal shear. The equivalent numerical value for a horizontal shear event is found by considering the time rate of headwind change experienced by an aircraft flying through vertical shear zone along the glidepath: a significant vertical shear of 4.5 kphf would be experienced as a headwind change of 2.4 knots (1.2 m/sec) in 1000 feet (300m) of travel along a 3^{o} glide slope. An aircraft traveling at 160 knots (82 m/sec) would experience a headwind change of 0.65 knot (0.33 m/sec) per second: at 120 knots (62 m/sec), the headwind change would be 0.5 knot (0.25 m/sec) per second. Thus 0.5 knot per second or more is considered a significant headwind gradient, and 2.5 knots (1.3 m/sec) per 1000 feet (300 m) is considered a significant horizontal shear.

The severity of the shear event is not only related to the shear intensity, but also to the duration of the event and the total change in wind speed. Typical profiles, somewhat oversimplified, are shown in Figure 3-13; the first two profiles are the kind that would be encountered by an aircraft flying down through a warm front, or a thunderstorm initial gust front. Downburst cell profiles would be more like that of Figure 3-13c.

The total wind change is important because the time required for the stabilization of an aircraft in the new air mass field depends on it. Accuracy for the measure of total wind change is less critical than it is for the measurement of shear intensity.

In fact it is evident that for profiles a and b of Figure 3-13 there exist some equivalences between shear intensities and total changes, at least for a given aircraft: for example, a shear of 8 kphf (0.13 m/sec/m) with a total wind change of 20 knots (10 m/sec) might have a similar effect on an aircraft as a shear of 12 kphf (0.20 m/sec/m) with a total wind change of 10 knots (5 m/sec). More work needs to be done in this area because it may relax the accuracy requirements and improve the effectiveness

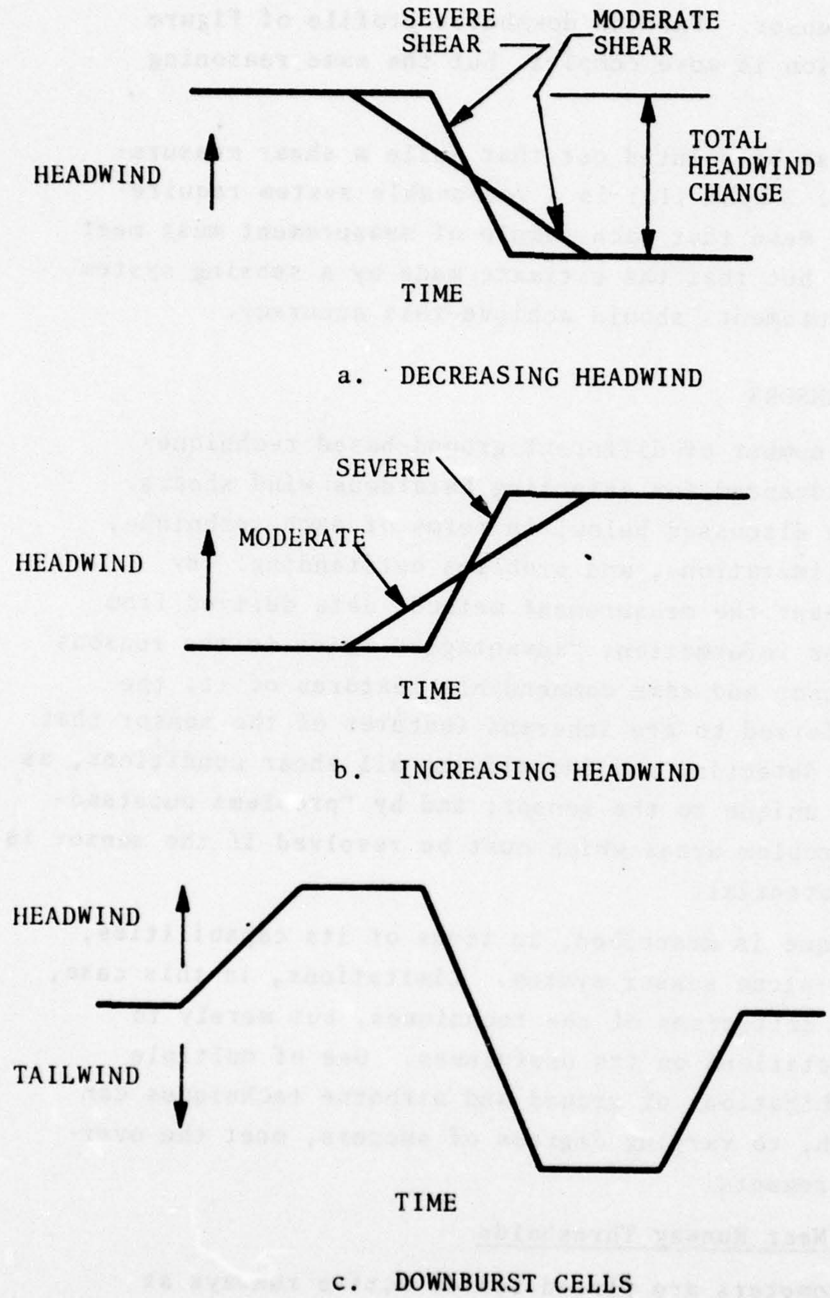

FIGURE 3-13. HEADWIND PROFILES ENCOUNTERED BY A MOVING AIRCRAFT FOR VARIOUS SHEAR CONDITIONS

of a particular sensor. For the downburst profile of Figure 3-13c, the situation is more complex, but the same reasoning applies.

It should also be pointed out that while a shear measurement accuracy of 1-2 kphf (1σ) is a reasonable system requirement, it does not mean that each sample of measurement must meet this requirement, but that the estimate made by a sensing system based on the measurements should achieve this accuracy.

3.5 CANDIDATE SENSORS

There are a number of different ground-based techniques which have been advanced for detecting hazardous wind shears. Some of these are discussed below, in terms of each technique, its advantages, limitations, and problems outstanding. By "technique" is meant the measurement method, data derived from it, and use of the information; "advantages" refer to the reasons for using the sensor and some commendable features of it; the "limitations" referred to are inherent features of the sensor that preclude it from detecting and identifying *all shear conditions*, as well as problems unique to the sensor; and by "problems outstanding" are meant problem areas which must be resolved if the sensor is to achieve its potential.

Each technique is described, in terms of its capabilities, etc., as a stand-alone sensor system. Limitations, in this case, are not meant as criticisms of the techniques, but merely to delimit the expectations on its usefulness. Use of multiple sensors, and combinations of ground and airborne techniques can be employed which, to varying degrees of success, meet the overall system requirements.

a. <u>Anemometers Near Runway Thresholds</u>

Technique: Anemometers are placed beside active runways at each end. Readings are relayed via radio link or ground lines to the tower. Pilots are alerted as to ground wind speed and direction at the appropriate runway, either by the controller or the ATIS broadcast. Departing aircraft would be advised if the vector difference between wind velocities at opposite ends of the runway exceeded some threshold like 15 knots.

Advantages: Inexpensive and utilizes familiar and relatively simple equipment.

Limitations: Does not detect shear events beyond airport boundaries; does not provide advance warning of shear events moving into the corrdor; does not detect synoptic shears above the airport.

Problems Outstanding: Establish whether tradeoff between false alarms caused by gusts and time lag associated with smoothing is feasible.

b. <u>Anemometers Beyond the Middle Markers</u>

Technique: Anemometers are placed approximately 2 miles from threshold. Readings are telemetered or relayed via telephone lines to central facility, along with airport centerfield anemometer reading. A pilot is notified by the local controller if the vector difference between the distant sensor and the centerfield sensor exceeds some threshold, such as 15 knots.

Advantages: Low/moderate cost and maintenance; uses familiar and relatively simple equipment. Detects outflow associated with gust fronts or downburst cells. Detects passage of fronts having sharply defined wind shift boundaries.

Limitations: Does not provide advance warning of shear events moving into the corridor; does not provide location of aircraft encounter with frontal boundary (slope information is not obtained); does not detect synoptic shear above airport environs.

Problems Outstanding: Establish whether tradeoff between false alarms caused by gusts and time lag associated with smoothing is feasible; establish a threshold which results in an acceptable miss/false alarm tradeoff; establish whether density of anemometers is sufficient to prevent misses of small wind shear events.

c. Array of Anemometers Around Airport

Technique: Anemometers are placed as in a and b above, and additional anemometers are placed farther out and in other sectors. Readings are relayed by telephone line or microwave link to central facility. A pilot is notified if wind patterns indicate a shear event moving into an active approach/departure corridor. Pilots are alerted as to ground wind speed and direction at runway threshold. Departing aircraft would be advised if anemometer readings at opposing ends of the runway indicated significantly different winds, or if a shear event were located at or moving into the departure corridor.

Advantages: Moderate cost and maintenance; uses familiar and relatively simple sensor equipment. Detects outflow associated with gust fronts or downburst cells. Detects passage of frontal boundaries. Provides advance warning.

Limitations: Complex network of sensors may prove costly to maintain; real estate and availability of vandalproof structures may prove difficult to acquire. Does not provide location of aircraft encounter with frontal boundary; does not detect synoptic shears above airport environs.

Problems Outstanding: Establish whether resulting wind patterns provide signatures that can be identified by a central processor; establish a threshold and averaging time which results in an acceptable miss/false alarm tradeoff.

d. Array of Pressure Jump Sensors

Technique: Pressure jump sensors are placed in a grid surrounding the airport. Readings are relayed by telephone line to central facility. Pressure jumps indicate onset of thunderstorm gust front, and time sequences of jumps are analyzed to estimate time of arrival of gust front at operating corridors. A pilot is alerted if a shear event is located in, or is moving into active corridor.

Advantages: Advance warning provided for thunderstorm gust fronts. Low/moderate cost, using relatively simple sensors; can be mounted on telephone poles.

Limitations: Does not provide an all-clear indication when shear event has passed. Does not measure winds directly. Does not detect frontal passage or any synoptic shear events.

Problems Outstanding: Establish that pressure jumps are associated with most hazardous wind shears; establish that false alarms (e.g., caused by gravity waves) are sufficiently infrequent or are recognizable; establish means of estimating shear intensity.

e. Acoustic Sodar

Technique: The acoustic sodar is installed beside a shelter on the airport surface. The sodar points upward, and measures the two horizontal wind components at heights from 100-1500 feet (30-450m). Vertical wind shears, winds aloft, and surface winds are measured and made available to controllers and pilots.

Advantages: Detects synoptic shears and locates altitudes of aircraft encounters with vertical shear events. Detects passage of fronts having sharply defined wind shift zones. Moderately high costs.

Limitations: Susceptible to noise from aircraft, rain patter. Requires expensive bunker installations to obtain data above 500 feet (150 m). Does not detect gust fronts or downburst cells; does not detect cold fronts before they arrive at airport.

Problems Outstanding: Establish operational feasibility in noisy airport environment, in rain, and in conditions which exist when nocturnal boundary layer shears are present. Assess reliability and maintenance costs.

f. FM/CW Microwave Radar

Technique: The radar is installed beside a shelter on the airport surface. The radar points upward,* and measures the three wind components at heights from 50-10,000 feet (15 m - 1 km). Vertical wind shears, winds aloft, and surface winds are measured and made available to controllers and pilots.

Advantages: Detects synoptic shears and locates altitudes of aircraft encounters with vertical shear events. Detects passage of fronts having sharply defined wind shift zones.

Limitations: Moderately high cost, complexity, antennas are bulky, require some ground installation. Does not detect gust fronts or downburst cells; does not detect cold fronts before they arrive at airport.

---

*Actually the radar is pointed about 30° from the zenith. Clutter prevents the antenna from pointing up the glide slope; thus its use is limited to synoptic measurements.

Problems Outstanding: Establish whether returns are obtained in nocturnal boundary layer atmospheric conditions, i.e., establish all-weather potential. Assess reliability and maintenance costs.

g. CW Laser Radar

Technique: The laser is placed in a shelter on the airport surface. The laser beam points upward, and measures the three wind components at heights from 50-1000 feet (15 m - 300 m) above the surface. Vertical wind shears, winds aloft, and surface winds are measured and made available to controllers and pilots.

Advantages: All-weather operation. Detects all synoptic shears and locates altitudes of aircraft encounter with vertical shear events. Detects passage of fronts having sharply defined wind shift zones. Compact scanning and sensor equipment.

Limitations: Does not detect gust fronts or downburst cells; does not detect cold fronts before they arrive at airport. Moderately high cost, complexity.

Problems Outstanding: Establish turn-key operational capability, eliminating need for frequent cryogenic and laser gas refills. Assess reliability and maintenance costs.

h. Pulsed Doppler Microwave Radar

Technique: A highly sensitive Doppler radar is installed on the airport surface, and scanned near the horizon. Returns from precipitation or index-of-refraction variations in the atmosphere permit a line-of-sight wind profile to be obtained. Horizontal shears along the radials are detected, and wind shear events can be tracked. Controllers and pilots are alerted if windshear events are located in or are approaching active runway corridors.

Advantages: System range in precipitation is more than adequate; update rate is likewise more than adequate. The shear component measured corresponds essentially to headwind gradients encountered by the aircraft. Provides advance warning for thunderstorm gust fronts and downburst cells. Air traffic control equipment and maintenance personnel shelters can be shared.

Limitations: Utilizes large (10-15 feet, or 3-5 meters) antennas requiring tower installation; moderately high cost, moderate complexity. Vertical beam size (somewhat greater than one degree) results in a limitation on pointing near horizon (caused by clutter) and results in masking of shears associated with winds having significant vertical gradients. Does not directly measure downdrafts.

Problems Outstanding: Establish capability of obtaining clear air returns in thunderstorm gust front and downburst cells where precipitation is nonexistent. Establish reasonable cost/size/ performance tradeoffs to assess ultimate costs. Establish signature recognition capability and false alarm (e.g., due to gusts) rejection capability.

i. Pulsed Doppler Laser Radar

Technique: A narrow-beam laser radar is placed in a shelter on the airport surface or on top of a building, and scanned close to the horizon. Returns from particulate aerosols, fog, and rain permit a line-of-sight wind profile to be obtained. Horizontal shears along the radials are detected, and wind shear events are tracked. Controllers and pilots are alerted if wind shear events are located in or are approaching active runway corridors.

Advantages: Provides advance warning for thunderstorm gust fronts and downburst cells. The shear component measured corresponds essentially to headwind gradients encountered by aircraft. Compact equipment can be placed in a variety of locations without installation costs associated with heavy equipment. Beam can be raised in elevation to provide synoptic shear measurements. Beam is extremely narrow, and can be pointed very close to horizon without clutter problems or masking of non-horizontal shears.

Limitations: Range is limited in heavy rain, fog, and snow. Does not directly measure downdrafts. Does not measure winds at or above the sensor. Moderately high cost, complexity.

Problems Outstanding: Establish signature recognition capability and false alarm (e.g., due to gusts) rejection capability; establish system range capability in thunderstorm environment. Establish turn-key operational capability; eliminate need for frequent cryogenic and laser gas refills. Assess reliability and maintenance costs.

Clearly, many of the limitations listed above are inherent: i.e., the sensors are proposed to solve only one problem. Thus used in combinations, they cover the gamut of wind shear events. For example, at Dulles Airport (Langweil, 1976) a combination of acoustic sodar, a small pulsed doppler radar, and an array of pressure jump sensors are utilized to provide advance warning of gust fronts, and to measure synoptic conditions.

The combination of a CW laser and a pulsed laser complement each other. The pulsed laser does not measure winds above the airport; although the elevation angle can be raised to, say, 6 degrees, and synoptic shears can be detected under most conditions, under conditions of heavy fog or rain the penetration would be inadequate. Raising the elevation angle higher results in a loss of altitude resolution. Thus a vertical-looking CW laser radar, which operates in all weather conditions, would measure the vertical wind shears in fog conditions which frequently accompany warm fronts, where a pulsed laser could not. The fortuitous feature of the laser approach is that most of the equipment which comprises the system are common: scanner, telescope, optics, detector, signal processor, and data processor. The CW laser can also function as a master oscillator for the pulsed system. The result is that the capital equipment needed to achieve pulsed operation over and above that required for CW operation costs is on the order of 20 percent or less of the CW system cost. Furthermore, it is possible to switch quickly between CW and pulsed modes of operation, thus achieving a hybrid CW/pulsed operation with no loss of performance except the time lost by the time-sharing scheme.

The sections which follow are addressed to the particular features, problems, and characteristics of laser radar systems. The system requirements developed up to this point apply to any ground sensor, but the remaining sections develop the particular laser design constraints these requirements entail.

4. SENSORS AND PROPAGATION CHARACTERISTICS

4.1 BASIC FEATURES OF THE MEASUREMENT

The fundamental property of the atmosphere that is exploited by a laser radar, or lidar, is the presence of particles which are large in comparison with the air molecules, and move essentially with the air mass. The particles, which are plentiful except in rare dry, clean conditions, are dust particles, moisture droplets, fog droplets, raindrops, or particulate pollution, frequently all grouped under the name "aerosol." The laser transmitter directs a beam toward a narrow volume of air; some radiation is scattered and some absorbed by each aerosol in the beam path, and thus never reaches the backscattering volume; this causes an attenuation of the beam. Some of the radiation reaching the backscattering volume is scattered back toward the laser (backscatter) by aerosols in the volume, and is again attenuated by aerosols in the return path (see Figure 4-1). The signal received is detected by heterodyning with a local oscillator whose frequency is tightly controlled. The Doppler shift principle dictates that the frequency of the backscattered signal differs from that of the transmitted signal by an amount proportional to the velocity component, parallel to the beam, of the particles in the volume. Thus the measurement of this frequency difference is a measure of the velocity of the air mass of the volume in the direction of the beam.

It is informative to consider the effect of aerosol densities on the received signal (see Figure 4-2). Suppose the volume of interest is fixed at some distance from the laser, and the density of particles, of a given size distribution, increases from zero: at very low density, attenuation is negligible, but backscatter is very small, resulting in a small signal; as the density increases, the attenuation remains small, backscatter is high, resulting in a large signal; eventually a point is reached where attenuation reduces the signal at the same rate that backscatter increases it, and the signal is maximized; beyond that, attenuation reduces the signal much faster than backscatter increases

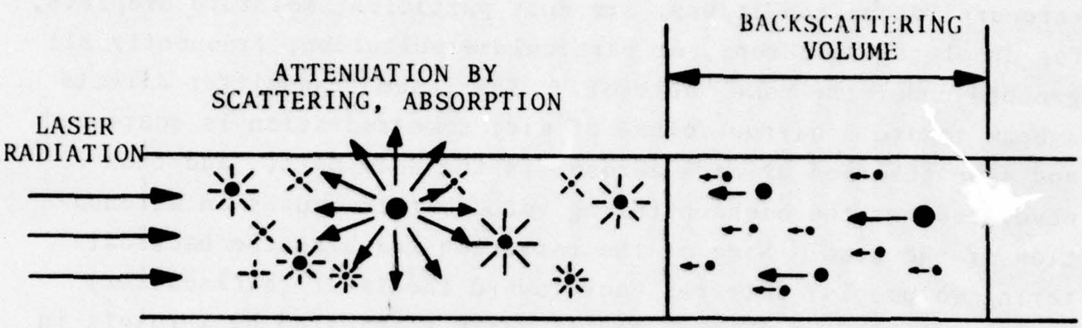

FIGURE 4-1. ATTENUATION AND BACKSCATTERING OF A LASER BEAM

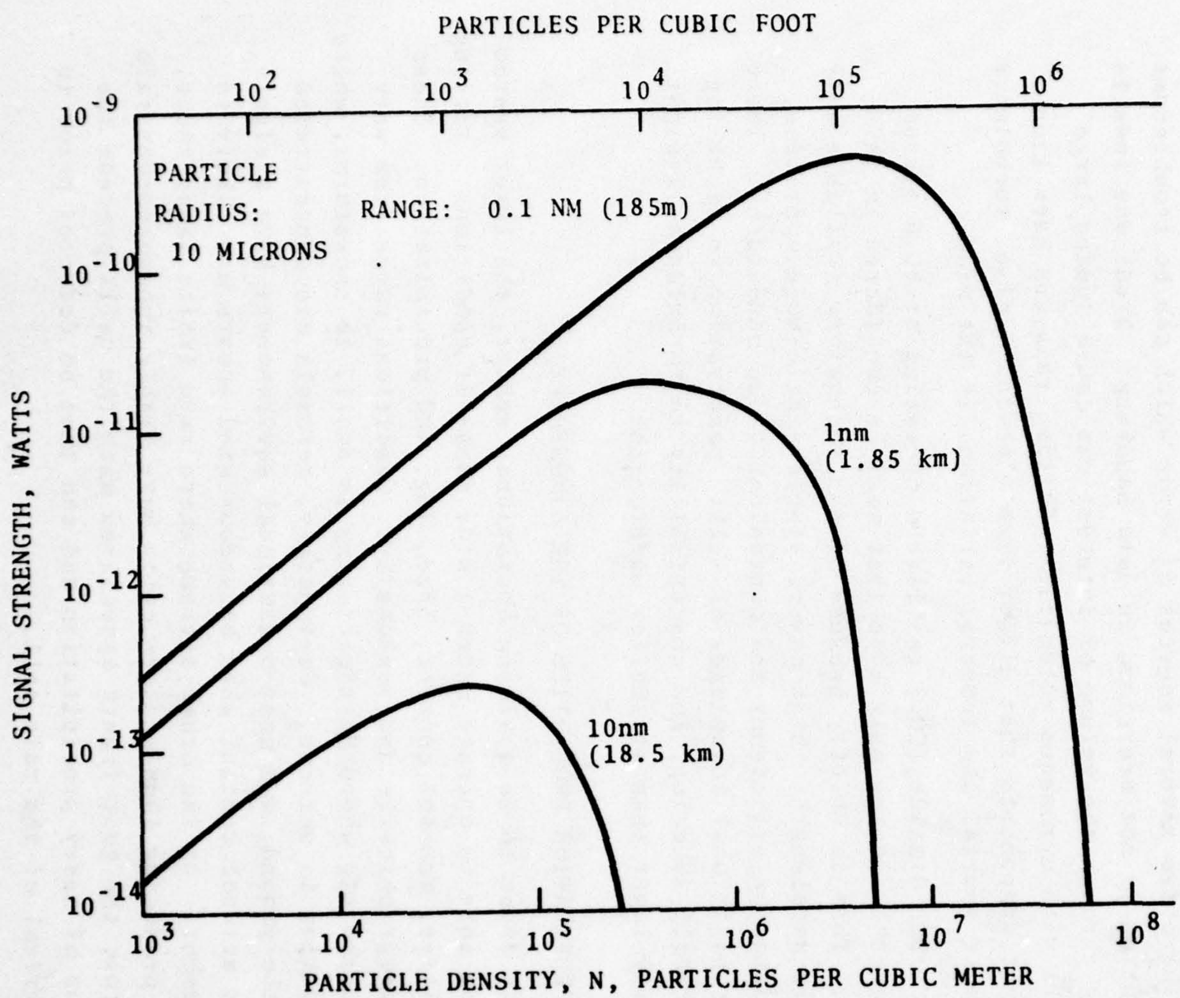

FIGURE 4-2. SIGNAL VARIATIONS AS A FUNCTION OF PARTICLE DENSITY

it, resulting in a rapidly decreasing signal. Some fogs and heavy rain can cause loss of signal at 2-3 nautical miles range (4-6 kilometers) with present day lasers.

There are several sources of error which can be troublesome if caution is not exercised in data handling: birds and insects flying through the volume of interest can cause sudden large signals with erroneous velocities; falling rain can have line-of-sight components that differ from the winds; also, turbulence can cause spatial and temporal variations in the wind.

Carbon dioxide (CO_2) gas lasers operating at 10.6 micron wavelengths are the only type that will be considered in this study. This is chiefly because of the technology available only at this wavelength: high power, stable single-mode operation, high detector efficiency and convenient video bandwidths. There are propagational advantages as well: penetration in light fog is markedly superior, and susceptibility to turbulence is significantly lower than at smaller wavelengths.

4.2 PROPAGATION PROPERTIES OF THE ATMOSPHERE

In order to be a viable operational sensor, the laser system must be able to operate under a wide range of conditions: varying humidities, aerosol content, haze, fog, and precipitation. These vary geographically and seasonally. Conditions range from very dry, clean air where backscattering is small, to snowstorms, where attenuation is extreme. Fortunately, aerosols are concentrated near the ground, and most operational environments have a significant aerosol content when hazardous wind shears are likely to be present. At the other extreme where rain limits laser range, shear-producing thunderstorm cells have highly inhomogeneous rain patterns; the gust fronts associated with the cells precede the regions of heavy precipitation and can thus be detected prior to the arrival of the rain cell.

There are several physical mechanisms which affect the amplitude of the received signal: (1) attenuation, by aerosol scattering and absorption; (2) backscatter by the aerosol assemblage; (3) fluctuations of the backscattered signal; (4) fluctuations of the attenuation by scattering; (5) scintillation, i.e., amplitude fluctuations caused by index-of-refraction and aerosol inhomogeneities in the beam path; and (7) beam spread, caused by scattering.

Of the 7 factors, only (1)-(3) and (6) are believed to be significant in the present application. Fluctuations of the attenuation are small. Scintillation is likewise small, even with considerable turbulence. Angle-of-arrival variations are not significant, because reciprocity requires the transmitted and received paths to be the same. Phase front distortion, however, can be significant in heavy turbulence, since it reduces the effective receiving aperture. Beam spread by scattering occurs under high attenuations, where range is primarily limited by the attenuation; the beam spread signal loss is small compared with the attenuation loss.

4.2.1 Attenuation

Each particle between the transmitter and the volume of interest scatters some energy into a 4π steradians of solid angle; in addition some energy is absorbed by the particle and converted to heat. Particles smaller than a wavelength scatter relatively weakly (Rayleigh scattering) while particles larger than a wavelength scatter an amount approximately proportional to the cross-sectional area (Mie scattering). Thus for a given beam volume the attenuation depends on the particle size distribution, the number of particles, the wavelength, and the particle indices of refraction.

In clear air molecular absorption, rather than aerosol absorption or scattering, appears to be the limiting factor. The values for attenuation published by McClatchey, et al. (1972) indicate that the attenuation by molecular absorption ranges from

0.63 dB/nm (0.34 dB/km) in winter to 2.9 dB/nm (1.6 dB/km) in summer. Clear air aerosols would only give about 0.07 dB/nm (0.04 dB.km), while haze by itself would cause about 0.4 dB/nm (0.2 dB/km).

In light developing fogs and mist, the attenuation is small, typically 2-3 dB/nm (1-1.6 dB/km); under these conditions the wavelength of 10.6 microns has significantly greater penetrating capability than optical wavelengths. The primary reason for this is that the particles are primarily of a size which results in weak (Rayleigh) scattering at infrared and strong (Mie) scattering at optical frequencies. In denser fogs, the average drop size also increases, and attenuation can reach extreme values of up to 75 dB/nm (40 dB/km). For a given water density the attenuation at 10.6 micron wavelength is relatively insensitive to drop size distribution (but highly sensitive at optical wavelengths); it can be approximated by:

$$\alpha = 0.5\ \rho\ \text{dB/km}$$

where ρ is the water density in milligrams per cubic meter. If ρ is given in pounds per cubic foot, α is approximately:

$$\alpha = 6\times10^{-8}\rho\ \text{dB/nm}\ .$$

A typical light fog has a water density of 5 mg/m^3 (3×10^{-7} lb/ft^3) while a typical dense fog may reach 100 mg/m^3 (6×10^{-6} lb/ft^3).

In rain, only Mie scattering occurs; the attenuation varies inversely with the drop diameter for a given water density. Drop sizes typically range between 0.2 mm (0.008 in) and 6 mm (0.2 in) in diameter. Rainfalls observed in nature have a wide spread of drop sizes for any rainfall rate, but they can be characterized by the following behavior: the most prevalent drop size increases with rain rate. This is shown in Figure 4-3, which is taken from Kerr (1951), based on measurements by Laws and Parsons (1943). Using this model, Chu and Hogg (1968) calculated the attenuation as a function of rainfall rate; this is shown in Figure 4-4. It is evident that heavy rainfall rates

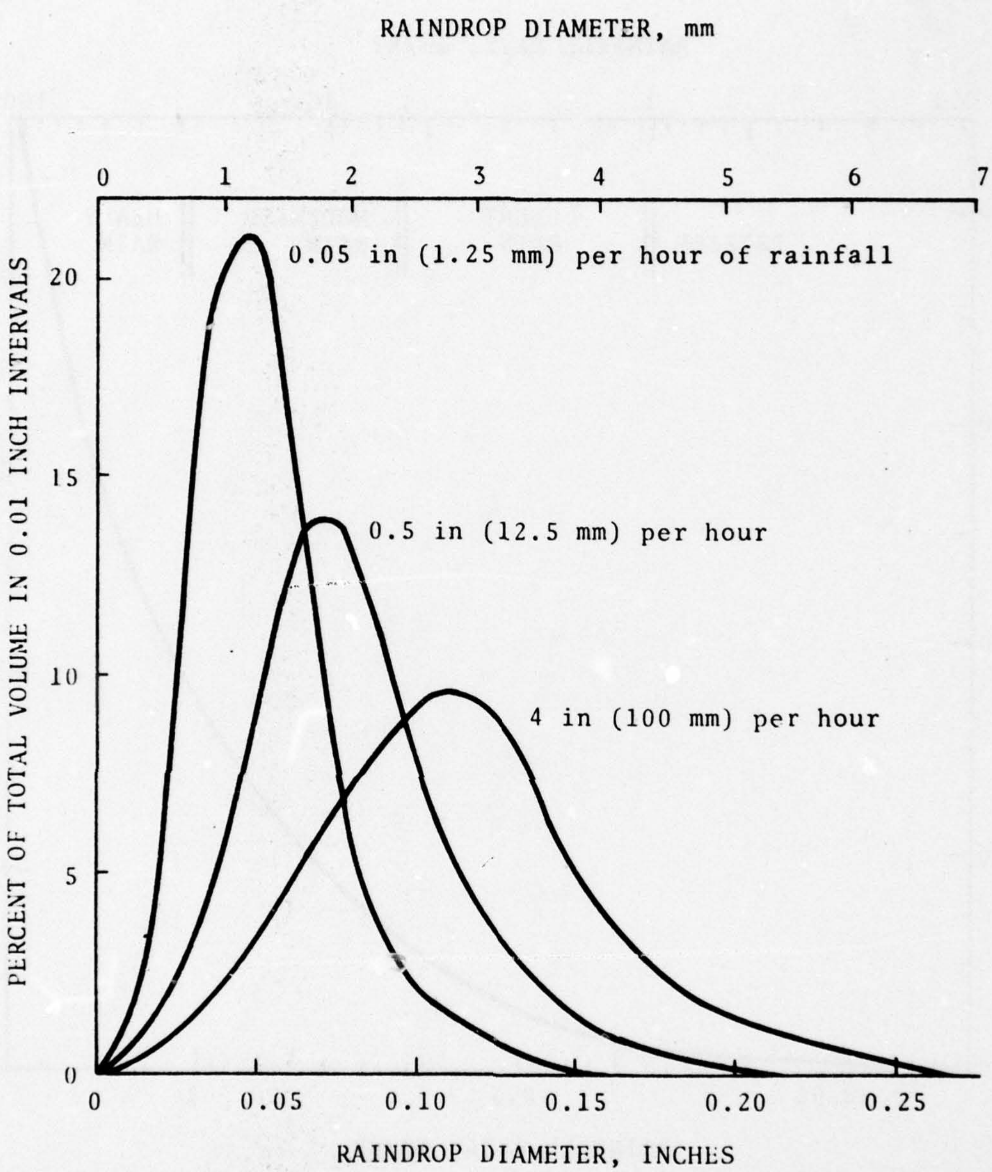

FIGURE 4-3. RAINDROP SIZE DISTRIBUTION
(FROM LAWS AND PARSONS 1943)

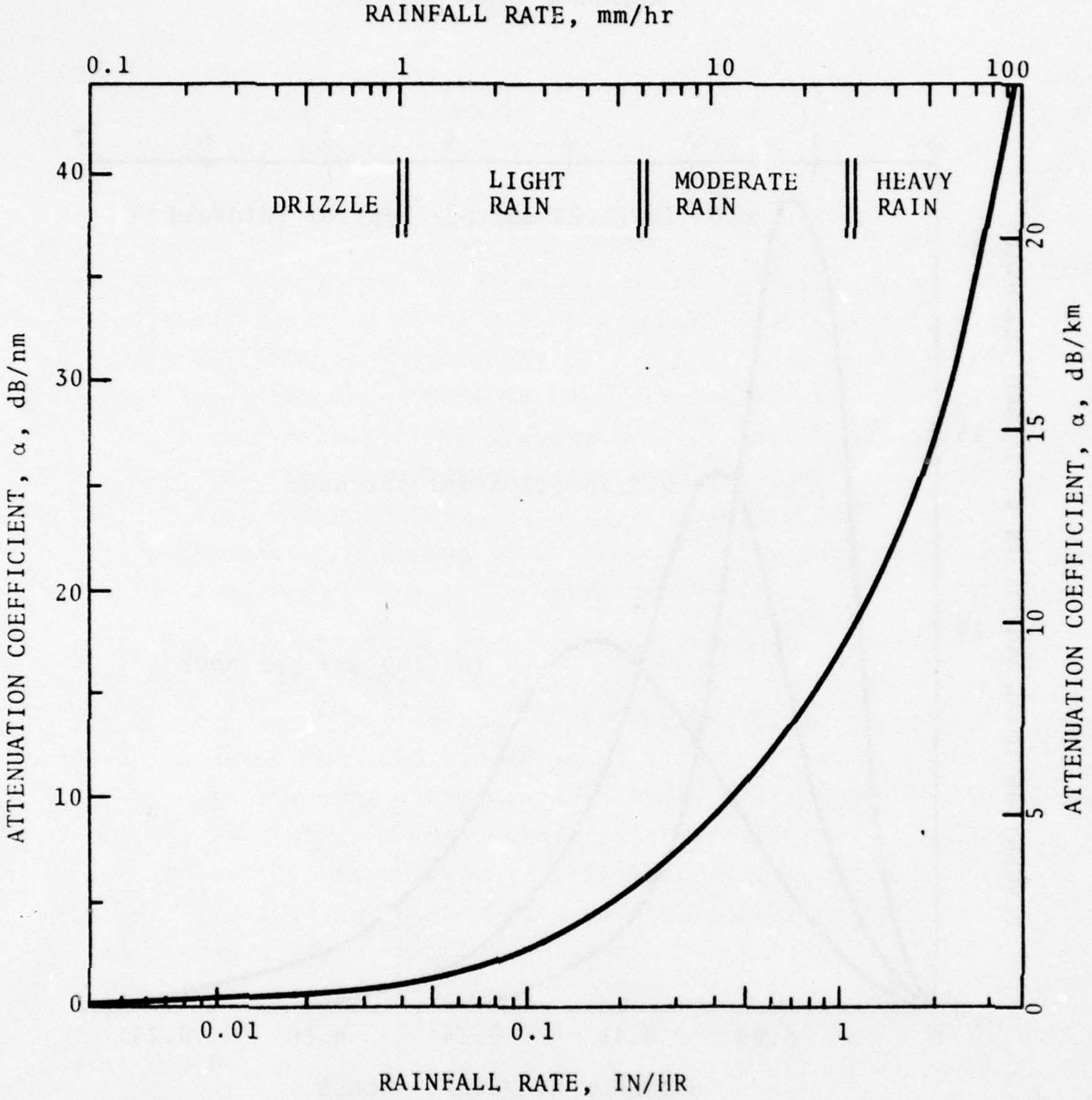

FIGURE 4-4. ATTENUATION COEFFICIENTS IN RAIN
(FROM CHU AND HOGG 1968)

greatly reduce the signal strength.

4.2.2 Backscatter

Each particle in the volume of interest scatters some energy back toward the telescope. As in the case of attenuation, weak (Rayleigh) scattering occurs in clear air and haze, due to the existence of a few aerosols which are usually present. Fog and rain result in an enhanced backscattered signal, but since attenuation also increases, the net result is a reduced signal at long range.

The backscattering coefficient $\beta(\pi)$ varies by several orders of magnitude, depending on conditions. In clear air and haze $\beta(\pi)$ generally varies from 10^{-9} to 10^{-6} $m^2/sr/m^3$*. In fog, $\beta(\pi)$ varies from about 10^{-6} to $4x10^{-5}$ $m^2/sr/m^3$; in rain, from about 10^{-6} to $2x10^{-5}$ $m^2/sr/m^3$. The backscattering coefficient expresses the equivalent cross-sectional area, presented by a cubic meter of scattering particles to the incident beam, that would scatter the same fraction of energy per unit of solid angle back toward the transmitter.

There is obviously a connection between the backscatter coefficient and attenuation coefficient (α), since they exhibit the same dependence on dielectric constant and drop diameter. However, the scattering diagram of a drop varies considerably as a function of drop size. But, since these variations are due to resonances, the fact that drops of varying sizes are present in a volume has the effect of averaging the resonances, and a reasonable estimate at a relation between the two averaged coefficients can be made for water droplets larger than a wavelength. This is done in Appendix B. The result is:

*In general, dual units are employed. However, there are some quantities that are rarely, if ever, expressed in nonmetric units.

$$\beta(\pi) = \frac{\alpha}{80\pi} \; m^2/sr/m^3$$

where α is the attenuation in nepers per meter. (α in nepers per meter is equal to α in dB/km divided by 4343, and to α in dB/nm divided by 8035.)

The relation between α and $\beta(\pi)$ used here holds for large droplets, but the assumptions break down for droplet diameters of less than 5-10 microns. Nonetheless, it is still a good working figure down to about 2 microns; below that, attenuation is due mostly to absorption, not scattering. Backscattering is strongly dependent on drop diameter, while absorption is not, so that the ratio of $\beta(\pi)$ to α decreases for smaller droplets. This means that for attenuations less than 2 dB/nm (1 dB/km), backscattering estimates are too high, the actual values being highly dependent on the drop sizes present: the smaller the droplets, the smaller the backscattering coefficient.

At the one extreme of heavy rain or dense fog, the signal at any significant range is limited by attenuation. At the other extreme, the signal is limited by the lack of backscatter. The latter situation does not appear to be a serious problem, because most airports are near urban centers, where particulate pollution is present or near salt water where salt particles act as hydroscopic nuclei. In fact, even in relatively clean air, there are generally a sufficient number of aerosols between 1-20 microns in diameter to provide a detectable signal. An extreme example was observed in a recent measurement program (Brashears, et al, 1977) utilizing a CW laser. After a cold front passed through on a dry winter day at Table Mountain in Boulder, Colorado, a noticeable drop in signal occurred: the backscatter coefficient was estimated to be about 10^{-10} m^3. Even here, the signal was sufficient to establish the wind velocity. These relatively rare conditions are not believed to be associated with hazardous wind shears.

A phenomenon which is encountered by a focused laser is that for rain the backscattering volume may be so small that on the average less than one raindrop is present at a time. In this case the backscattering is provided by aerosols; however, there are still many particles in the path to cause attenuation. This phenomenon does not occur in fog, where the particle density is much higher; nor does it occur for pulsed lasers (focused at infinity) where the volume is orders of magnitude larger.

4.2.3 Fluctuations of the Backscattered Signal

The backscattered signal is the sum of the returns from particles in the volume of interest. On the scale of the inter-particle spacing, the locations of the various particles are random and independent. Thus the phases of their returns can be considered to be random and independent. This gives rise to a combined signal exhibiting Rayleigh statistics. If all the particles in the volume are moving with the same velocity, the frequency of the combined signal will be Doppler-shifted from the transmitted frequency by a fixed amount, and the amplitude will be random, with a Rayleigh probability distribution. If w is the rms value of the intensity of the return from each particle, the mean intensity is given by $\pi Nw/4$, where N is the number of particles. The standard deviation of the intensity is given by Nw. Thus, the standard deviation approximates the mean. This means that the signal fluctuates quite widely. The probability that the received signal (s) exceeds some intensity value (S) is given by

$$P\ (s > S) = 1 - \exp\ (-S^2\pi/4M)$$

where M is the mean intensity; this is shown in Figure 4-5. From this it can be seen that 5 percent of the returns will either exceed the mean by 6 dB or be down 12 dB or more below the mean.

The question of coherent detection naturally arises: is the coherence time of the phenomenon long enough that waveforms from successive pulses could be combined to reduce the effect of noise? The answer appears to be negative, since in the presence

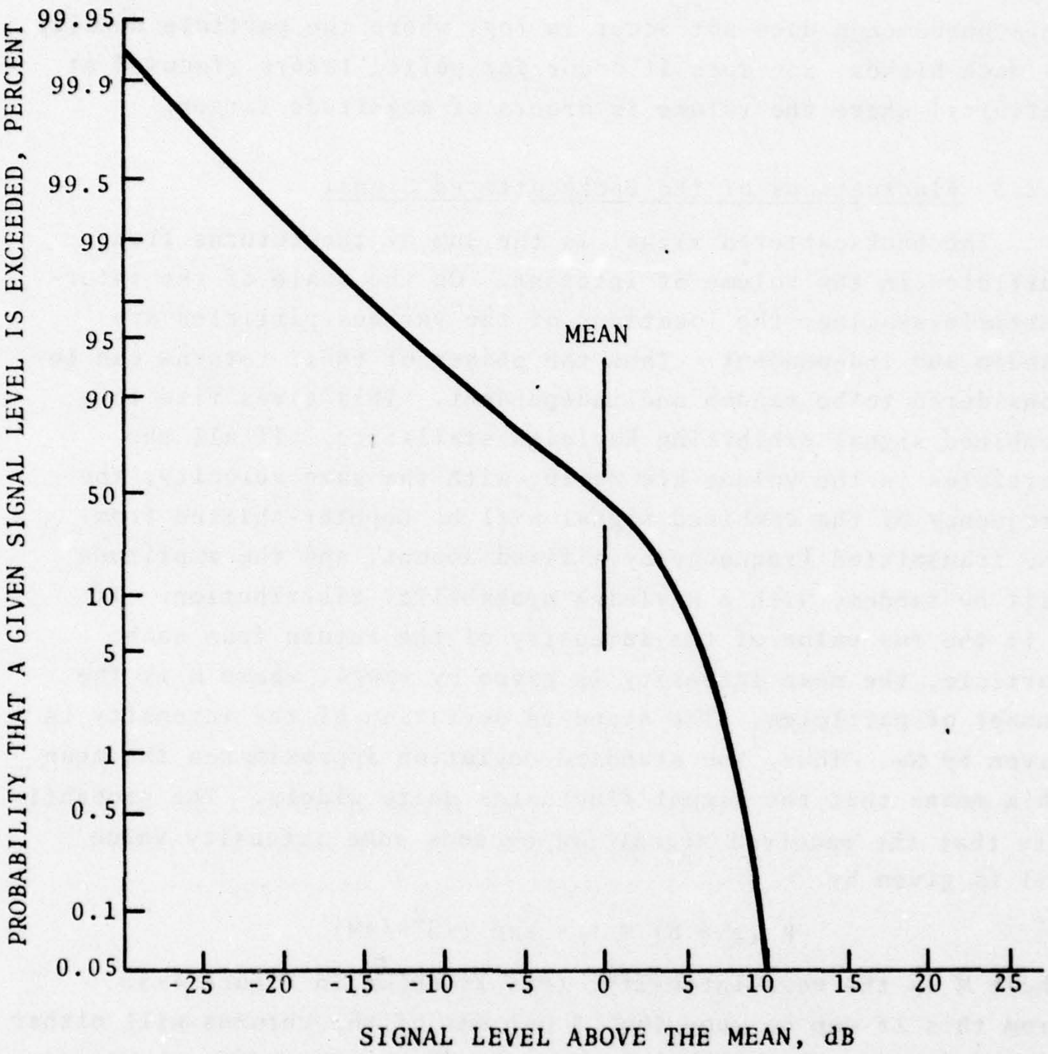

FIGURE 4-5. RAYLEIGH DISTRIBUTION

of a shear, different portions of the volume have a relative motion which destroys coherence on a time scale of microseconds. The shear also causes a spectral spread (another manifestation of the same thing).

This does not say that averaging is not helpful; incoherent averaging is useful because while the noise mean does not improve, the noise variance is reduced. This allows postintegration thresholding to be performed prior to data processing, where parameter estimation processing takes place. Also, the processor can be designed to ignore samples where the signal-to-noise ratio (SNR) drops below some threshold (e.g., 3dB), so that signal dropouts do not degrade the averaged SNR.

4.2.4 Fluctuations Due to Beam Path Disturbances

As a laser beam travels through the atmosphere, there are a number of mechanisms which alter its shape, direction and intensity. Depending on the cause of these disturbances, different characteristics are affected at different wavelengths.

At wavelengths near 10.6 microns, turbulence effects, which cause index-of-refraction variations, are much smaller than at optical wavelengths; they must be considered, however. The attenuation and changes in attenuation caused by turbulence are not significant. Phase front disturbances, on the other hand, can limit performance. Small eddies encountered by the propagating beam cause the beam to spread, and cause phase front perturbations, while large eddies actually deflect the beam (Fante, 1975). For a heterodyned laser beam the beam deflection (also called beam wander or spot dance) is not a problem, since the effect is merely to change the volume of scatterers being illuminated: by reciprocity, the return signal traverses the same path back to the telescope. Beam spread caused by turbulence is also small (see equation (37) of Fante, 1975). The phase front perturbations have the effect of limiting the dimension across the phase front over which coherence is maintained. Stated another way, for a given rms phase ripple increasing telescope diameter will not be effective (Goldstein, Miles, and Chabot, 1965 and Strohbehn, 1968).

Thus the effect of turbulence can be summed up as limiting the effective diameter of the collecting optics. This effective diameter is given by (Goldstein et al., 1965):

$$D_{eff} = \left(\frac{0.0588\ \lambda^2}{C_n^2 R} \right)^{3/5} \text{ meters}$$

where λ is the wavelength in meters, C_n^2 is a measure of the level of turbulence having the units of -2/3 meters, and R is the path length (two-way) in meters.

For typical values of turbulence near the ground, C_n^2 is about $4 \times 10^{-16}\ m^{-2/3}$, which yields an effective diameter of 0.76 m (2.5 ft) for 26 km (14 nm) of path length. For strong turbulence, C_n^2 is about $10^{-14}\ m^{-2/3}$, which yields an effective diameter of 0.11m (0.36 ft). In order that 1 foot (0.3m) optics be effective at ranges of 7 nm (26 km two-way path), the average value of C_n^2 would have to be less than $2 \times 10^{-15}\ m^{-2/3}$. Whether this poses a serious limitation is not known.

Turbulence which causes the index-of-refraction variations is associated with wind shears and thermal convective heating from the ground (Strohbehn, 1968). The latter causes turbulence which is strongest in the lowest 100 feet (30 m), and thus is less of a problem for a laser beam which will be looking up the glide slope. However, whether values of C_n^2 in excess of $2 \times 10^{-15}\ m^{-2/3}$ are encountered in thunderstorm outflows is not known.

Particle scattering primarily causes attenuation. Systematic density variations in the transverse direction could in principle cause beam bending, but there is no reason to believe that particle densities exhibit such variations. Forward scattering could conceivably cause beam spread, and this has been observed in measurements in rain and snow (Chu and Hogg, 1968). However, since the attenuations calculated for particle scattering already account for the energy not available to the backscattering volume, it does not appear that the beam spread represents an additional loss over and above the attenuation value.

Phase fluctuations caused by particle scattering are believed to be small, but there are no rigorous calculations or experiments which verify this.

4.3 CW LASERS IN THE VAD SCAN MODE

4.3.1 Basic Measurement Technique

A CW heterodyned laser can obtain wind profiles in a volume above the laser by employing a VAD (Velocity Azimuth Display) scan, similar to that described by Lhermitte and Atlas (1961) for radar. In this mode the range is varied by focusing the beam at the range of interest, and scanning the beam in azimuth, while holding the angle from the zenith constant (typically 30 degrees) (see Figure 4-6). If the horizontal wind remains constant during the time of a complete rotation, the line-of- sight Doppler velocity component recorded will be a sine wave whose amplitude is a measure of horizontal wind direction, and whose average value is a measure of vertical draft speed. By refocusing the telescope to a series of heights, a profile of the three wind components can be mapped out.

Deviations from a sine wave denote nonuniformity of the wind field, or changes in the wind field with time. Turbulence would cause both of these variations, so that the nonuniformity can potentially be used as a measure of turbulence. This is discussed further in Section 4.3.6.

Laser systems have been fabricated and tested which use this principle (Brashears and Hallock, 1976). They have been successfully employed and tested against tower anemometer measurements. As a result, the requirements of the following sections are based on the observed behavior of an operating system.

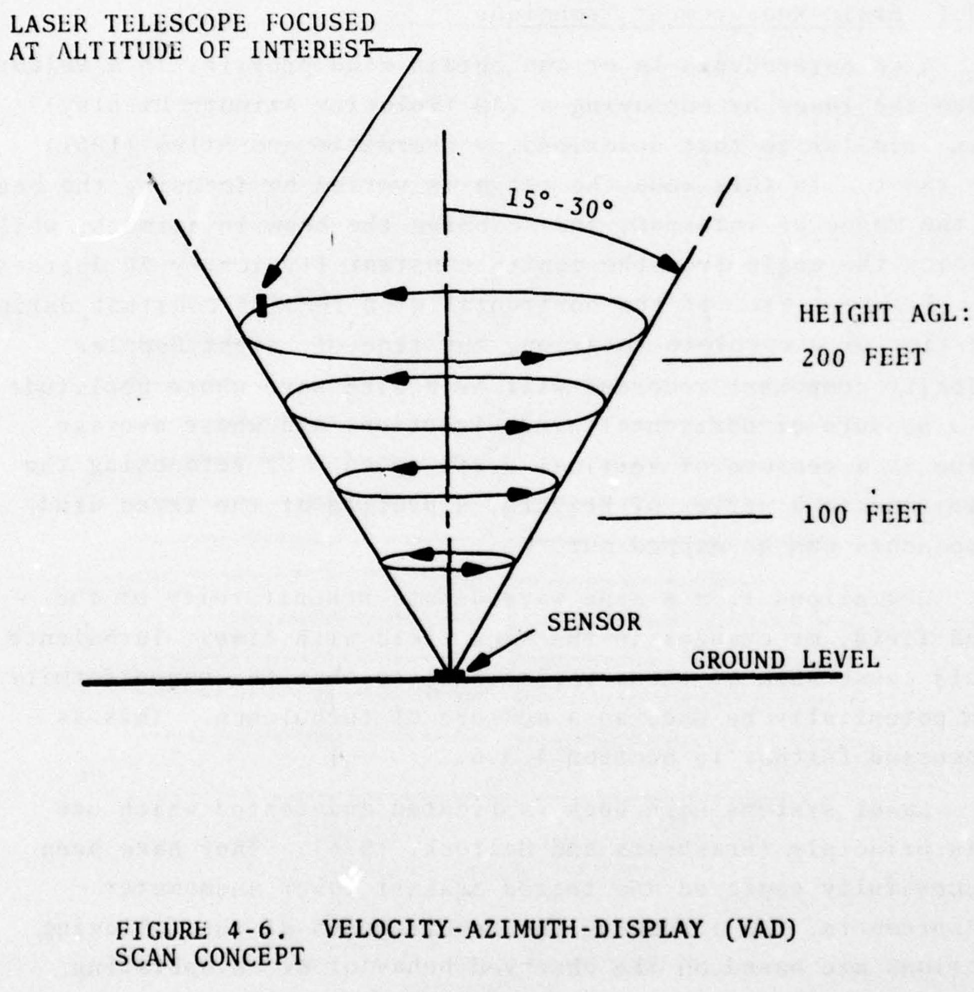

FIGURE 4-6. VELOCITY-AZIMUTH-DISPLAY (VAD) SCAN CONCEPT

4.3.2 Scanning Techniques

There are two scanning modes which may be employed: (1) Ring Scan, which is a rapid azimuth scan (e.g., 0.5 revolution per second) combined with a stepped range scan (e.g., at 50 foot (15 m) increments) (see Figure 4-7); or (2) Finger Scan, which is a rapid range scan (e.g., 0.3 Hz) combined with a slow azimuth scan (e.g., 2 revolutions per minute) (see Figure 4-8). There is a wide latitude of choices, because for synoptic phenomena, changes take place slowly, and there is no need for a rapid update rate. A CW laser sensor operating full-time would utilize extensive averaging, and take much longer than the 40 second update rate used to derive the parenthetical numbers listed above.

The reason for minimizing the total measurement period is in anticipation of the combined CW/pulsed operation: there the need for rapid updating of information for the pulsed mode of operation is such that as little time as necessary, for a reliable synoptic measurement, should be allocated to the CW mode of operation. A measurement of 40 seconds duration every 10-15 minutes is probably adequate.

4.3.3 Altitude Resolution

The rationale for an altitude resolution has already been developed in Section 3.3, where a 50 foot (15 m) altitude resolution is recommended to properly characterize frontal shears (see especially Figure 3-9).

4.3.4 Accuracy

In section 3.4 the recommended system accuracy was determined to be 1-2 kphf (0.017-0.034 m/sec/m). Since the measurement technique yields the magnitude and phase of the horizontal winds (plus net vertical flow), a polar-to-rectangular transformation is necessary, where the rectangular coordinate axes are aligned with the runway in order to provide headwind (and crosswind) profiles. From the headwind profile successive

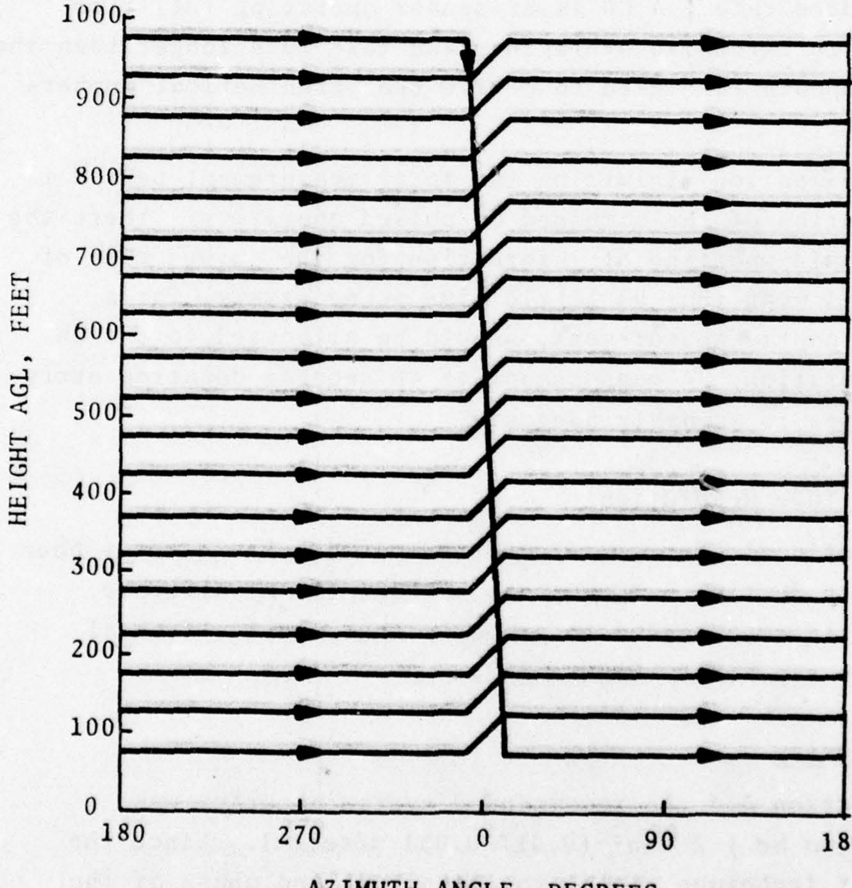

FIGURE 4-7. RING SCAN FOR WIND PROFILE MEASUREMENTS

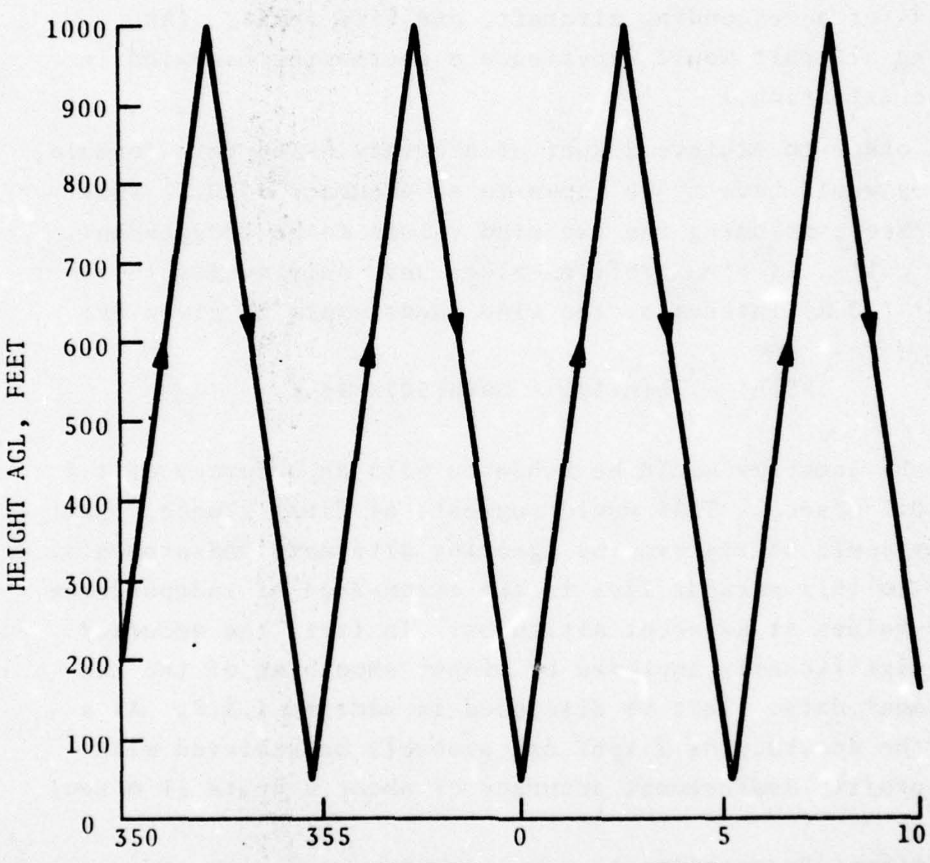

FIGURE 4-8. FINGER SCAN FOR WIND PROFILE MEASUREMENTS

differences between altitudes at 50 foot (15 m) intervals would give the shear:

$$WS(h) = 2\Big(HW(h-25) - HW(h+25)\Big)\,\text{kphf}$$

where h is the height AGL, height units are in feet, and headwinds are in knots; a positive shear indicates an increasing headwind for a descending aircraft, and vice versa. (An ascending aircraft would experience a decreasing headwind in the same situation.)

In order to achieve 2 kphf of accuracy using this formula, the winds would have to be known to an accuracy of 0.71 knot (0.36 m/sec), assuming the two wind values to be independent. Paradoxically, if wind profile values were only available at 100 foot (30 m) intervals, the wind shear would be given by:

$$WS(h) = HW(h-50) - HW(h+50) \quad \text{kphf}$$

and 2 kphf accuracy would be achieved with an accuracy of 1.4 knots (0.7 m/sec). This would suggest, at first glance, that accuracy could be improved by ignoring alternate measurements. The key to this paradox lies in the assumption of independence of wind values at adjacent altitudes. In fact, the accuracy can be significantly improved by proper smoothing of the two-dimensional data. This is discussed in section 4.3.7. As a guess, the accuracy of 2 kphf can probably be achieved with a wind profile measurement accuracy of about 2 knots (1 m/sec).

4.3.5 Signal Processing

The signal processing operates on the raw signal, and produces a frequency domain set of descriptors: either the entire spectrum, or a set of parameters, e.g., the strongest frequency, the amplitude at the strongest frequency, and the highest and lowest frequencies of the spectral bandwidth. The processing can be thought of as a Fourier transform operation, with or without interpretation. In addition, signal processing may include rejection of low-amplitude frequencies.

The sample period is quite arbitrary, but is typically tens of milliseconds. The spectra which result from the processing by a spectrum analyzer typically look like Figure 4-9a and b: the first spectrum is for a steady wind, where only one wind velocity is present; the second spectrum is broadened, which could be caused by a shear over the volume, or by turbulence, where several wind velocities are present.

For one-foot (0.3 m) optics, the focal volume is approximately a cylinder whose diameter varies from 0.04 inch (1 mm) at a 50 foot (15 m) range, to 0.5 inch (12 mm) at 1000 feet (300 m); its length varies simultaneously from 0.6 foot (0.2 m) to 200 feet (60 m), respectively. Thus near the ground the focal volume is so small that individual spectra are quite narrow, and turbulence is seen rather as a sample-to-sample variation. Higher up, however, the focal volume is large enough to incorporate a large number and size of eddies, and turbulence will be seen as a spectral broadening, indicating that there are wind speed variations within the volume.

The characteristic sine wave of the VAD scan is a plot of the frequency (proportional to the wind velocity) versus the scan angle. Thus one of the problems is to choose the frequency parameter that best characterizes the average frequency of a given spectrum. Some candidate parameters are the following:

a. Frequency at the peak amplitude - This is simplest, but noise spikes cause significant errors.

b. Average of minimum and maximum frequencies of the spectral band - This is better, but any skew tends to be accentuated where particulate concentration is high.

c. Average of minimum and maximum frequencies of the spectral band, measured at some fraction of the peak amplitude - This is a more consistent measurement, but somewhat complicated to implement.

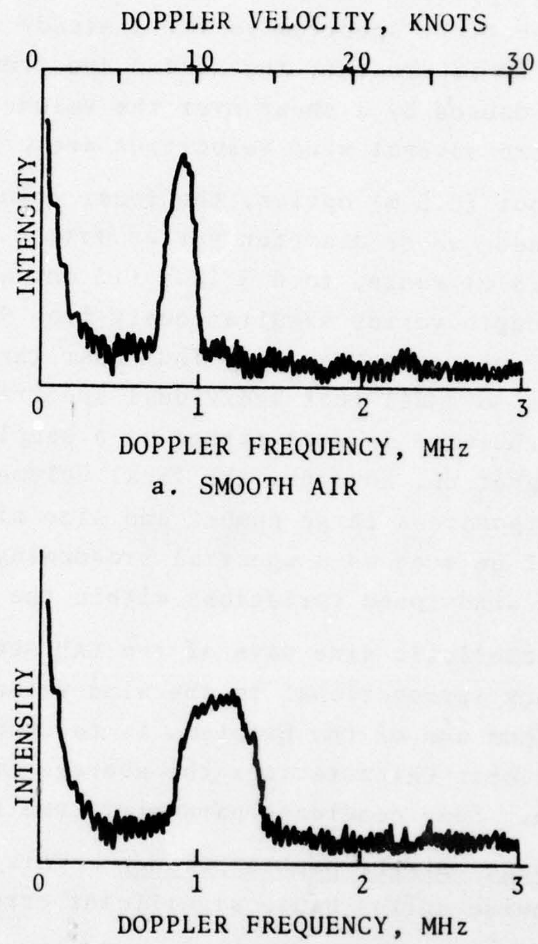

FIGURE 4-9. DOPPLER WIND SPECTRA

d. Centroid of spectral band - Probably the best measurement, but complicated.

It should also be pointed out that the difference between signal processing and data processing is not precise: parameter determination may well be implemented in software.

If signal processing is performed in hardware, it must be able to handle unusual situations like insect replies, as well as returns from falling rain. Both of these cause "double-peaking" in the spectrum, since there are two or more distinct velocities present in the return. Some form of outlier rejection scheme in the data processing could help in the case of insects, while choosing the slower of two or more sustained peaks would result in the correct characterization of the wind in the presence of rain.

4.3.6 Data Processing

In both scan modes (Ring Scan and Finger Scan) the result is a collection of Doppler velocities at a number of azimuth angles for each range, or height. Figure 4-10 shows a measurement example (Brashears, et al, 1976): the missing values between ±2 knots are the result of preprocessing thresholding. It is evident that several different methods could be used for estimating the wind speed and direction from the data. Some of these are discussed below:

a. Peak Algorithm: take the largest value of wind speed, and use that value as the wind speed, and the associated phase as wind direction. This has the result of always estimating high in wind speed, and is not reliable in direction.

b. Filtered Peak Algorithm: use some averaging or filtering technique to reduce the effect of noise, and proceed as in "a" above. This reduces the effect of noise, but still gives errors due to turbulence and gusts, which cause systematic deviations from a sine wave.

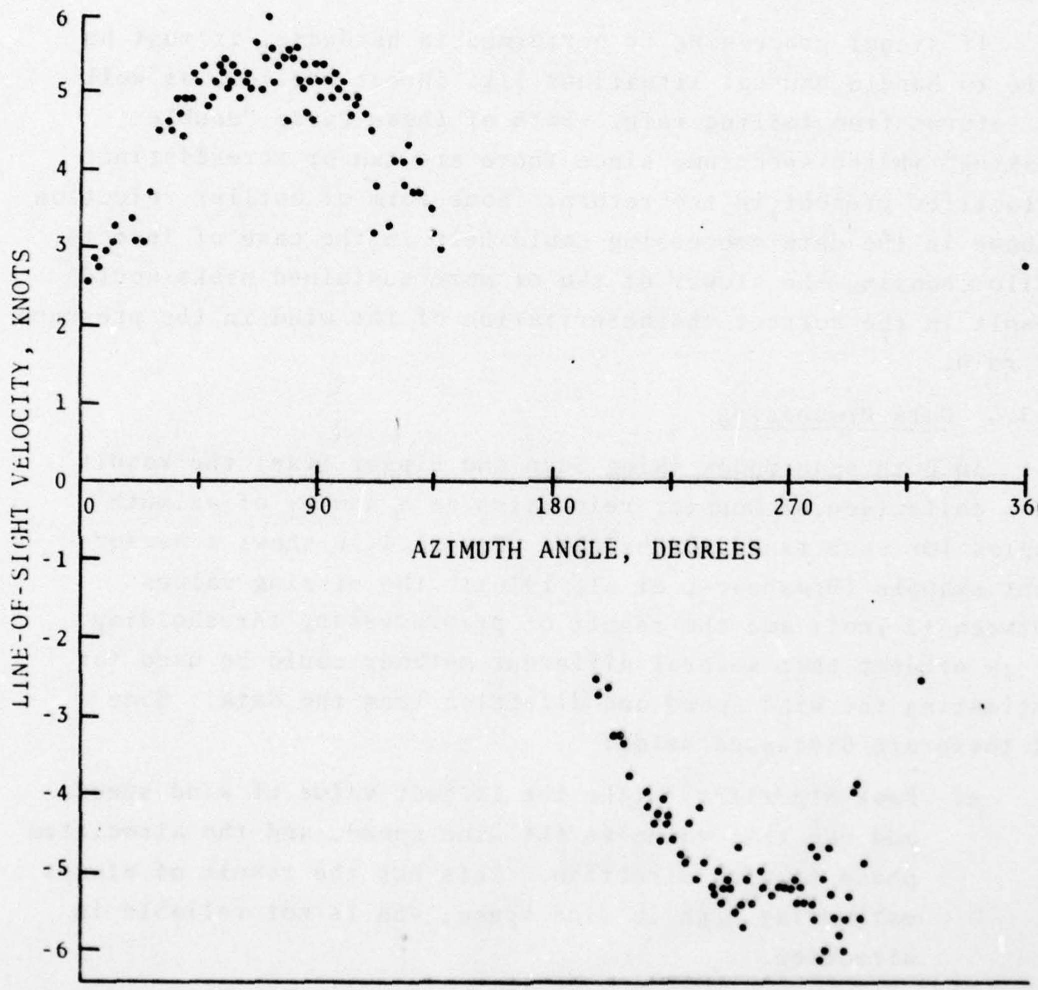

FIGURE 4-10. MEASURED VAD SCAN DATA

c. Fourier Transform Technique: recover the fundamental frequency sine wave by a digital Fourier transform calculation, and use the resulting sine wave to estimate wind speed and direction. This takes some computation, but provides the best estimate.

Algorithms b and c above can be improved by some form of outlier rejection scheme, whereby data which vary from their neighbors by some amount are rejected

There are some differences between the two scanning modes that favor the Finger Scan mode. For one thing, turbulent eddies whose characteristic lifetimes are longer than the Ring Scan period (e.g., 2 seconds), but are less than the total measurement period (e.g., 40 seconds) will tend to be averaged out in the Finger Scan mode, while they will tend to bias the results in the Ring Scan mode. For another, in the Finger Scan mode, samples are taken at more altitudes (and less azimuth angles); equivalent accuracy and resolution with the Ring Scan mode can be obtained by averaging the samples within the altitude resolution cell. Alternatively, the additional altitude samples can be used to obtain a higher altitude resolution, albeit at a reduced accuracy. This feature may be useful in assessing the intensity and extent of shear zones.

Once a profile is obtained, the result can be further scrutinized to see if it is physically realizable. For example, synoptic profiles approach logarithmic in the lowest 100 feet (30 m); a sequence of +10, +10, -8, +10 knots (+5, +5, -4, +5 m/sec) at 50 foot (15 m) altitude increments would not be physically realizable. As more shear data are obtained, other physically realizable constraints can be brought in to improve confidence in predicted shears and reduce false alarms due to spurious measurements.

4.3.7 CW Laser Hazard Limitations

Laser hazards potentially exist within the shelter and outside. The hazards within the shelter can be minimized by proper enclosures and precautions. Outside the shelter, there are the questions of hazards to maintenance personnel on the roof of the shelter or in the area of the shelter, people in the airport buildings, and passengers and crew in aircraft.

Considering only maximum intensity, there are regions where the beam is focused (the focal volume) where intensities are quite high. For example, the worst case is at minimum range (50 feet, or 15 m), where the beam is focused down to a volume 1 mm (0.04 in) in diameter. There a 10 watt laser would result in a peak intensity of 1270 watts/cm^2*, which is definitely dangerous to skin and eyes; however, a maintenance man on the roof of the shelter would experience at most only 0.02 watt/cm^2, a safe amount. Furthermore, if the scanner were in motion, the amount of time that a spot would be illuminated would be small, which is not as dangerous as continued irradiation.

The Food and Drug Administration has issued standards on laser radiation (FDA, 1975), which define three classes of at CO_2 wavelengths (Class II does not apply to CO_2 wavelengths):

Class I: For a scanned laser, the radiant energy through a 7 mm diameter aperture shall not exceed $4.4\times10^{-3}\ t^{1/4}$ joules where t is the duration of the irradiation in seconds. For a fixed beam laser, the radiant power through an 80 mm diameter aperture shall not exceed 7.9×10^{-4} watts.

---

*The units of watts per square centimeter and joules per square centimeter are standard for laser hazard definitions and will be used here and in Section 4.4.7.

Class III: For a scanned laser, the radiant exposure through a 7 mm diameter aperature shall not exceed 10 joules/ cm^2. For a fixed beam laser, the radiant power through an 80 mm diameter aperture shall not exceed 0.5 watt.

Class IV: Does not meet Class III requirements.

In its intended operational modes, the laser beam will always be scanning. Using the worst case of a focal volume at a 50 foot (15 m) range, Figure 4-11 shows the Class I limits and the energy levels attained by a scanning CW laser for different emitted powers. Since even at 20 watt laser actually emits less than 10 watts of power, due to transmission losses, it appears that CW lasers up to 70 watts can be utilized without violating Class I standards. (Class III standards are about 3 orders of magnitude more lenient.)

The laser system should have provisions to shut off the transmitter if the scanner stops during operation. With these provisions, Class I limits will not be exceeded.

4.4 PULSED LASERS IN THE HORIZON SCAN MODE

4.4.1 General Description

A pulse transmitted from a laser will travel along a narrow beam at the speed of light, illuminating at every instant a tubular volume whose length is proportional to the pulse width. The received signal at an instant some time after the transmission represents the sum of the scattered energies from that volume illuminated at half that time after transmission. By examining the return signal during periods of duration equal to the pulse width, a series of velocities can be generated for each transmitted pulse, each associated with a different range interval, or bin. This is discussed in detail in Section 4.4.5. For example, a two microsecond pulse is associated with a 1000 foot (300 m) range resolution cell. By examining the return signal during successive two-microsecond periods, the Doppler velocities can be extracted from a series of 1000 foot (300 m) range bins. Figure 4-12 shows a number of range bins and the relative weighting

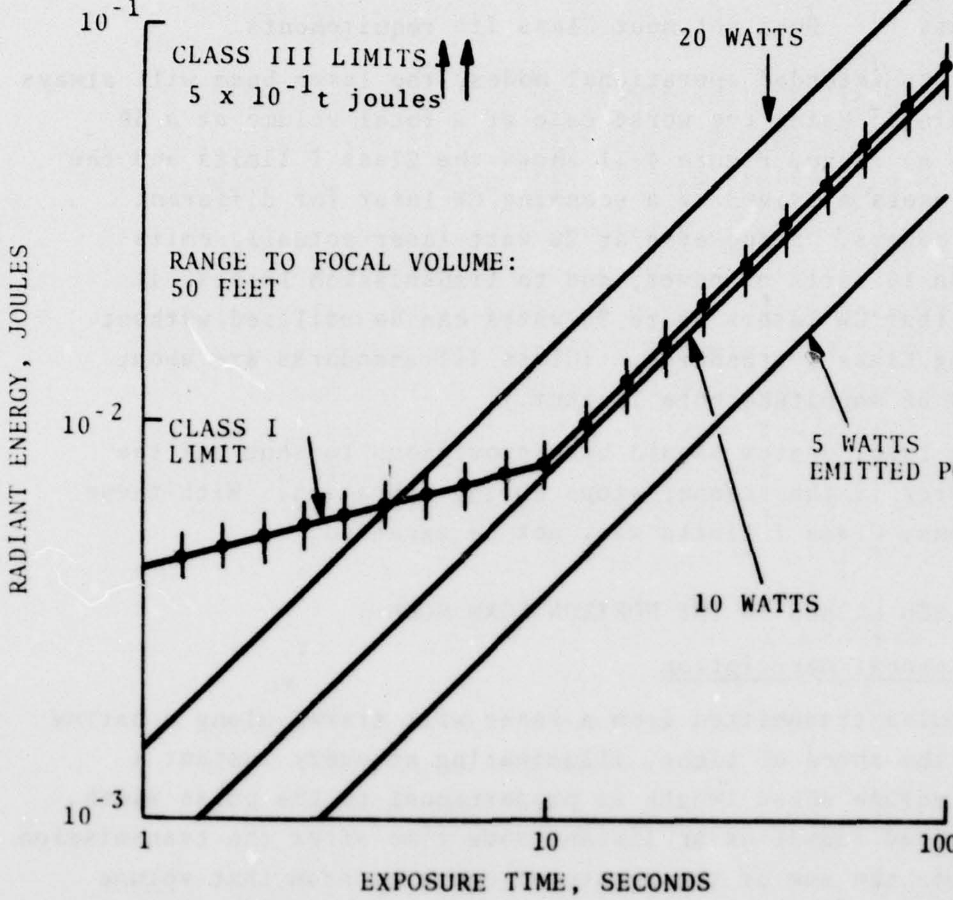

FIGURE 4-11. EMISSION LEVELS FOR CW SCANNING LASERS

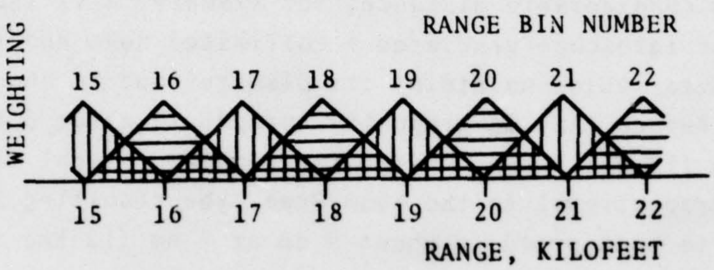

FIGURE 4-12. RELATIVE WEIGHT ATTACHED TO RETURNS FROM PARTICLES IN EACH RANGE BIN

attached to signal returns from particles at different ranges; e.g., the particles at 19.5 kilofeet range contribute equally to the signals in bins 19 and 20, and not at all to bins 19 and 21. Thus there is some overlap, but 75 percent of the energy in the return signal is from within ±500 feet (150 m) of the range bin center.

For a minimum range of 0.5 nm (1 km) and a maximum range of 7 nm (13 km), there are 39 range bins, and a doppler velocity can be estimated for each range bin on each transmitted pulse.

The transmitted beam has the property of maintaining its diameter for a considerable distance; for example, a 12 inch (0.3m) diameter telescope generates a collimated beam about 12 inches in diameter which maintains its diameter out to about 2 nm (4 km). Beyond that it gradually spreads to about 3 feet (0.9m) at 7 nm (12 km) range. Since the received signal intensity is inversely proportional to the beam area, the resulting loss of signal due to beamspread is about 9 dB at 7 nm (12 km) range.

Shears will be evidenced by variations in the Doppler velocities in successive ranges. The gradients in these line-of-sight wind velocities are essentially the headwind shears that would be experienced by an approaching or departing aircraft. This is due to the geometry, whereby a sensor located near the center of an airport has radials which are nearly parallel to the approach and departure lanes (see Figure 5-1).

4.4.2 Range Capability

A pulsed laser system will not achieve the desired system range of 7 nm under all conditions: under conditions of heavy fog or moderate-to-heavy rains, the range will drop due to severe attenuation. This limitation poses the largest problem to the deployment of pulsed laser sensors. Fortunately, heavy fogs are usually associated with warm front shears, rather than thunderstorms; in the latter case some inconsequential light fogs may accompany rain. It is not anticipated that pulsed lasers would be used to detect warm front shears.

The features of thunderstorm related shears that are encouraging are that (1) gust fronts and secondary surges of the cold air outflow precede the rainfall of a parent thunderstorm, and thus can be readily detected in advance (see Goff, 1976); and (2) downburst cells usually have heavy rain within the cell but are surrounded by areas of light rainfall or no rainfall (Fujita, 1975, and NTSB, 1974b, 1976a, and 1976c). In these conditions pulsed lasers would be able to achieve adequate system ranges. The evidence is not as extensive as one would like, and needs further experimentation.

The effect of attenuation on range can be seen from Figures 4-13 and 4-14, which are calculated using system parameters which are believed to be readily achievable with today's technology (see Appendix A). It can be seen that a system range 7 nm (13 km) can be achieved for attenuations less than 2 dB/nm (1.1 dB/km) (assuming a SNR threshold of 3 dB). Comparing this to Figure 4-4, it can be seen that this corresponds to about 2 mm/hr. Thus if the average rainfall along the beam path does not exceed 2 mm/hr, the system range can be achieved with 10 kilowatts of transmitter power.

Higher laser performance would be helpful in improving the range but not as much as one might expect. For example, a 1000 percent increase in transmitter power would allow system ranges of 7 nm in average rainfalls of up to 3mm/hr (0.1 in/hr). Another 1000 percent increase in transmitter power would increase this to about 4 mm/hr.

An interesting point to note is that a line-of-sight sensor pointing up the glide path will not detect downburst cells beyond about 1-2 miles from touchdown even if system range were unlimited. This can be seen from Figure 4-15: above the outwash of a downburst cell the wind currents are essentially downdrafts, which couple weakly into the line-of-sight velocity component. This, of course, can be alleviated by pointing the laser below the glide path. It is suggested that the beam be pointed at such an elevation angle that it crosses the glidepath at about 250-300

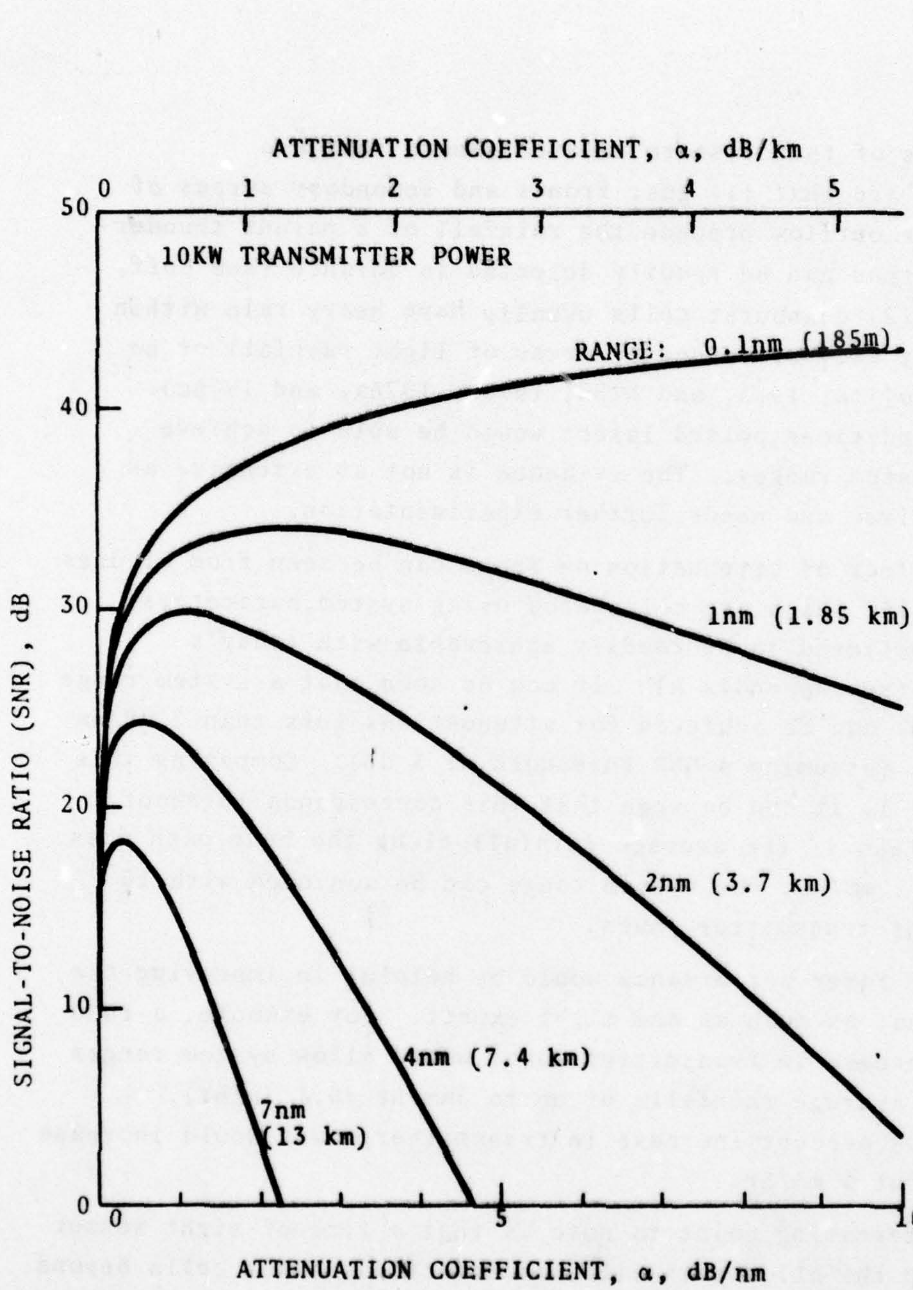

FIGURE 4-13. SIGNAL-TO-NOISE DEPENDENCE ON ATTENUATION COEFFICIENT

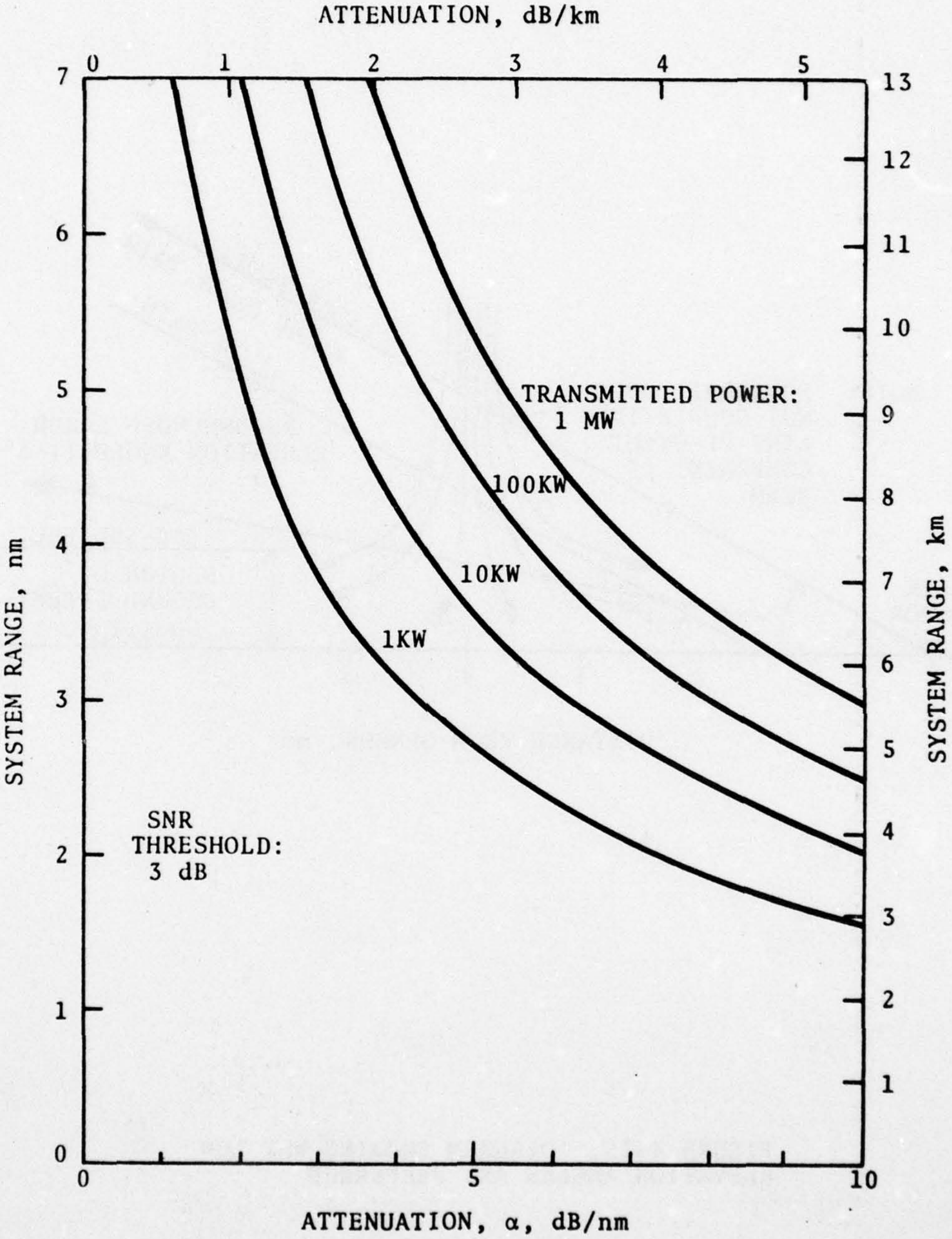

FIGURE 4-14. SYSTEM RANGE DEPENDENCE ON ATTENUATION AND TRANSMITTED POWER

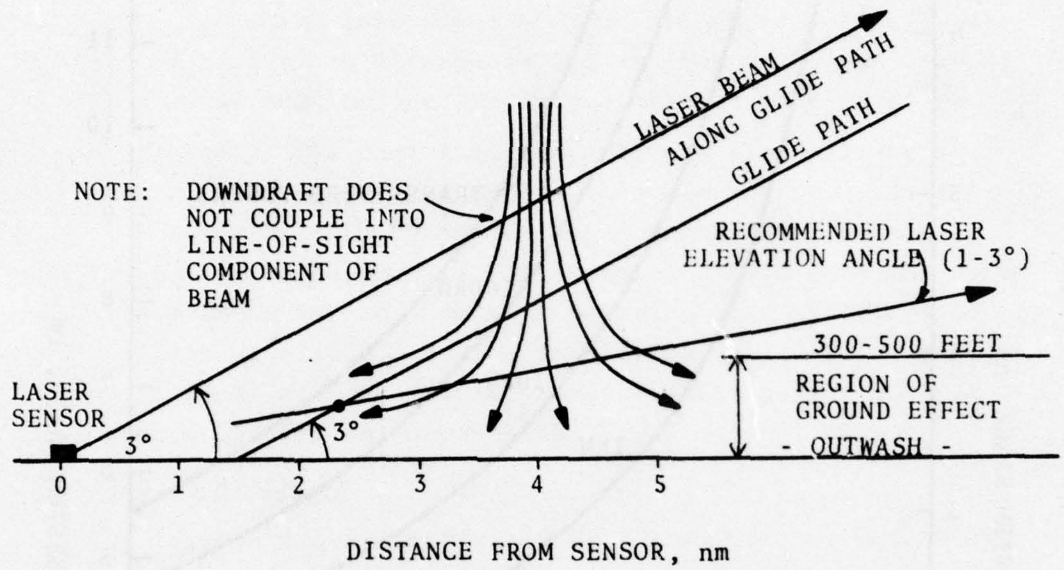

FIGURE 4-15. DIAGRAM SHOWING WHY LOW ELEVATION ANGLES ARE PREFERRED

feet (75-90 m) in altitude, as shown in Figure 4-15. It can be seen that the outwash of the cell will be detected by the laser sensor at much longer ranges when it is pointed at lower angles.

4.4.3 Scanning Capability

Before scan speed and data update rate are discussed, the need for scanning must be established. First of all, without scanning, a sensor would have no advance warning capability. It would answer the question, "Is there a wind shear event in the corridor?", but not, "Is there a wind shear event approaching the corridor?" Secondly, unless a separate sensor were placed at each threshold, a scanning mechanism would still be required for pointing successively at different approach corridors. To require a separate sensor for each approach/departure zone would be prohibitively expensive for most airports.

For wide-scale synoptic phenomena such as inversions and warm fronts, it is less critical to have advance information. In the case of rapidly advancing cold fronts and thunderstorm outflows, however, a hazardous situation could arise in the two minutes it takes a typical aircraft to travel from the outer marker to decision height. In these two minutes a thunderstorm system moving at 30 knots would travel a nautical mile. Since the scan capability is required, anyhow, it should be used to detect the incoming hazard.

The discussion on update rate in Section 3.2 concludes that an update rate of two per minute is adequate to detect fast-moving fronts, gust fronts, and downburst cells. Since the storm system (or front) can approach from any direction, it is desirable to have 360 degree coverage, especially until a storm system and its motion have been established. The scan rate for a two-per-minute update rate is 360 degrees in 30 seconds, or 12 degrees per second. It turns out that speed of light limitations do not allow faster scan rate if the azimuth scanner is smoothly rotated; this can be demonstrated by the following argument: the half-power beamwidth of a

AD-A054 174   TRANSPORTATION SYSTEMS CENTER CAMBRIDGE MASS   F/G 4/2
WIND SHEAR REQUIREMENTS AND THEIR APPLICATION TO LASER SYSTEMS.(U)
FEB 78   R M KALAFUS
UNCLASSIFIED   DOT-TSC-FAA-77-5   FAA/RD-77-120   NL

2 OF 2
ADA
054174

END
DATE
FILMED
6-78
DDC

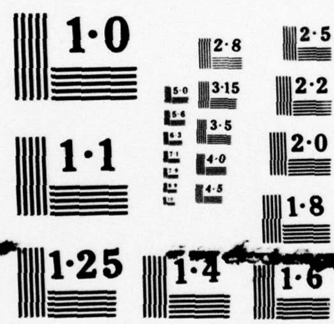

NATIONAL BUREAU OF STANDARDS
MICROCOPY RESOLUTION TEST CHART

laser using 1 foot optics is given by 1.3 λ/D radians, or 0.046 milliradian. At a range of 7 nm (13 km), it takes 84 microseconds for a round trip; thus at a scan rate of 12 degrees per second, the scanner has moved $12 \times 84 \times 10^{-6} = 10^{-3}$ degrees, or 0.0175 milliradian, or 3/8 of a beamwidth. This represents a signal loss of about 1 dB, which is acceptable. A telescope twice as large would lose about 6 dB of signal at 7 nm (13 km), or would be limited to a range of 3.5 nm (6.5km). Thus larger apertures would not improve system performance in a scanning mode.

Fortunately, the fact that convenient optics sizes are concomitant with the desired update rate means that a constant rate of scan in azimuth can be employed (otherwise, a step scan mode would have to be used). For example, a 12 degree per second scan with a laser having a pulse repetition rate of 24 per second yields a mapping with 0.5 degree resolution, which corresponds to 370 feet (113 m) at 7 nm (13 km) range. These parameters are quite reasonable for the application.

4.4.4 Pulse Width

The pulse width is determined by a tradeoff between range resolution and velocity resolution. Figure 4-12 shows the relative signal weighting attached to returns from particles associated with a given range for a two microsecond wide square pulse. While returns from a 2000 foot (600 m) volume figure in the total, 75 percent of the return comes from the central 1000 feet (300 m) (see Section 4.4.5 for a full discussion of this); for this sensor, a two microsecond wide pulse is said to be associated with a 1000 foot (600 m) range resolution cell.

Velocity resolution is directly related to the frequency resolution of the return signal and the signal processor. Generally the signal processor bandwidth is matched to the pulse spectral width. For a two microsecond pulse, the processor bandwidth would be 500 kHz, and for a four microsecond pulse, 250 kHz. Roughly speaking, one knot of speed corresponds to 100 kHz (actually, 97.16 kHz). Thus a 500 kHz bandwidth corresponds to about 5 knots of resolution. The tradeoff is shown in Figure 4-16.

The velocity accuracy, as opposed to resolution, depends on the signal-to-noise ratio as well as the signal processor

$$\Delta V \approx \frac{\lambda\ \Delta f}{2\sqrt{SNR}} = \frac{10.3\ B}{\sqrt{SNR}} \quad \text{knots}$$

where B is the bandwidth in megahertz. For example, for signal-to-noise ratios greater than 14 dB, the theoretical accuracy (per pulse) is better than 1 knot. The next section discusses the implications to the signal processing techniques to be employed. The important conclusion is that there appear to be methods available to achieve wind speed accuracies of 1-2 knots (0.5-1 m/sec) with two-microsecond pulses.

4.4.5 Averaging and Signal Processing

It was mentioned in the previous section that the inherent accuracy of the velocity estimate is better than the matched filter resolution. It is also true that proper averaging of velocity estimates from successive pulses will improve the final velocity estimate for the range bins associated with a particular azimuth. The purpose of averaging and signal processing is to obtain the best estimate of the velocity characteristic of the volume of interest.

In principle a complete velocity spectrum is received at every range for each transmitted pulse: at every instant of time after the pulse begins to leave the transmitter it illuminates some volume along the beam line of sight. Assuming a simple square pulse, the volume is approximately a cylindrical tube, having a beam diameter equal to the telescope diameter initially, and a length equal to the speed of light times the pulse width. For a 2 microsecond pulse width, the tube is about 2000 feet (600 m) long at any instant. The situation is shown in Figure 4-17a. The returns at t_5, for example, are made up of the returns

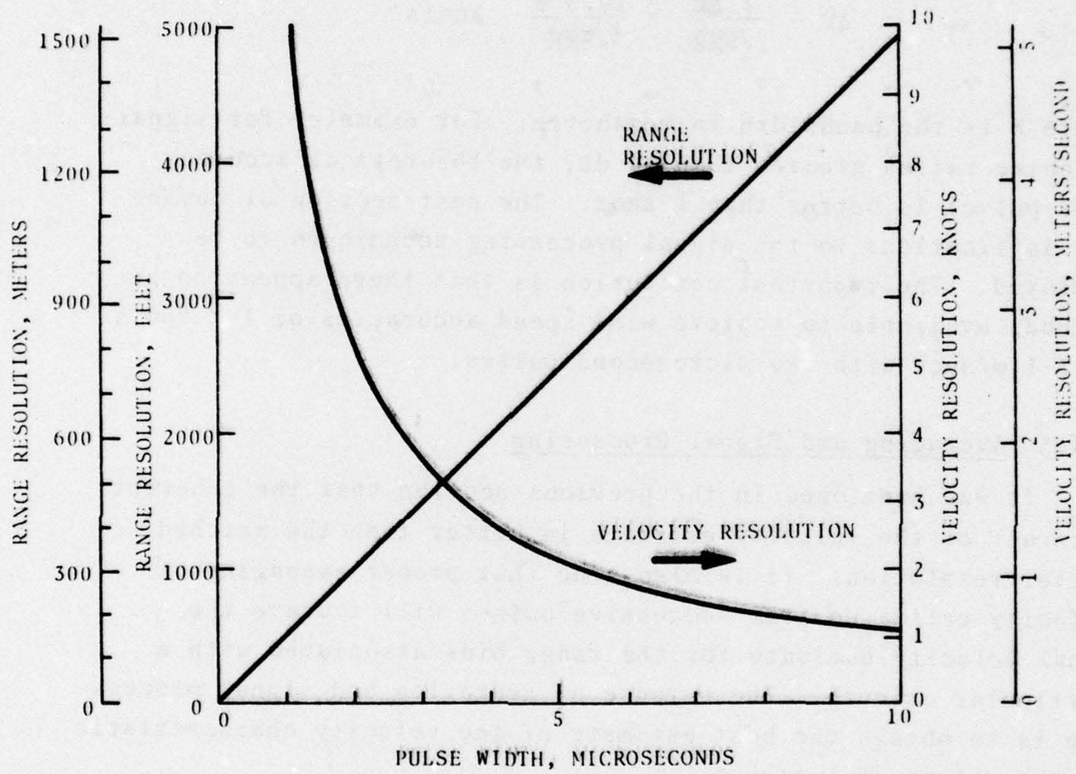

FIGURE 4-16. TRADEOFF BETWEEN RANGE RESOLUTION AND VELOCITY RESOLUTION

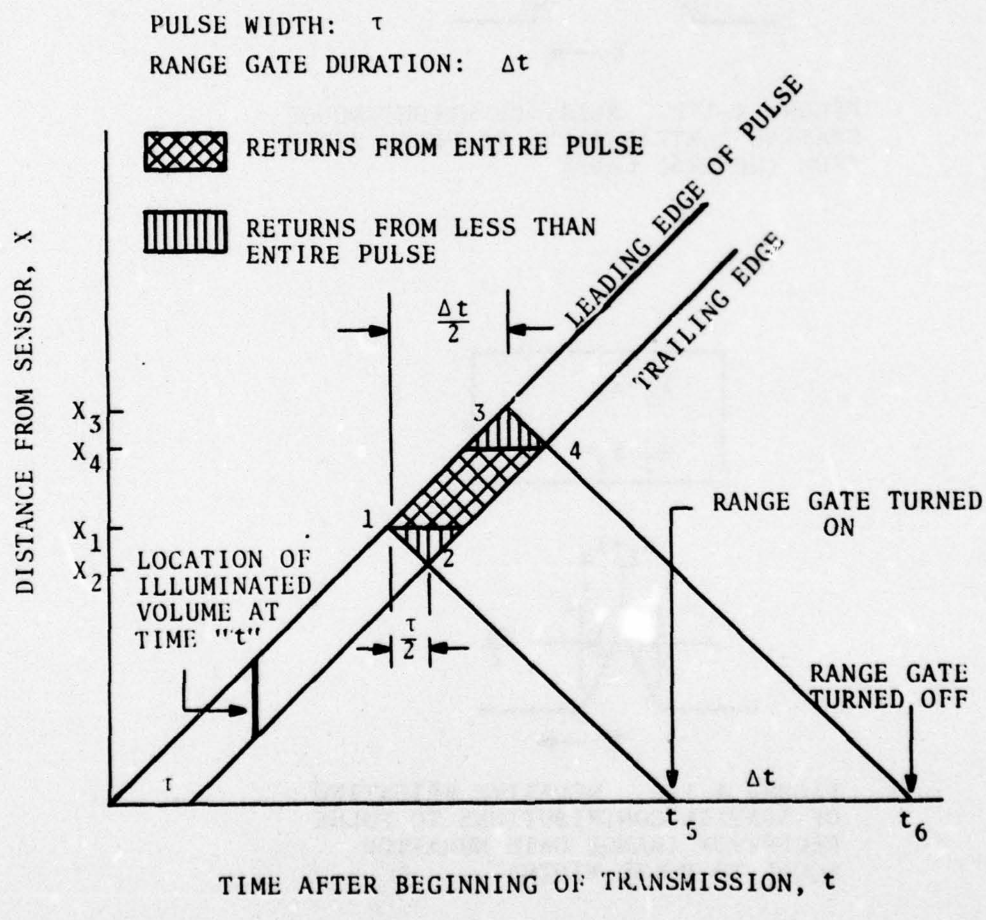

FIGURE 4-17a. TIME-RANGE DIAGRAM

$$X_1 - X_2 = X_3 - X_4 = c\tau/2$$

$$X_3 - X_1 = X_4 - X_2 = c\Delta t/2$$

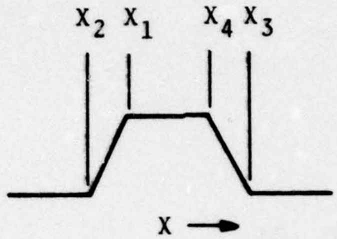

FIGURE 4-17b. RELATIVE WEIGHTING OF SPATIAL CONTRIBUTIONS TO PULSE RECEPTION (GENERAL CASE)

$$X_1 = X_4$$

$$X_3 - X_2 = c\tau$$

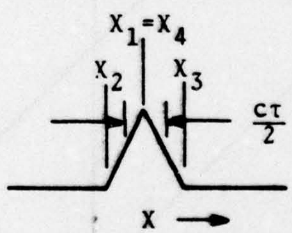

FIGURE 4-17c. RELATIVE WEIGHTING OF SPATIAL CONTRIBUTIONS TO PULSE RECEPTION (RANGE GATE DURATION EQUAL TO PULSE WIDTH)

from X_1 to X_2. If the range gate is left on for a duration longer than the pulse width, the received signal is made up of contributions from X_1 to X_4 weighted as shown in Figure 4-17b. If the range gate is matched to the pulse ($\Delta t = \tau$), the triangular weighting function of Figure 4-17c applies. Here 75 percent of the return signal originates from the central portion, $c\tau/2$ wide; thus for a 2 microsecond pulse, 75 percent of the energy received during the range sample emanates from the central 1000 feet of the volume.

The Doppler shift ranges from about 100 kHz for 1 knot winds to 6 MHz for 60 knot winds. It is anticipated that the received signal will be heterodyned with a local oscillator signal at a frequency higher (or lower) than the transmitted frequency in order to distinguish positive and negative velocities. Assuming a frequency offset of 30 MHz, there will between 24x2=48 and 36x2=72 cycles received for each range within a 2 microsecond pulse. This is a long enough record to enable a spectrum analysis for each pulse and each range bin.

A filter bank having filter bandwidths matched to the pulse width will produce at any given time a set of outputs whose amplitudes provide a sampled measure of the velocity spectrum of the corresponding range bin. For example, a filter bank matched to a two microsecond pulse width would have filters 500 kHz wide; 24 filters would cover the velocity range of ±60 knots (±30 m/sec). If 40 range bins were utilized, the filter outputs would be sampled 40 times at 2 microsecond intervals. The same considerations apply here as for the CW laser (see Section 4.3.6) except that the velocity resolution here would be almost 5 knots (2.5 m/sec). Turbulence and wind gradients cause a spreading of the spectrum. For example, a significant gradient of 2.5 knots per thousand feet (0.4 m/sec/km) (see Section 3.4) would have a spectral spread of about 250 kHz, wide enough so that significant amplitudes would be found in two or three adjacent velocity samples. This would allow interpolation to estimate the velocity centroid to better than the nearest 5 knot increment. Other techniques could also be employed to this data granularity problem.

One approach to improving the accuracy would be to store the waveform from pulse to pulse and analyze the extended record. This would be quite beneficial if pulse-to-pulse transmitter coherence were maintained, and if the returns maintained their phase correlation from pulse to pulse. However, in the inter-pulse period the particle configuration changes enough to destroy the phase correlation: a mild horizontal shear of 1 knot per 1000 feet (0.16 m/sec/km) results in a relative motion of 50 wavelengths per millisecond; thus decorrelation takes place in microseconds, and coherent averaging is not feasible. Furthermore, for pulse repetition rates less than 1000 pps, the sample volume has completely changed, since the scanner is moving in azimuth.

Even with a lack of phase coherence, averaging is beneficial. It reduces the noise variance, thus allowing tighter thresholding to be employed. Incoherent averaging can take a variety of forms, one of which is to store the amplitude of each velocity bin (for each range) after spectral processing, and add the contents from pulse to pulse for a period of time determined by the azimuth sampling rate.

Signal processing must be sophisticated enough to reject spurious measurements and measurements whose SNR falls below some threshold, e.g., 3dB. The latter situation will routinely occur due to backscattering variations, described in Section 4.2.3. Other improvements will be possible when more field data become available.

Considering the benefits of averaging, it is evident that the pulse repetition rate should be as high as laser technology, budget considerations, processing time, and safety considerations will allow; also, full use should be made of the information available on each pulse. The NASA Clear Air Turbulence (CAT) detector employs a laser amplifier operating at 140 pulses per second (pps) (Sonnenschein, et al, 1970). A modern off-the-shelf

TEA laser typically provides 2 pps, while 20 pps have been readily obtained in laboratory setups; although there are technical problems encountered at higher repetition rates for TEA lasers, there appears to be no fundamental reason why 200-1000 pps cannot be obtained. Electron-injection techniques have been demonstrated which achieve megawatt outputs and kilohertz repetition rates simultaneously.

4.4.6 Data Processing

Data processing treats the samples that emerge from the signal processor and is concerned with the reasonableness of the data sample, its internal structure, and the sample-to-sample consistency. Problems that data processing should be able to handle include the following:

a. Spectral broadening due to turbulence and shear.
b. Double-peaking caused by heavy objects such as hailstones, large raindrops, insects, and birds that are in motion with respect to the local air mass.
c. Spurious errors that cause data outliers.

Data processing also includes signature recognition algorithms which involve a priori knowledge of wind shear descriptors, so that shears can be distinguished from short term, large scale gusts, and so that downdraft cells can be distinguished from frontal shears. It is difficult to state precisely the requirements of such algorithms without field data. Some reasonable map signatures are shown in Figure 4-18 for some well-defined situations, but these are qualitative only. It may be, for example, that downdraft identification may require different thresholds than other shear types. Turbulence may prove to be highly correlated with certain shear regimes, so that the spectral width variations may be useful. Certainly the amplitude of the return signal is related to the precipitation level through the attenuation and backscattering mechanisms. For example, a heavy precipitation would cause the signal to decrease with range at a much more rapid rate than would be true in light rainfall. This information would be used to help identify downdraft cells, which

(+) INCREASING HEADWIND TO APPROACHING AIRCRAFT

(–) DECREASING HEADWIND TO APPROACHING AIRCRAFT

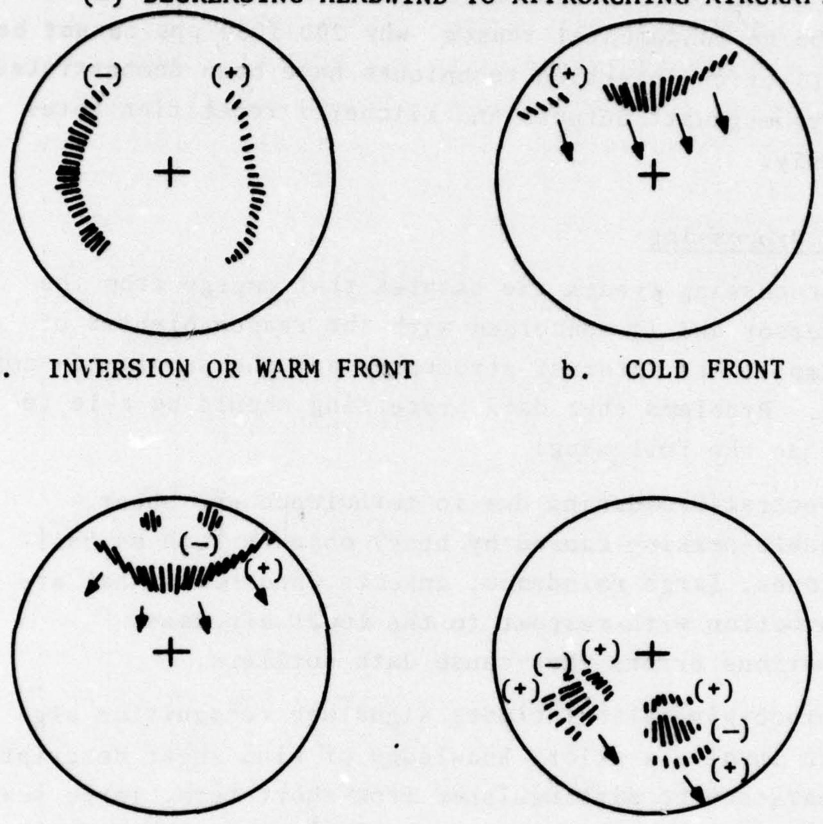

a. INVERSION OR WARM FRONT

b. COLD FRONT

c. THUNDERSTORM GUST FRONT

d. DOWNBURST CELLS

FIGURE 4-18. PULSED LASER MAP SIGNATURES OF WIND SHEAR EVENTS

usually have heavy precipitation within.

Signature recognition is clearly an area where more work needs to be done. Field data obtained during shear events will prove invaluable here.

4.4.7 Laser Hazard Limitations

The safety requirements for a pulsed laser must be calculated in a manner different from those for the CW laser. For one thing, the pulsed laser is only on for a burst of a few microseconds: This, coupled with the fact that laser damage to human and animal life is a function of average power rather than peak power, allows quite high peak power levels to be reached safely. For another, the pulsed laser beam is collimated; the CW beam on the other hand, is focused on a small region, wherein high local intensities can be reached.

Reasonable safety precautions will eliminate situations where accidental irradiation could occur:

a. The space through which the laser beams travel within the housing should be enclosed to prevent accidental insertion of hands or other members into the active region; removal of the cover by unauthorized personnel should automatically shut down the laser.

b. The scanner should not be located anywhere that people are likely to be working; it should be placed above such an area.

c. The scanner should have mechanical limits to prevent it from pointing down.

d. Software should not allow the scanner to stop in one place for longer than some prescribed time, e.g., 0.3-1 second, in an operational environment. For test purposes this would not be necessary, since personnel operating the unit during tests would be trained.

e. Access to the scanner should cause the laser to shut down.

First, the limits of an operational (scanning) laser will be addressed. Within about 2-3 nautical miles of the laser, the telescope has collimated the radiation into approximately a tube, whose diameter is approximately that of the telescope, assumed here to be 1 foot. In this region intensity is highest, and the potential hazard is highest; it is conservatively assumed that all of the radiated energy is in this tubular beam. For a scanning beam, an aperture of 7 millimeters diameter is utilized for the standard (see section 4.3.8 and FDA (1975)), which states that, to meet Class I limits, the radiant energy detectable within an aperture of 7 millimeters diameter shall not exceed 4.4×10^{-3} $t^{1/4}$ joules, where t is the exposure time in seconds. Note that the measurement aperture is small compared with the beam diameter, unlike the case for CW operation, where the reverse is true. If the pulse repetition frequency is small enough, the 7 mm test aperture will be illuminated only once per scan. At higher repetition rates, the beam will have moved less than a beam width between pulses, and several illuminations will occur. Figure 4-19 shows the limits on peak power and pulse repetition rate imposed by Class I limits. The flat portion results from the limit of energy per pulse, and the sloping region from energy per scan. The long-term limit is less stringent and is not shown.

From Figure 4-19, it can be seen that the present TEA laser operation is at the Class I limits within 10 meters of the scanner (actually, transmission losses between laser and telescope output, typically 3-5 dB, bring the operation well within the limits). The maximum anticipated operation will likewise be within Class I limits when transmission lasers are included for ranges greater than 100 m. It is certainly desirable to meet Class I requirements, since the precautions that are required are minimal. However, if it proves necessary, these can be exceeded; operation will still remain within the Class III limits. Extra precautions and justification would then be required.

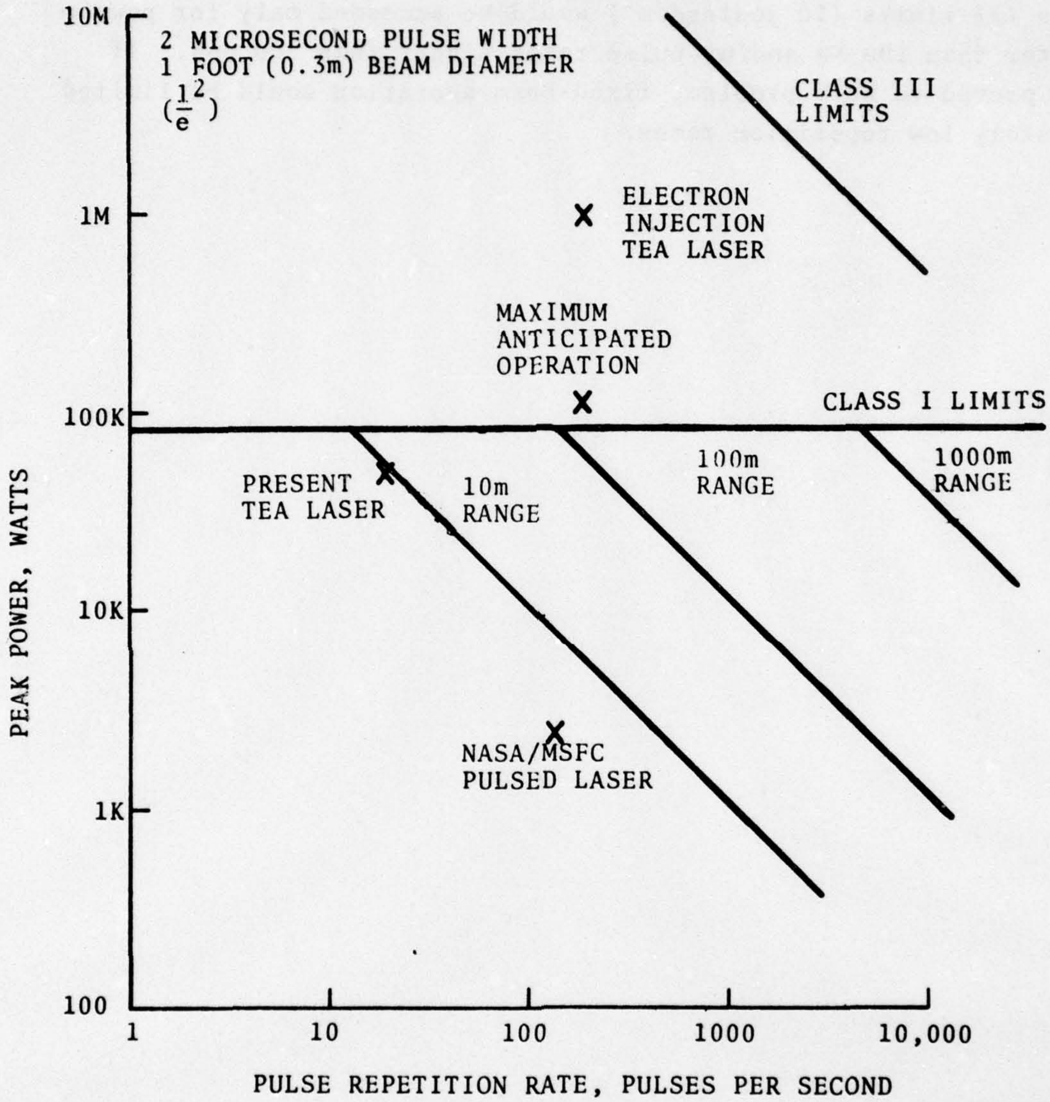

FIGURE 4-19. EMISSION LEVELS FOR PULSED, STEP-SCAN LASER OPERATION

The previous discussion applies to an operational sensor. For experimental purposes, Class III (or even Class IV limits) can be applied. For fixed beam operation, e.g., for calibration, Class III limits (10 joules/cm^2) would be exceeded only for powers greater than 100 KW and/or pulse rates higher than 500 pps. If this proved to be a problem, fixed-beam operation could be limited to safely low repetition rates.

5. SYSTEM CONCEPT AND RECOMMENDATIONS

5.1 PROPOSED SYSTEM CONCEPT AND ALTERNATIVES

5.1.1 Preferred System Concept

The system concept proposed here is that of a single centrally located, scanning laser sensor, which will provide approach and departure corridor protection, and advance warning of shear events. The laser scanner is lightweight, typically 75-100 lb., while the laser itself is compact, with processing electronics which can be located atop a building, or on a small shelter on the airport surface (see Figure 5-1).

The laser is a hybrid pulsed/CW unit: the pulsed amplifier can be bypassed such that the primary laser oscillator can radiate directly, in a continuous wave (CW) Velocity-Azimuth-Display (VAD) mode, which employs a conical scan at elevation angles of 60-75 degrees above the horizon. The system operates periodically (e.g., once every 15 minutes) in the VAD mode to measure wind speed and direction at several altitudes; this information, which could be incorporated in the ATIS meteorological broadcasts, serves a dual purpose: (1) to detect any synoptic vertical shears, and (2) to provide a two-altitude (e.g. surface and 1000 feet altitude) wind report to assist the pilot in choosing his approach speed.

In the pulsed mode, the unit scans 360 degrees of azimuth every 30 seconds.

The elevation angle is programmed to intersect the glide path of each runway at about 300 feet (see Figure 5-2). Note that this improves downburst cell detection at ranges farther out than 1 nm from touchdown (see Section 4.4.3).

Staggering is employed in range to reduce the effects of quantization. On successive pulses, the range starting point is changed by half a resolution cell; e.g., the old sweeps might employ range bins centered at 1000 feet, 2000 feet, 3000

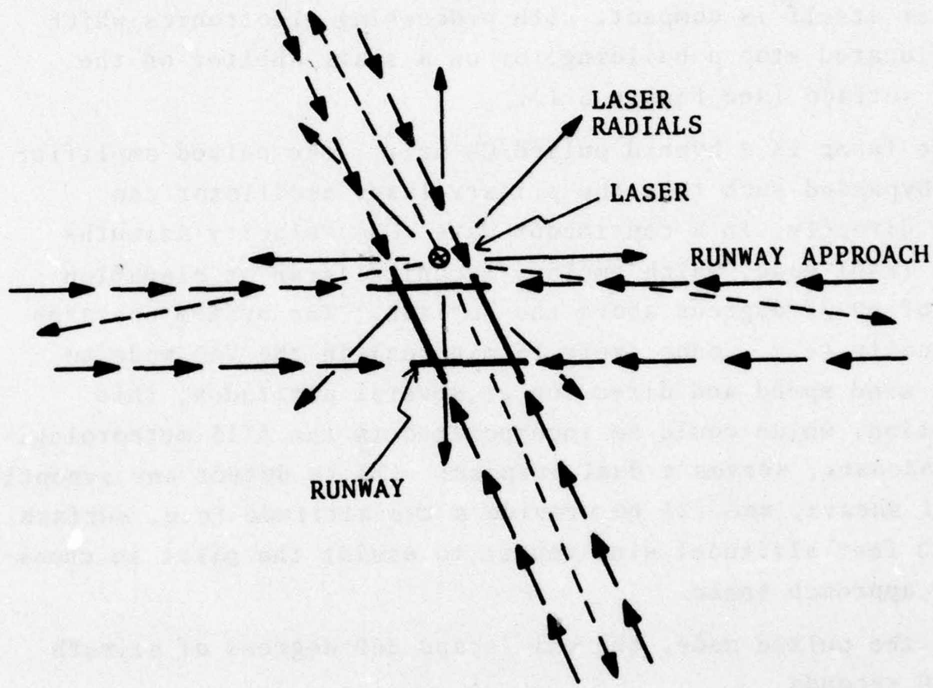

FIGURE 5-1. TYPICAL AIRPORT LAYOUT SHOWING LASER LOCATION FOR COMPARISON BETWEEN HEADINGS OF RUNWAY CORRIDORS AND LASER LINE-OF-SIGHT RADIALS

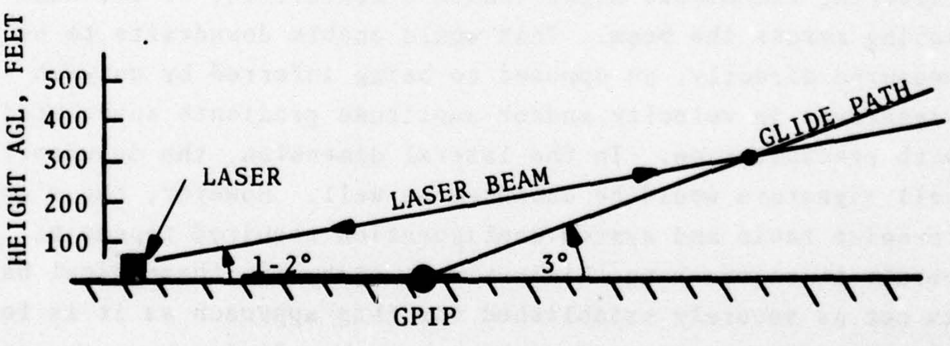

FIGURE 5-2. PULSED MODE ELEVATION ANGLE

feet, etc. This technique helps better locate and assess the shear event.

The system relies on line-sight velocity components to derive the necessary information. Since approaches and departures are nearly radial outside of a mile of the airport, a centrally located line-of-sight sensor will detect primarily headwind changes, which are more important than crosswind changes (Figure 5-1).

The data processor identifies shear zones and estimates their intensity and spatial extent. Vertical shears are identified by height AGL, and are calculated for each corridor orientation. Horizontal shears are located, tracked, and estimates are made of the time of arrival of the shear event at each corridor to be protected. This information is made known to the control tower. The manner in which the information is to be displayed has not yet been determined.

5.1.2 Alternative 1 Laser System: Cross-Beam Velocities

Studies conducted to date (Lee, 1976) indicate that spatial filtering techniques might enable a measurement of the wind moving across the beam. This would enable downdrafts to be measured directly, as opposed to being inferred by outwash signatures in velocity and/or amplitude gradients associated with precipitation. In the lateral dimension, the downdraft cell signature would be enhanced as well. However, the signal-to-noise ratio and system configuration required appear to result in severe range limitations; also, the theoretical basis is not as securely established for this approach as it is for the conventional line-of-sight approach. It is, however, an area that warrants further study.

5.1.3 Alternative 2 Laser System: Dedicated Corridor System

An expensive, but possible, alternative is to dedicate a laser system to one corridor, or one approach-departure corridor pair. The advantage of this is that even under heavy rainfall or fog, the system range would still be 1-2 nautical miles, and would provide excellent corridor protection. By eliminating the scan requirement, some cost could be eliminated, but this is minimal; it would be better to reduce the coverage and increase the update rate, thereby improving system performance.

This alternative appears to have no drawback or special considerations beyond the increased cost. It would be located near threshold and operate at an elevation angle equal to or slightly below the glideslope. It would "see" the same headwinds as the aircraft.

This alternative would be impractical for an application to wind shear only; it has, however, the capability of measuring vortices, by merely adding software. Thus it could be an element in a Wake Vortex Avoidance System. Additionally, a remote visibility sensor could share much of the same equipment, since it would be colocated. A multifunction system like this could be economical for some airports.

5.2 OPERATIONAL AND DISPLAY CONSIDERATIONS

It would be inappropriate in this analysis to design the operational interfaces, since these should be determined by the ultimate users of the system, the pilots and controllers. Furthermore, the laser system is flexible enough that the laser concept need not be tied in with a particular operational procedure. However, there are some well-accepted guidelines which are useful to mention here, that are important in the development of the ultimate sensor. These are enumerated below:

a. System startup should be a simple switch. No personnel should be required to tune or adjust equipment at start-up, nor should any gas fill or refrigerant supply be necessary. Start-up should be possible by a remote switch.

b. Maintenance should be minimal and simple in nature. Once per week maintenance for about half an hour should be sufficient. If laser heads are to be exchanged, realignment should be minimal, not requiring special training. A software diagnostic routine should be available, and be simply initiated.

c. Displays to the controller should not require constant surveillance. The display should be silent and blank, except when shear events have been detected. When activated, the controller's attention should be flagged, probably by an aural cue.

5.3 REQUIREMENTS SUMMARY

5.3.1 CW System Performance Requirements

Height Range - From 50 to 1000 feet above mean ground level.

Height Resolution - 50 feet or less, for heights up to 500 feet; 100 feet or less, for heights of 500 to 1000 feet.

Wind-Speed Range - ±60 knots, headwind and crosswind; ±(1-20) knots, vertical draft.

Measurement/Averaging Time - A complete set of range/angle measurements shall take place in 40 seconds or less; the averaging time shall not exceed 20 seconds; if exponential averaging is used, the time constant shall not exceed 8 seconds.

Wind Speed Accuracy - ±1.5 knots, all components; noise ±1 knot, all components. It is assumed that these measurements are taken at 50-foot height intervals below 500 feet, and include the effect of any averaging over small height intervals below 500 feet, as well as over smaller height resolution cells.

Wind Shear Accuracy - ±1 kphf for heights up to 500 feet; ±2 kphf for heights from 500 to 1000 feet. It is assumed that these measurements are taken at 50-foot intervals below 500 feet.

Scanning Speed - The scanner shall be capable of conical scan at speeds from 0.025 to 0.5 Hz, at an elevation angle of 60 degrees above the horizon.

Environmental Conditions - The equipment shall be entirely enclosed. The system shall meet the specifications of 5.3.1 under the following conditions:

a. 30 knot surface winds
b. Rainfall rate: 25 mm/hr.
c. Snowfall rate: 80 mm/hr.
d. Fog: RVR of 1200 feet
e. Temperature: -10 to 110 degrees F
f. Humidity: 10 to 100 percent RH.

RFI Environment - The equipment shall operate without degradation in a severe airport noise environment.

Personnel Hazard - The radiation intensity shall not exceed the safety limits of the standard for lasers (4.3.8) for airline passengers, crew, airport maintenance personnel, operating personnel, or other personnel in the area. If radiation safety limits are exceeded at the scanner, a safety switch shall be installed on any ladder to prevent accidental exposure to personnel attempting to approach the scanner. Range scan control limits shall be employed to prevent focusing of dangerous radiation at close range; similarly, elevation control limits shall prevent scanning below 1 degree above the horizon. A convenient means of absorbing the laser radiation during extended standby periods shall be provided.

5.3.2 Pulsed System Performance Requirements

Slant Range - 0.3 to 7 nautical miles.

Slant Range Resolution/Accuracy - 1000 feet, at all ranges. Accuracy better than 1 percent of range.

Wind Speed - ±60 knots, line of sight, with wind sense determined by the system.

Wind Speed Accuracy - ±1.5 knots between adjacent range cells; ±3 knots absolute, at all ranges up to 5 nautical miles.

Measurement/Averaging Time - Variable, to be determined.

Pulse Repetition Frequency - 20 pps required; design goal 200 pps.

Pulse Width - Nominally 2 microseconds.

Peak Power - 50 KW minimum; 200 KW design goal.

Focus - Nominally set for infinite range (collimated beam).

Elevation Angle - Variable, from at least 1 to 6 degrees during operation.

Azimuth Scan Rate - 0.008 Hz to 0.05 Hz, average.

Environmental Conditions - The equipment shall be enclosed. In addition the system shall meet the specifications above under the following conditions.

a. 30 knot surface winds.
b. Temperature: 10 to 110 degrees F
c. Humidity: 10 to 100 percent

RFI Environment - The equipment shall operate without degradation in a severe airport noise environment.

Personnel Hazard - As per paragraph 5.3.2, except that the standards described in 4.4.7 shall be employed.

APPENDIX A. RANGE CALCULATIONS

The signal-to-noise ratio (SNR) for a pulsed system is found by (Sonnenschein and Horrigan, 1971):

$$SNR = \frac{\eta_d P_t \beta(\pi) D^2 \; \Delta R \; \eta_t \; \pi \; e^{-2\alpha R}}{8 \; B \; h\nu \; R^2 \left[1 + \left(\frac{\pi D^2}{4\lambda R} \right)^2 \right]}$$

where
- η_d: is the quantum efficiency of the detector
- P_t: is the peak power of the transmitter, in watts
- $\beta(\pi)$: is the backscattering coefficient, in $m^2/sr/m^3$
- D: is the telescope diameter, in meters
- ΔR: is the range resolution, in meters
- B: is the filter bandwidth, in Hertz
- $h\nu$: is the photon energy, in joules
- η_t: is the transmission efficiency of the optical system
- R: is the range, in meters
- λ: is the wavelength, in meters
- α: is the attenuation coefficient, in nepers per meter.

As an example which uses values representative of laser technology today, the following numbers are used:

η_d = 50 percent

η_t = 5 percent

P_t = 10 KW

$D = 0.3$ m

$\Delta R = 300$ m

B = 500 KHz

$h\nu = 1.88 \times 10^{-20}$ joules

$\lambda = 10.6 \times 10^{-6}$ m

$\beta(\pi) \triangleq \alpha/80\pi \; m^2/sr/m^3$ (See Appendix B) .

In the near field, $R << \frac{\pi D^2}{4\lambda}$ and the SNR becomes:

$$SNR = 2.5 \times 10^7 \alpha e^{-2\alpha R} .$$

In the far field, $R >> \frac{\pi D^2}{4\lambda}$ and the SNR becomes:

$$SNR = 1.1 \times 10^{15} \alpha e^{-2\alpha R}/R^2 .$$

The signal-to-noise ratio is usually expressed in decibels:

$$SNR\ (dB) = 20 \log_{10} (SNR)$$

Note that SNR is a ratio of intensities, and therefore unitless.

The attenuation coefficient α is expressed here in nepers per meter; more convenient units are decibels per kilometer and decibels per nautical mile. They are related to α by the following relations:

$$\alpha(dB/km) = 4343\ \alpha\ (nepers/m)$$
$$\alpha(dB/nm) = 8043\ \alpha\ (nepers/m) .$$

These formulas and values are used to determine the curves of Figures 4-13 and 4-14.

APPENDIX B. THE RELATION BETWEEN BACKSCATTER AND ATTENUATION COEFFICIENTS FOR WATER DROPLETS

The calculation of backscatter and attenuation (also called extinction) coefficients are both derived from the classic problem of scattering of a plane wave by a dielectric sphere. This seemingly simple problem is in fact a complex one, and many books and thousands of articles have appeared on the subject. A typical curve of total scattered power as a function of drop size is shown in Figure B-1; the behavior of the backscattered component is similar, but is much more pronounced at the resonant peaks and valleys. If backscattering and total scattering tracked precisely, the coefficients would be related by a constant. In the regime where the drop diameter is large in terms of wavelengths, the total scattering cross section of each drop is approximately twice the projected area of the sphere, regardless of dielectric constant. The resonances cause variations around this value. Since drop distributions are not uniform, we may assume that the resonant effects will average out. A heuristic argument is now presented relating average backscattering and attenuation coefficients for diameters large compared to a wavelength.

The method is to begin with the ratio of backscatter coefficient to extinction coefficient for water at visible wavelengths, and successively account for absorption and index of refraction changes at 10.6 micron wavelength.

At visible wavelengths, it is generally agreed that the average value of this ratio (ζ) is given by (Lifsitz, 1974):

$$\zeta \triangleq \frac{\beta(\pi)}{\alpha} = \frac{0.6}{4\pi} ,$$

where $\beta(\pi)$ is the backscatter coefficient in $m^2/sr/m^3$, and α is the extinction coefficient in nepers per meter. A plot of the ratio from another set of calculations is given in Figure B-2, taken from Twomey & Howell (1965); it can be seen that $4\pi\zeta$ is well approximated by 0.6.

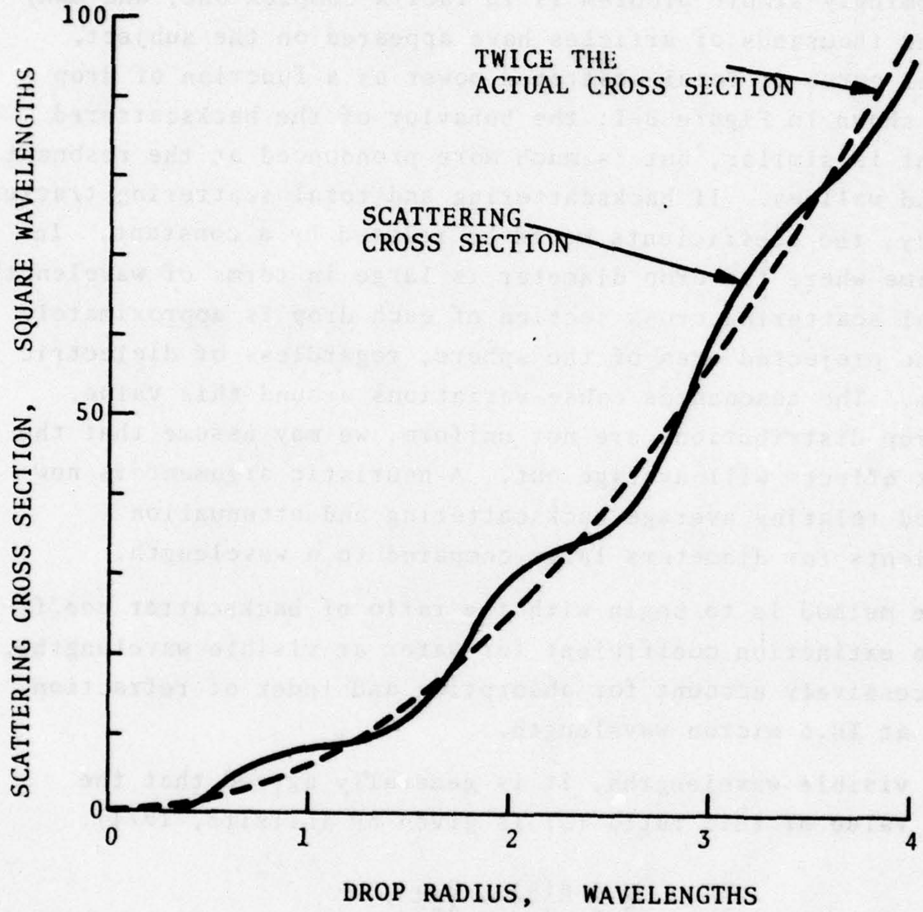

FIGURE B-1. TYPICAL SCATTERING CROSS SECTION OF A DIELECTRIC SPHERE

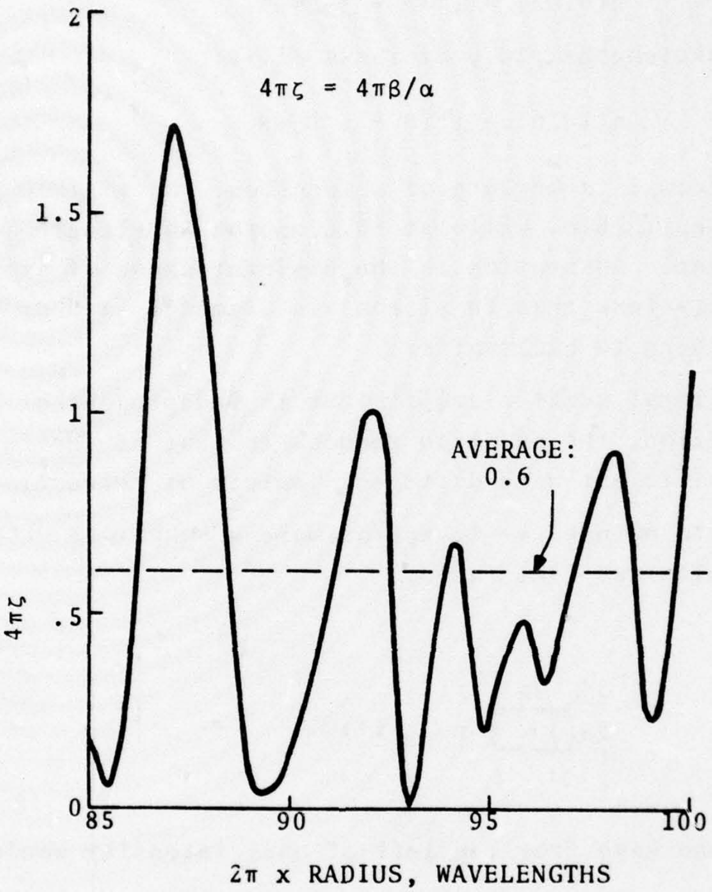

FIGURE B-2. RATIO OF BACKSCATTERING TO ATTENUATION COEFFICIENTS AT VISIBLE WAVELENGTHS FOR A TYPICAL WATER DROPLET (FROM TWOMEY AND HOWELL, 1965)

The index of refraction of water at visible wavelengths (0.63 micron in particular) is:

$$n(0.63) = 1.33 + j\,10^{-6},$$

while at CO_2 wavelengths (10.6 microns) it is:

$$n(10.6) = 1.18 + j\,0.08.$$

The imaginary term is a measure of absorption. At visible wavelengths it is negligible, while at 10.6 micron wavelength it is quite significant. Absorption is the dominant cause of attenuation for droplets less than 10 microns in diameter (and of course contributes nothing to backscatter).

Since the total scatter coefficient is independent of the index of refraction, the question reduces to that of the relative backscatter coefficient with different indices of refraction.

The model to be used is to approximate a spherical drop by a cylinder with two flat faces:

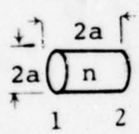

$n_o \approx 1 + j0.$

An incident plane wave from the left of unit intensity would reflect $\left(\frac{n-1}{n+1}\right)^2$ units of intensity times πa^2, the projected area, and transmit the rest $\left(\frac{4n}{(n+1)^2}\right)^2$ into the drop. At visible wavelengths, none would be absorbed in the drop, and $\left(\frac{n-1}{n+1}\right)^2$ would be reflected by face 2 back through the drop; transmitted back through face 1 would emerge an intensity equal to:

$$\left(\frac{n-1}{n+1}\right)^2 \cdot \left(\frac{4n}{(n+1)^2}\right)^2 .$$

As the diameter varies, the backscattered reflections go in and out of phase, resulting in large variations in backscattered signal. (Since the total scattering does not vary appreciably, the energy is scattered in other directions when the backscatter is low.) On the average, the total intensity is just the sum of the two reflected intensities. For n = 1.33, the intensity is proportional to:

$$I(0.63) \sim \left(\frac{n-1}{n+1}\right)^2 \cdot \left(1 + \frac{16n^2}{(n+1)^4}\right) = 0.0393 \ .$$

At 10.6 microns, there is no second reflection, since all energy entering the droplet is absorbed. Thus

$$I(10.6) \sim \left(\frac{n-1}{n+1}\right)^2 = 0.0068$$

for n = 1.18. The ratio between these is

$$\frac{I(10.6)}{I(0.63)} = 0.17 \ .$$

Additionally, the total attenuation is due to scattering and absorption; half the energy is absorbed at 10.6 microns, while none is absorbed at visible wavelengths. Thus the ratio of backscatter to attenuation at 10.6 microns is approximately

$$\zeta(10.6) \simeq \frac{1}{2} \cdot \frac{0.6}{4\pi} \cdot (0.17) = \frac{0.05}{4\pi}, \text{ or}$$

$$\beta \approx \frac{\alpha}{80\ \pi} \ m^2/sr/m^3$$

if α is expressed in dB/km,

$$\beta = 9.2 \times 10^{-7}\ \alpha\ (dB/km) \qquad m^2/sr/m^3$$

or approximately,

$$\beta \simeq 10^{-6}\ \alpha\ (dB/km) \qquad m^2/sr/m^3 \ .$$

A number of points from results by Rensch and Long (1970) were checked, and the ratio ζ was found to vary between $\frac{0.02}{4\pi}$ and $\frac{0.12}{4\pi}$, so that $\frac{0.05}{4\pi}$ represents some middle value. Even though the assumption breaks down in fog, representative values of ζ for fog also yield values of about $\frac{0.05}{4\pi}$. For drop sizes below 2 microns in diameter, absorption exceeds scatter, and the ratio rapidly decreases for decreasing drop size. Thus, in a fog, the backscatter is primarily due to the drops greater than 2 microns in diameter, but smaller drops can cause attenuation by absorption.

APPENDIX C. BOUNDARY-LAYER SHEARS (HALLOCK, 1976)

The surface boundary layer is that region of the atomsphere where the shear stress is practically constant. The region extends from the surface to a few tens of meters in altitude on clear nights with light winds and to about two thousand meters in altitude on sunny summer afternoons. In the surface boundary layer, only the surface conditions, the stability condition, and altitude affect the wind and turbulence structure. The logarithmic wind law as derived from the Monin-Obukov similarity theory and experiments for neutral, stable, and unstable conditions is, in simplified form, given by:

$$u = (u^*/k)\left[\ln\left(\frac{z+z_o}{z_o}\right) + \psi\left(\frac{z}{L}\right)\right]$$

where u is the wind magnitude, u* the surface friction velocity, k the von Karmon's constant ($k \approx 0.4$), z the measurement height, z_o the roughness length, and L the Monin-Obukov stability length. The function $\psi(\frac{z}{L})$ is an empirically derived universal function of z/L:

$$\psi\left(\frac{z}{L}\right) = 0 \qquad \text{(neutral)}$$

$$\psi\left(\frac{z}{L}\right) = 5.2\,\frac{z}{L} \qquad \text{(stable)}$$

$$\psi\left(\frac{z}{L}\right) = \int_{z/L}^{z/L} \frac{L}{z}\,\{1-(1-18\tfrac{z}{L})^{-1/4}\}\,d\left(\frac{z}{L}\right) \qquad \text{(unstable)}$$

For every stable condition, the logarithmic law is not valid; the layers of the atmosphere become disconnected and large scale frontal motions define the wind profile shape.

The net effect of turbulence in the atmosphere is the production of a thoroughly mixed state by the transport of fluid properties down their respective gradients. In the friction layer of the atmosphere, the turbulence operates to transport momentum from the higher layers of the atmosphere downward toward the ground layer to replace the momentum lost through frictional dissipation. If the mixing process were not present, the wind shear near the ground would become very large, being governed only by surface drag and the kinematic viscosity. Consequently, for any given atmospheric state, the maximum value of wind shear may be expected to occur just prior to the onset of the mixing process.

Low-level wind shears result from the interaction of synoptic scale flow with the surface of the earth. The boundary layer can be segmented into a constant wind direction layer (where the winds behave as in the equations above) and a wind turning layer. The constant wind direction layer extends from the surface up to about 150 meters and wind shear results from the boundary condition that the steady-state wind speed must be zero at the ground. The turning layer occurs above the constant wind direction layer and exhibits a marked turning of the steady-state wind vector with an increase in altitude.

Consider first the constant wind direction layer. When the temperature lapse rate is neutrally stable, the mechanical production of turbulent kinetic energy is neither augmented by the buoyant production of turbulent kinetic energy (as in the unstable case) nor suppressed by thermal stratification (as in the stable case). Although strong wind shears accompany neutral conditions, the shear is confined to below about 10 meters. Unstable conditions are synonymous with convective mixing. Thus, both neutral and unstable conditions should not produce wind shears that are hazardous to aviation. Stable conditions, on the other hand, can lead to dangerous shear conditions. Negative buoyant forces suppress the turbulence and decouple the layers allowing them to slip relative to each other. Large mean flow wind shears can then result. With very stable conditions the flow is laminar, very little mixing occurs, and the overriding air remains separated from the underlying air. Large changes in wind direction (in excess of 45 degrees) and/or magnitude (in excess of 8 knots) are possible in altitude changes of only tens of meters.

Innumerable wind profiles are possible in the turning layer. Stable conditions produce the most dangerous shears in the turning layer with typical angle changes of 30 to 50 degrees. The stable turning layer is the least understood layer due to the decoupling of the layers as a result of the decreased turbulence. During the night, an inversion can build up and relax the constraint imposed on the wind by day-time mixing. As a result, the wind at the top of the inversion accelerated, becomes supergeostrophic, and oscillates inertially-- a low level nocturnal jet. The low-level jet is a thin, well-defined region of high-speed air at a typical altitude of about 300 meters, with no indication of such a wind near the ground. The jet begins to build up in the late afternoon, reaches its maximum in the middle of the night, and decays in the early morning. The nocturnal jets can produce significantly large values of low-level wind shear. At the peak of the jet, the winds in its core, between 250 and 700 meters in altitude, can attain between 40 and 70 knots, decreasing to 10 or 20 knots between 1000 and 1400 meters, and to 0 at the ground. It is a local phenomenon but can be 1500 kilometers long and 70 to 700 kilometers wide. In the United States, the occurrence of the nocturnal jet is most pronounced in the Great Plains. Tower measurements have recorded low-level jet shears in excess of 12 meters/second/30 meters.

APPENDIX D. ANALYSIS OF WIND SHEAR ERRORS AND THEIR EFFECTS ON SYSTEM PERFORMANCE

If the wind shear criterion could be simply characterized by two states (i.e., Severe and Not Severe), the problem could be classically stated in terms of False Alarms and Misses, where a False Alarm indicates a "Severe" indication when the actual shear is "Not Severe" and a "Miss" indicates a "Not Severe" when the actual shear is "Severe." If more states are desired (i.e., Light, Moderate, Strong, Severe), the characterization is more complicated.

Staying with the two-state criterion, it is convenient to use a mixed continuous/discrete description whereby wind shear is characterized by whole kphf; where, for example, 5 kphf means a shear between 4.5 and 5.5 kphf . Let W_T be the threshold value, and W the shear:

$|W| > W_T$ implies a Severe shear, and

$|W| < W_T$ implies a Non-Severe shear,

where W_T is half integer value (e.g., 4.5 kphf, 5.5, etc.) The probability of a False Alarm, P_{FA}, is:

$$P_{FA} = P\left(|W_M|>W_T \,\Big|\, |W_A|<W_T\right) \qquad \text{(D-1)}$$

where W_M is the measured shear, and W_A is the actual shear. For example, if W_T = 4.5 the event $|W_A|<W_T$ means that W_A can be -4, -3, -2, -1, 0, 1, 2, 3, or 4 kphf; however, in general, the probabilities of these subevents are not uniform, but depend on the probable density of the phenomenon, $p_s(W_A)$.

The ICAO paper on Low Level Wind Shear and Turbulence (ICAO, 1976) suggests the following values for the probability of exceeding the values shown:

3 kphf - 50 percent
5 kphf - 17 percent
8 kphf - 2 percent
10 kphf - 0.4 percent

where the percentage values refer to:

$$\int_{|W_o|}^{\infty} p_s(W_A)\,dW_A \overset{\Delta}{=} P_s(W_o) \quad . \qquad \text{(D-2)}$$

A little curve-fitting yields the following approximation:

$$p_s(W_A) = 0.09\; W_A^{0.72} \quad \exp\{-0.105\; W_A^{1.72}\} \qquad \text{(D-3)}$$

and $P_S(W_o) = \frac{1}{2}\exp\{-0.105|W_o|^{1.72}\}$.

We take $p_s(m)$ here to mean:

$$p_s(m) \overset{\Delta}{=} \left| P_s(|M-\tfrac{1}{2}|) - P_s(|M+\tfrac{1}{2}|) \right| \quad . \qquad \text{(D-4)}$$

Thus for any event A:

$$P(A \,\big|\, |W_A|<W_t) = \frac{\sum_{n=-[W_T]}^{[W_T]} P(A \,\big|\, W_A=n)\,p_s(n)}{\sum_{n=-[W_T]}^{[W_T]} p_s(n)} \qquad \text{(D-5)}$$

where [x] is the largest integer less than or equal to x. Here A is the event that $|W_M|>W_T$. Assuming Gaussian errors with zero mean and a standard deviation of σ kphf:

$W_M = W_A + \varepsilon$

where $E\{\varepsilon\} = 0$, and $E\{\varepsilon^2\} = \sigma^2$. (D-6)

For example, suppose $W_A = 3$ kphf. A False Alarm occurs

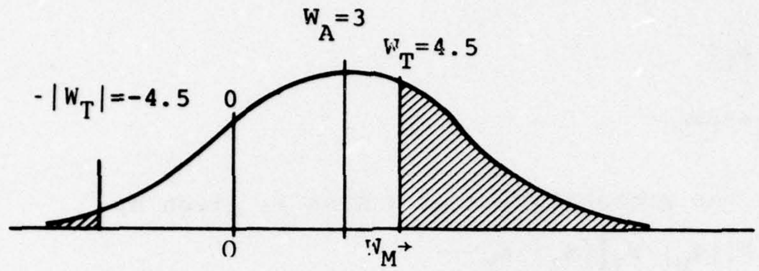

if $|W_M|>4.5$ shown by the shaded regions; the density distribution is given by

$$P(W_M) = \frac{1}{\sigma\sqrt{2\pi}} \exp\{-\frac{(W_M - W_A)^2}{2\sigma^2}\} \qquad \text{(D-7)}$$

and the shaded regions by

$$P(|W_M|>W_T) = \left(\int_{W_T}^{\infty} + \int_{-\infty}^{-W_T}\right) p(W_M)\,dW_M \qquad \text{(D-8)}$$

$$= 2 - \frac{1}{2}\,\mathrm{erf}\left(\frac{W_T - W_A}{\sigma\sqrt{2}}\right) - \frac{1}{2}\,\mathrm{erf}\left(\frac{W_T + W_A}{\sigma\sqrt{2}}\right) \qquad \text{(D-9)}$$

where erf (x) is the Error Function, found in several available tables. For our problem, where the condition is that $W_A=n$, we have

$$P\left(|W_M|>W_T \middle| W_A=n\right) = 2-\frac{1}{2}\,\mathrm{erf}\left(\frac{W_T - n}{\sigma\sqrt{2}}\right) - \frac{1}{2}\,\mathrm{erf}\left(\frac{W_T + n}{\sigma\sqrt{2}}\right). \qquad \text{(D-10)}$$

We are now in a position to calculate the values: the probability of a False Alarm is given by

$$P_{FA} = \frac{\sum_n^* P(|W_M|>W_T \mid W_A=n)\,P_S(n)}{\sum_n^* P_S(n)} \qquad \text{(D-11)}$$

where $P(|W_M|>W_T|W_A=n)$ is given by (D-10), $p_s(n)$ is given by (D-4), and

$$\sum_n^* = \sum_{n=-[W_T]}^{[W_T]} .$$

Similarly, the probabilities of a Miss is given by

$$P_M = P(|W_M|<W_T \,\big|\, |W_A|>W_T)$$

$$= \frac{\sum_m^* P(|W_M|<W_T \,\big|\, W_A=m)\; p_S(m)}{\sum_m^* \; p_S \; (m)} \qquad \text{(D-12)}$$

where $\sum_m^* = \sum_{m=-\infty}^{-[W_T]-1} + \sum_{m=[W_T]+1}^{\infty}$, and

$$P(|W_M|W_T \,\big|\, W_A|=m) = \tfrac{1}{2}\mathrm{erf}\left(\frac{m+W_T}{\sigma\sqrt{2}}\right) - \tfrac{1}{2}\;\mathrm{erf}\left(\frac{m-W_T}{\sigma\sqrt{2}}\right) . \qquad \text{(D-13)}$$

This gives the following results for $W_T = 4.5$:

σ	P_{FA}	P_M
1	.087	.154
2	.189	.257
2.8	.261	.307
4	.360	.350 .

Changing the threshold to $W_T = 7.5$ gives:

σ	P_{FA}	P_M
1	.018	.190
2	.055	.297
2.8	.097	.344
4	.166	.385 .

GLOSSARY

Aerosols - Particles suspended in the atmosphere: dust particles, moisture droplets, soot. Sometimes fog and rain droplets are also called aerosols.

AGL - Above mean Ground Level; used to denote height above a runway. It is used in contradistinction to altitude, which is referenced to mean sea level.

ATIS - Automated Terminal Information Service; a recorded weather advisory for pilots, broadcast from selected airports.

Backscatter coefficient - A coefficient which denotes the relative strength of the laser signal reflected from a volume of aerosols back toward the laser.

Boundary layer - The lowest kilometer of the atmosphere; so named because the effect of the ground is to retard the winds near the ground.

Clutter - The unwanted radar returns from vegetation and buildings; clutter tends to mask the returns from desired targets.

Collimated beam - A beam of radiation that remains in a column for some distance from the telescope used to shape the beam.

CO_2 laser - A laser operating at one or more of several wavelengths very close to 10.59 microns, characteristic of carbon dioxide molecular vibrational resonances.

CW - Continuous wave, used to describe a signal which remains on for long periods of time; as opposed to pulsed signals.

Downburst cells - Tightly confined downdrafts which occur as secondary surges behind the gust front of a thunderstorm outflow; they frequently contain rain (see Section 2.3).

Glidepath - The vertical guidance provided by an ILS; generally it is a plane oriented at about three degrees elevation, and intersecting the runway at the GPIP. The guidance is not usually reliable below 100-200 feet AGL.

GPIP - Glide Path Intercept Point, the point on the runway centerline that the glidepath would intercept if the straight-line guidance were projected to the ground. It is usually located about 1000 feet from threshold.

Gust front - The leading edge of the cold air outflow from a thunderstorm; sometimes used to denote the zone behind the leading edge, where gusty winds and vertical drafts occur.

Heterodyne - A technique for receiving returns from a target, wherein the detector mixes signals from the return signal with a local oscillator signal to achieve high detection efficiency.

Hit - Used here to denote the detection of a shear event by a laser sensor during one scan. Hits on successive scans provide a track of a shear event, and allow an estimate of its velocity.

Horizontal shear - In its ideal form, a wind condition wherein wind velocities have gradients in the horizontal plane, but are constant in a vertical line above the ground; used here to denote a condition where horizontal gradients are larger than vertical gradients.

ILS - Instrument Landing System, a guidance system associated with a runway, which provides deviation from runway centerline and glidepath to instrumented aircraft. An outer marker is generally employed about 5 miles out, which provides timing information; a middle marker is also employed, located about half a mile out.

Isotach - Contours on a wind map showing lines of constant wind speed.

KIAS - Knots of Indicated Air Speed, the speed of the aircraft relative to the air mass.

kphf - Knots Per Hundred Feet, a unit used here to describe the intensity of a vertical shear; 2 kphf is mild, 5 kphf is significant, and 12 kphf is treacherous.

Localizer - The transmitter used in an ILS to provide lateral guidance in the form of deviations from runway centerline; it is generally located about 1000 feet beyond the stop end of the runway.

Matched filter - A filter in a signal processor/receiver which is shaped to optimize the SNR to a known transmitter pulse shape.

Middle marker - A transmitter in an ILS which provides a signal, generally audible, to the pilot of an approaching aircraft that he is about half a nautical mile from the runway.

Nocturnal jet - A thin, well-defined region of high-speed air that occurs at about 1000 feet AGL in the late afternoon and night; it would not be detected by an anemometer near the surface.

Outlier - A measurement which differs so much from other measurements proximate in space or time that it is highly unlikely to be valid, and is probably spurious.

RH - Relative Humidity

Scan - A complete set of measurements; in the case of a laser scanner, a scan denotes a complete cycle of range and angle variations.

SNR - Signal-to-Noise Ratio, a measure of the goodness of the signal received; low SNR's result in loss of accuracy and increased uncertainty.

Sweep - A set of measurements associated with a single pulse, in a pulsed laser or radar; the set of sweeps comprising the azimuth scan form a scan.

System range - Used to denote the maximum distance from the sensor system for which a useful signal is obtained; as opposed to "range," which is the distance from the sensor to some point implied by the context.

VAD - Velocity Azimuth Display, a scanning measurement technique used by CW radars and lasers to obtain wind profiles (see Section 4.3).

Vertical shear - A wind condition wherein horizontal winds exhibit significant gradients in the vertical direction, but change gradually horizontally.

BIBLIOGRAPHY

Brashears, M.R. and Hallock, J.N. 1976: The Measurement of Wake Vortices by Laser Doppler Velocimetry. 7th Conference on Aerospace and Aeronautical Meteorology, 175-181.

_________, Eberle, W. and Shrider, K., 1977: Laser Doppler Velocimeter Measurements and Comparison with Tower-Mounted Anemometers. FAA-RD-77-00.

Brundidge, K.C., 1965: The Wind and Temperature Structure of Nocturnal Cold Fronts in the First 1,420 Feet. Monthly Weather Review, 93, 587-603.

Caracena, F., 1975: Surface Winds in the Vicinity of Stapleton Airport at the Time of the Crash of Continental Flight 426 - Part II. NTSB Docket No. 76ADCAZ002.

_________, 1976: Surface Winds in the Vicinity of Stapleton Airport at the Time of the Crash of Continental Flight 426 - Part II. Private Communications.

Chu, T.S., and Hogg, D.C., 1968: Effects of Precipitation on Propagation at 0.63, 3.5, and 10.6 Microns. Bell System Tech J., 47, 723-759.

Coons, F.G., 1976: Aircraft-Derived Profiles in Frontal Shears. Private Communication.

_________, and Mandel, C., 1976: The FAA Wind Shear Research and Development Program--A Status Report. 7th Conference on Aerospace and Aeronautical Meteorology, 70-77.

Fante, R.L., 1975: Electromagnetic Beam Propagation in Turbulent Media. Proceedings of the IEEE, 63, No. 12, 1669-1691.

FDA (Food and Drug Administration), 1975: Performance Standard for Laser Products. Federal Register, 40, No.148, Part II, July 31, 1975.

Friedman, A., 1964: Analog Computer Study of Safe, Low Approach Decision Regions and Effectiveness of Glide Path Extension Techniques. Bendix Eclipse-Pioneer Division Final Report, Contract FAA-ARD-451. (See especially Figs. 6&7 and discussion.)

Fujita, T., 1976: Spearhead Echo and Downburst Near the Approach End of a John F. Kennedy Airport Runway, New York City. SMRP Res. Paper 137.

Goff, R.C., 1975: Thunderstorm-Outflow Kinematics and Dynamics. NOAA Technical Mem. ERL NSSL-75.

________, 1976: Some Observations of Thunderstorm Induced Low-Level Wind Variations. AIAA 9th Fluid and Plasma Dynamics Conference.

Goldstein, I., Miles, P.A. and Chabot, A., 1965: Heterodyne Measurements of Light Progagation through Atmospheric Turbulence. Proceedings of the IEEE, 53 No. 9, 1172-1180.

Hallock, J.N., 1976: Boundary-Laver Shears. Material on file at DOT/TSC, September 8, 1976.

ICAO (International Civil Aviation Organization), 1976: Explanatory Material on Low Level Wind Shear and Turbulence. Attachment B to ICAO State Letter AN 10/4.6-76/19.

Kalafus, R.M., and Hallock, J.N., 1976: Requirements for an Airport Ground-Based Wind Shear Detection System. 7th Conference on Aerospace and Aeronautical Meteorology, 182-187.

Kerr, D.E., 1951: Propagation of Short Radio Waves. Dover Publications.

Langweil, L., 1976: The Status and Direction of the Federal Aviation Administration Wind Shear Program. Paper 76-386, AIAA 9th Fluid and Plasma Dynamics Conference.

Laws, J.O., and Parsons, D.A., 1943: The Relation of Drop Size to Intensity. Trans. Am. Geophys. Union, p. 452.

Lee, R.W., 1976: Spatially Filtered Lidar Velocity Probes: A Feasibility Study. Stanford Electronics Laboratory TR 4511, July 1976.

Lhermitte, R.M. and Atlas, D. 1961: Precipitation Motion by Pulse Doppler Radar. Proc. 9th Weather Radar Conference, 218-223.

Lifsitz, J.R., 1974: Lidar Systems for Measuring Visibility--A Technical Assessment. DOT-TSC-FAA-74-15, FAA-RD-74-119, September 1974.

McClatchey, R.A., Fenn, R.W., Selby, J.E.A., Volz, F.E., Garing, J.S., 1972: Optical Properties of the Atmosphere (Third Edition). AFCRL-72-0497, August, 1974.

Nancoo, M.E., 1974: A Status Report on Low Level Turbulence and Wind-Shear Effects on Aircraft. ICAO Bulletin, Sep. 1974, pp.16-21.

NTSB (National Transportation Safety Board), 1974a: Aircraft Accident Report--Ozark Airlines--Fairchild Hiller FH-227B, Lambert-St. Louis International Airport. NTSB-AAR-74-5.

__________, 1974b: Aircraft Accident Report--Delta Airlines Douglas DC-9, Chattanooga Municipal Airport. NTSB-AAR-74-13.

__________, 1974c: Aircraft Accident Report--Iberian Airlines Douglas DC-10-30, Logan International Airport. NTSB-AAR-74-14.

__________, 1976a: Aircraft Accident Report--Eastern Airlines Boeing 727-225, JFK International Airport. NTSB-AAR-76-8.

__________, 1976b: Aircraft Accident Report--Continental Airlines--Boeing 727-224, Stapleton International Airport. NTSB-AAR-76-14.

__________, 1976c: Aircraft Accident Report--Eastern Airlines Boeing 727, Raleigh, N.C. NTSB-AAR-76-15.

Rensch, D.B. and Long, R.K., 1970: Comparative Studies of Extinction and Backscattering by Aerosols, Fog, and Rain at 10.6 μ and 0.63 μ. Applied Optics, 9, 1563-1573.

Snyder, C.T., 1968: Analog Study of the Longitudinal Response of a Swept-Wing Transport Aircraft to Wind Shear and Sustained Gusts During Landing Approach. NASA Technical Note D-4477, April, 1968.

Sonnenschein, C., Jelalian, A., and Keane, W., 1970: Development of CO_2 Laser Doppler Instrumentation for Detection of Clear Air Turbulence. Contract NAS-8-24742, Final Report, Raytheon, ER 70-4203, June 5, 1970.

_________, and Horrigan, F.A., 1971: Signal-to-Noise Relationships for Coaxial Systems that Heterodyne Backscatter from the Atmosphere. Applied Optics, 10, 1600-1604.

Stapleford, R.L., 1976: Thirteenth Monthly Progress Report, Computer Simulation of Wind Shear Hazard for Cine Transport Aircraft. Systems Technology Inc., Monthly Progress Report, Contract NAS2-8889.

Strohbehn, J.W., 1965: Line-of-Sight Wave Propagation Through the Turbulent Atmosphere. Proceedings of the IEEE, 56, No. 8, 1301-1318.

Tatarski, V.I., 1961: Wave Propagation in a Turbulent Medium. McGraw-Hill, ch. 3.

Twomey, S. and Howell, H.B., 1965: The Relative Merit of White and Monochromatic Light for the Determination of Visibility by Backscattering Measurements. Applied Optics, 4, 501-506.

200copies